Université Fédérale
Toulouse Midi-Pyrénées

Acknowledgements

Abstract

Arbuscular mycorrhization and rhizobial nodulation are two major root endosymbioses which play important roles in plant development by improving their mineral nutrition. Produced by Rhizobia bacteria and mycorrhizal fungi, lipo-chitooligosaccharides (LCOs) were shown to be essential for the formation of the rhizobial symbiosis and to have stimulatory effects on mycorrhization. In the legume *Medicago truncatula* three lysin motif (LysM) receptor-like kinases LYR3, NFP and LYK3 have been shown to be involved in LCO perception. Here work is presented aimed at the biochemical characterization and application of these important receptor proteins.

Cloned from several legume species orthologs of *M. truncatula* LYR3, except from lupin, were shown to bind LCOs with high affinity, but not structurally-related chitooligosaccharides (COs). Domain swaps between the lupin and *Medicago* proteins were used as a tool to decipher the molecular basis of LCO recognition and revealed the importance of the third LysM domain for LCO binding.
The possibility of exploiting the LCO-binding capacity of LYR3 in biotechnology, through the composition of chimeric receptors, was investigated by combining together the extracellular domain of LYR3 protein with the kinases of *Arabidopsis thaliana* immune receptors, AtCERK1 and EFR. The results suggest that LYR3 could be used for constructing biologically active chimeric proteins whose mode of activation needs to be improved.

Finally studies on the two LysM symbiotic receptors NFP and LYK3 suggest that they are regulated by changes in their phosphorylation after symbiotic treatments.

Together this work brings light on the mechanisms underlying LCO perception and the modifications that receptors undergo after their treatment with LCO.

Key words: Rhizobium/Legume symbiosis; receptor structure function; lipo-chitooligosaccharides; *Medicago truncatula*; LysM; Phos tag; plant defence; PAMPs

Résumé

Les symbioses rhizobienne et mycorhizienne à arbuscules sont deux endosymbioses racinaires jouant des rôles importants dans le développement des plantes en améliorant leur nutrition minérale. Les lipo-chitooligosaccharides (LCOs), produits par les bacteries Rhizobia et les champignons mycorhiziens, sont essentiels pour l'établissement de la symbiose rhizobienne et stimulent la mycorhization. Chez la légumineuse *Medicago truncatula*, trois récepteurs-like kinase à motifs lysin (LysM), LYR3, NFP et LYK3 sont impliqués dans la perception des LCOs. Le travail présenté a eu pour objectif la caractérisation biochimique de ces récepteurs et leurs applications potentielles.

Les orthologues de LYR3 de *M. truncatula* ont été clonés et se sont tous révélés, à l'exception de celui du lupin, capables d'établir une interaction d'affinité élevée avec les LCOs mais pas avec les chitooligosaccharides de structure apparentée. Afin de mieux comprendre les bases moléculaires de la reconnaissance des LCOs, des échanges de domaine entre les protéines LYR3 de lupin et de Medicago ont été effectués et ont révélé l'importance du troisième domaine LysM dans l'interaction.

L'exploitation des capacités de reconnaissance des LCOs par LYR3 à des fins biotechnologiques a été évaluée à l'aide de récepteurs chimériques constitués du domaine extracellulaire de LYR3 et du domaine kinase des récepteurs immunitaires AtCERK1 et EFR. Il est apparu que LYR3 peut être utilisé pour élaborer des récepteurs chimériques mais leur mode d'activation reste à optimiser.

Enfin l'étude des deux récepteurs symbiotiques NFP et LYK3 suggère qu'ils sont régulés par phosphorylation suite au traitement par les signaux symbiotiques.

L'ensemble de ce travail apporte un éclairage nouveau sur les mécanismes de perception des LCOs et sur les modifications associées à leurs récepteurs qui en résultent.

Mots-clés : Symbiose Rhizobium/légumineuse; récepteur structure-fonction; lipo chitooligosaccharides ; *Medicago truncatula* ; LysM ; Phos tag, défense des plantes; PAMPs

Content page

Introduction

The majority of land plant species possess the ability to form mutualistic root endosymbioses with several types of soil microorganisms. These symbiotic relations are beneficial for both partners and are based on the improvement of plant mineral nutrition provided by the microorganisms (particularly nitrogen and phosphorus). Microbes in return receive carbon containing compounds, necessary to support their life and growth, which are produced by the plant's photosynthesis (Denison and Kiers, 2011). The three most important mutualisms are formed between plants and arbuscular mycorrhizal fungi (the AM symbiosis), between different legume species and nitrogen-fixing Rhizobia bacteria (the RL symbiosis) and between certain non-legume "actinorhizal" species and actinomycete bacteria called Frankia (the AR symbiosis) (Parniske, 2008; Oldroyd et al., 2011; Kucho et al., 2010). All three symbioses are based on a commonality: genetic studies have shown that in plants a similar set of genes (common symbiotic pathway or CSP) are required for the formation of the AM, RL and AR symbioses. This similarity suggests a common evolutionary origin of these three mutualisms with the presumed evolution of both the actinorhizal and rhizobial symbioses from the much more ancient mycorrhizal association (Svistoonoff et al., 2014; Markmann and Parniske, 2009; Geurts et al., 2012).

Model plants

For research in the plant field, including plant microbe interaction studies, the use of model plants has led to major advances in the field. For symbiosis two model plants have been proposed (*Medicago truncatula* and *Lotus japonicus*) and work on symbiosis also uses model plants developed for more general plant studies (*Arabidopsis thaliana* and *Nicotiana benthamiana*).

For symbiotic studies

Medicago truncatula

Medicago truncatula Gaertn belongs to the Fabaceae family, Faboideae sub-family, Trifolieae tribe. *M. truncatula* was selected as a model plant for several reasons, among them is its rapid life cycle, small diploid genome (~5×10^8 bp) which was recently sequenced from the cultivar Jemalong, line A17 (Young et al., 2011), self-fertile nature, possibility for its genetic transformation (Barker et al., 1990; Cook, 1999). It possesses the ability to form symbiotic associations with both Rhizobia, resulting in the development of indeterminate nodules containing an active apical meristem (*Sinorhizobium meliloti*- genome was sequenced (Galibert et al., 2001)), and AM fungi. *M. truncatula* symbiotic relations with bacterial and fungal symbionts have been studied for many years which has led to the identification of genes required for establishment of both or either one of the symbiotic associations (Cook, 1999; Oldroyd et al., 2011).

Lotus japonicus

Belonging to the Fabaceae family *Lotus japonicus* owns a small genome (400 Mb), self-fertile nature, short life cycle (3-4 months) and can be easily transformed with Agrobacterium (Handberg and Stougaard, 1992). Being able to form both rhizobial and arbuscular mycorrhizal symbioses *L. japonicus* became a model plant used to study these symbioses. It forms determinate nodules with *Mesorhizobium loti.* As for *M. truncatula* a set of symbiotic genes has also been identified for *L. japonicus* (Sato and Tabata, 2006; Madsen et al., 2010).

For non-symbiotic studies (plant development, interactions with pathogens)

Arabidopsis thaliana

Arabidopsis thaliana belongs to the Brassicaceae family and does not form either the bacterial or fungal symbioses. *A. thaliana* owns several features that make it an excellent experimental model for studying plant development. It possesses one of the smallest plant genomes of about 125 Mb. Its life cycle is short (approx. 6 weeks) and results in high yields of produced seeds. *A. thaliana* can be efficiently transformed with *Agrobacterium tumefaciens* and a large number of mutant lines and ecotypes already exist and are available.

A. thaliana is studied by a broad research community and all arising information is collected in the opened for public access- Arabidopsis Information Resource (TAIR-http://www.arabidopsis.org/).

Nicotiana benthamiana

Nicotiana benthamiana belongs to the *Solanaceae* family. *N. benthamiana* is susceptible to a large number of plant viruses and other pathogens such as bacteria, oomycetes and fungi and thus is widely used in plant virology and for host–pathogen interaction studies. For the reason that its large leaves can be easily transformed with high efficiency with *Agrobacterium tumefaciens, N. benthamiana* is often used for transient protein expression and functional characterization (Goodin et al., 2008).

The Arbuscular mycorrhizal symbiosis

The AM symbiosis is suggested to have appeared approximately 460 million years ago (mya) and is currently wide-spread, affecting 70–90% of all terrestrial plants in the plant kingdom, including angiosperms, gymnosperms, pteridophytes, and some bryophytes (Harrison, 2005). AM fungi are a major contributor to the enhancement of plant nutrition with phosphorus, a mineral compound which is essential for plant growth, health, and productivity (Parniske, 2008). It has been reported that, through the AM symbiosis, all the phosphorus taken up by the plant could originate from its fungal symbiont (Smith et al, 2003). Mycorrhizal fungi, although being unable to fix atmospheric nitrogen, are however able to improve host nutrition with nitrogen and other minerals. AM fungi are obligate

biotrophs, depending entirely for their carbon nutrition on the host plants. Plants can use 4–20% of their photosynthate compounds to support AM fungi (Bago et al., 2000). Phylogenetically all AM belong to a single Glomeromycota phylum (Harrison, 2005), which currently contains more than 150 species (da Silva et al., 2008). Those studied to date (for example *Rhizophagus irregularis* and *Gigaspora* spp.) do not show host specificity as they can colonize a wide range of plants in laboratory conditions.

Development of the AM symbiosis

In the soil AM fungi exist in the form of spores. Germination of the spores and hyphae growth can occur in the absence of host plants, however these two processes can be notably intensified in the presence of root exudates and volatiles, including CO_2 (Harrison, 2005). Attracted by the plant, the hyphae grow through the soil toward the host root, where they differentiate and form a special penetration organ called the appressorium or hyphopodium. Formation of the appressorium initiates intracellular changes in the adjoining plant cells, aimed at preparing for fungal penetration. Thus within 4-5 hours after attachment of AM fungi the plant develops the so called prepenetration apparatus (PPA), a cytoplasmic tunnel crossing the vacuole of the cell aimed to direct the growth of fungi after its penetration (Genre et al., 2008). Once the PPA is formed, fungal hyphae invade the host root and grow intra and intercellularly towards the inner cortex. Next the hyphae penetrate the cortical cells and form branched tree-like structures, the so-called arbuscules, which are used for nutrient exchange with the host plant. Formed inside of the cell, arbuscules stay separated from the cytoplasm being surrounded with the extended plant plasma membrane. Newly formed arbuscules stay functional for only a few days after which they get degraded without harming the plant cell which can later host another arbuscule (Harrison, 2005; Parniske, 2008) (Fig.1)

The Rhizobia-legume symbiosis

To support their growth, most plants acquire nitrogen from the soil in the biologically active forms of nitrate and ammonia. Despite gaseous nitrogen (N_2) being the most abundant component of the Earth's atmosphere (78%) its biologically available forms are present in very limited concentrations. However, certain bacteria (termed diazotrophs) have acquired the ability to fix gaseous nitrogen and use it to support their growth. Some plants, mainly belonging to the large Fabaceae (formally Leguminoseae) family, have developed a beneficial symbiosis with soil diazotrophic bacteria, termed Rhizobia, that can convert dinitrogen into ammonia and thereby supply its host plant with this mineral (Oldroyd, Murray, 2011). Rhizobia are unicellular gram-negative bacteria which in contrast to AM fungi are phylogenetically diverse, with members belonging to both the alpha- and beta- proteobacteria (Masson-Boivin et al., 2009). The most widely studied species belong to the *Rhizobium*, *Mesorhizobium*, *Sinorhizobium* (also known as *Ensifer*), or *Bradyrhizobium* genera of alpha-proteobacteria. Each Rhizobia possesses host specificity and can establish a symbiotic association with either a few or several legume species (Perret et al., 2000), and also with one tropical

Labels in figure:
- Spore
- Mutual recognition 'presymbiotic phase'
- Strigolactone
- Myc factor
- Formation of PPA
- Fungal penetration
- Hyphopodium
- Calcium spiking
- Nucleus
- Arbuscule
- Plant root
- Epidermis
- Outer cortex
- Inner cortex
- Endodermis
- Vascular cylinder

Nature Reviews | Microbiology
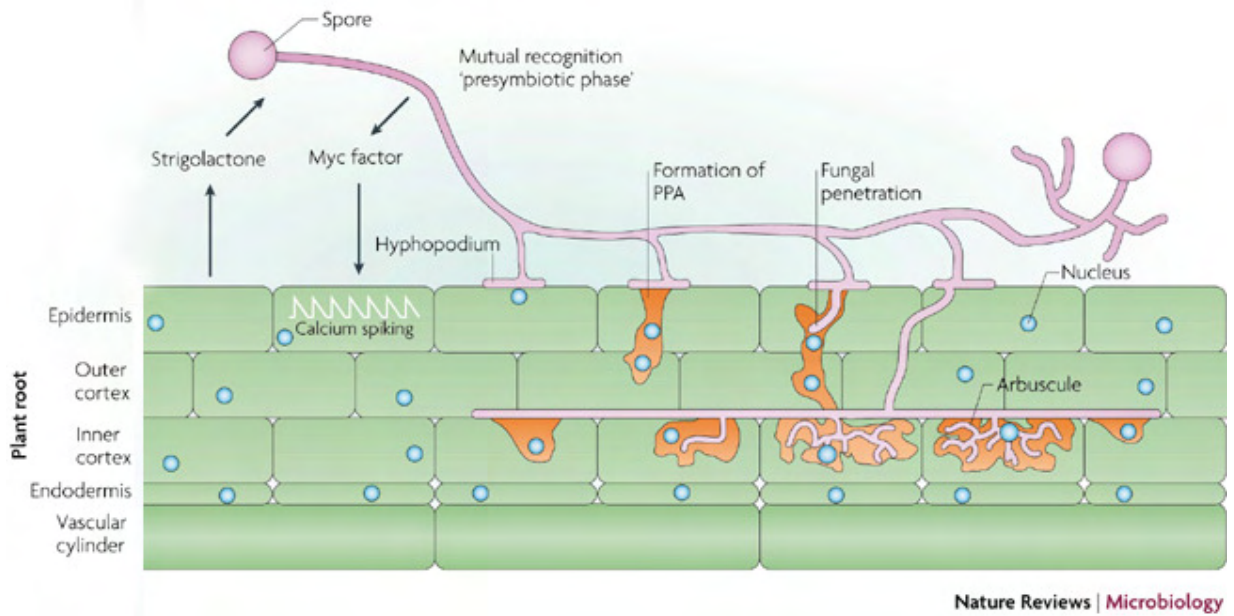
Fig.1 The different steps leading to the establishment of arbuscular mycorrhizal symbiosis.

In response to strigolactones, the spore germinates and the hypha grows towards the host root to form a fungal appressorium. After the formation of the prepenetration apparatus (PPA) by the plant, the fungal hypha penetrates the PPA and is guided towards the inner cortex where it branches to form arbuscules (adapted from (Parniske, 2008)).

tree *Parasponia andersonii* belonging to the Ulmaceae family (Op den Camp et al., 2012). The rhizobial symbiosis usually results in the development of root nodules, organs in which bacteria convert atmospheric nitrogen into ammonia, which is then assimilated by the plant. Similarly to the AM symbiosis, in return the plant provides the micro-symbiont with carbohydrates produced by photosynthesis. Nodules formed by different legumes can be divided into two major types according to their structural organization. *Phaseolus vulgaris*, *Lotus japonicus* and *Glycine max* form determinate nodules which are spherical in shape and lack a permanent meristem. *Medicago truncatula*, *Pisum sativum* and *Trifolium* form indeterminate nodules that are elongated and cylindrical in shape and contain a permanent apical meristem that continually generates new nodule cells which become infected by the Rhizobia present in the infection zone of the nodule (Oldroyd et al., 2011).

Being beneficial for both partners the symbiotic state is however not obligatory for either the host plants or for Rhizobia (Segovia et al., 1991). However this symbiosis is very important in both natural and agricultural ecosystems. Thus, for example, the list of important crops forming the rhizobial symbiosis includes *Glycine max* (soybean), *Phaseolus vulgaris* (common bean), *Pisum sativum* (pea), *Medicago sativa* (alfalfa), *Cicer arietinum* (chickpea), *Arachis hypogaea* (peanut) and a number of *Lupinus* species.

Development of the RL symbiosis: example of indeterminate nodule formation

To initiate the RL symbiosis, bacteria produce signal molecules which stimulate symbiotic responses in plant cortical cells provoking the formation of pre-infection threads (PIT), similar to the mycorrhizal PPA cytoplasmic tunnels crossing the cells. The signals also stimulate cell division in the inner cortex and pericycle, leading to the formation of the nodule primordium. Bacteria can enter the host root intracellularly through root hairs, by intercellular penetration (crack entry) or via intercellular infection (Oldroyd et al., 2011; Gage, 2004). Invasion through root hairs is the most common mode of rhizobial infection, for most of the agronomically important legumes. In this case, the bacteria signal to the root hair to trigger its deformation, ultimately resulting in the formation of a tight curl (shepherd's crook), surrounding and entrapping the Rhizobia which then divide to form a microcolony. Once such an infection pocket is formed, this initiates the development of an infection thread (IT), a special tubule that grows inside of the root hair that allows Rhizobia to reach and colonize the nodule primordium. IT formation starts with the degradation of the cell wall inside of the curl due to bacterial or/and plant enzymatic activities and allows invagination of the cell membrane. The invaginated membrane and newly deposited cell wall material forms the infection thread which continues its growth down through the root hair to the root epidermis, due to pressure from the dividing bacteria which thus continuously lead to extension of the tubule. Infection threads progress down through the cortical PITs and infect the divided cells of the nodule primordium. At this stage the outer cells of the nodule primordium form the nodule meristem, which continues its growth leading to the developing nodule emerging from the root. In the mature nodule the apical, distal meristem is followed by an infection zone in which infection threads are releasing bacteria into the cytoplasm,

surrounded by a plant membrane. Staying inside the nodule cells, the bacteria differentiate morphologically into a specific cell type, called bacteroids, which are capable of fixing dinitrogen (Timmers et al., 1999; Gage, 2004; Masson-Boivin et al., 2009; Oldroyd et al., 2011) (Fig.2).

Actinorhizal symbiosis

The acinorhizal symbiosis is formed between a nitrogen-fixing gram positive actinomycete called Frankia and roots of dicotyledonous plants belonging to eight plant families *Betulaceae, Casuarinaceae, Myricaceae, Elaegnaceae, Rhamnaceae, Rosaceae, Coriariaceae, Datisticaceae* and 25 genera (Pawlowski and Demchenko, 2012). Similarly to Rhizobia, in the AR symbiosis Frankia supplies the host plant with biologically-fixed nitrogen and, in return, obtains carbon compounds produced by the plant. Fixation of nitrogen occurs in the nodules formed on the host plant roots after their infection with Frankia. Actinorhizal nodules consist of several lobes each representing a modified lateral root lacking a root cap and containing infected cells in the cortex. Frankia is not an obligate biotroph and can exist in the soil in a free-living state in three cellular forms, filaments, nitrogenase-containing vesicles and multilocular sporangia (Wall, 2000).

Development of AR symbiosis

Frankia enters the root either through the root hairs or via intercellular infection. Invasion through the root hairs develops in a similar way as in the rhizobial symbiosis consisting of such steps as root hair curling and infection/pre-infection thread formation. Simultaneously with the infection thread progression cell divisions are induced in the cells of the outer cortex. Newly formed tissue becomes next infected with the bacteria which differentiate after being released into the nitrogen fixing vesicles. This newly formed structure is typical and specific for some actinorhizal plants and is called the pre-nodule. Cell divisions in the pericycle then give rise to the nodule primordium. Growing through the root, the future nodule merges with the pre-nodule tissue (Fig.3) (Wall, 2000; Kucho et al., 2010).

Plant and Microbial signal molecules required for establishment of AM, RL and AR symbioses

Signals released during AM symbiosis

It is suggested that the release of carotenoid-derived hormones strigolactones by the host plants underlies their ability to stimulate formation of the AM symbiosis. This statement arises from the positive effect of strigolactones on AM fungi metabolism (Besserer et al., 2006) and hyphal branching (Akiyama et al., 2005). Strigolactones may form a concentration gradient in the rhizosphere and are hypothesized thereby to either attract the AM fungi to the proximity of a host root (Parniske, 2005) or to direct it to suitable special penetration zones of the root (Kretzschmar et al., 2012).

A number of studies have shown that AM fungi produce diffusible signals which stimulate different plant symbiotic responses (Kosuta et al., 2003; Weidmann et al., 2004; Olah et al., 2005; Gutjahr et al., 2009; Kuhn et al., 2010). Recently two related types of symbiotic signal molecules were
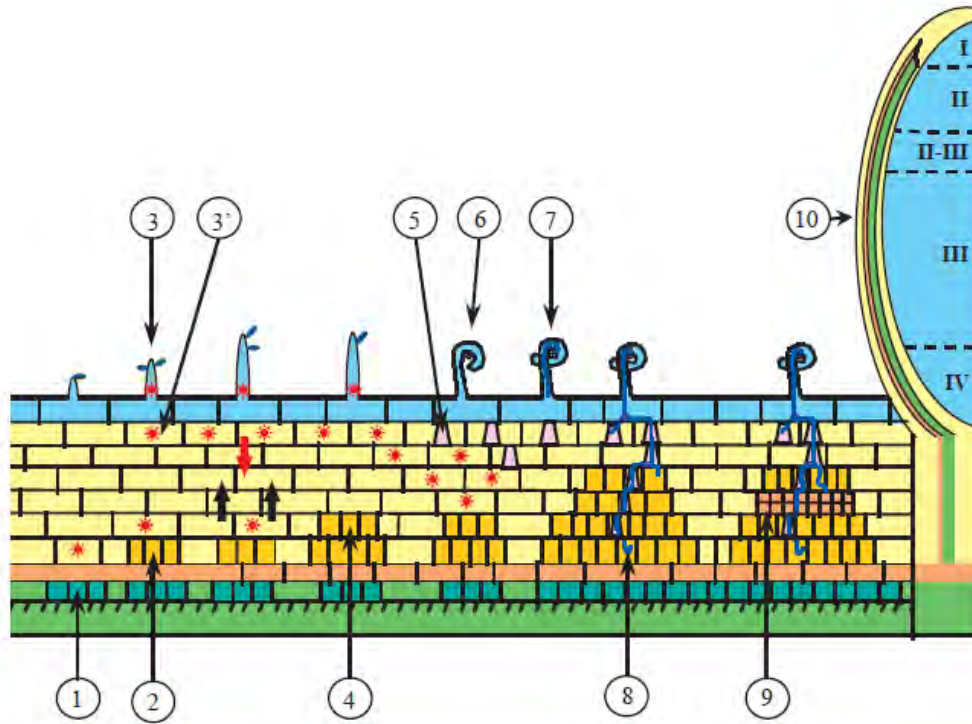
Fig.2 The different steps in the establishment of symbiosis between *Medicago truncatula* and *Sinorhizobium meliloti*.

Following inoculation, molecular and morphological responses occur simultaneously in the epidermis and in internal tissues of the root: microtubular cytoskeleton rearrangements and corresponding cellular changes in the pericycle (1); activation of cells in the inner cortex and formation of the first division which will lead to the nodule primordium (2); activation of root hairs (3) and of outer cortical cells (3'); activation of the middle cortex and extension of the nodule primordium (4); formation of pre-infection threads (5); root hair curling (6); formation of infection threads (7); growth of the infection threads towards the nodule primordium (8); formation of the nodule meristem from middle primordial cells (9); growth and emergence of the nodule (10). Adapted from (Timmers *et al.*, 1999).

identified for *Glomus intraradices* (*Rhizophagus irregularis*) (Maillet et al., 2011; Genre et al., 2013). The first class of compounds, extracted from mycorrhized roots and spores, and named Myc-LCOs are structurally similar to Nod factors produced by Rhizobia (see next section) and consist of tetrameric or pentameric N-acetyl glucosamine backbones with C16:0 or C18:1 N-acyl chains attached to the non-reducing sugar. On the reducing terminal sugar Myc-LCOs can be decorated with a sulphate group (Fig.4A). Myc-LCOs were shown to stimulate mycorrhization in legume (*M. truncatula*) and non-legume (*Tagetes patula* and *Daucus carota*) species, induce symbiotic gene expression (ENOD11) and influence root architecture (root branching). Whether the synthesis of Myc-LCOs is stimulated by strigolactones, has not yet been shown.

Other signal molecules were detected in the exudates of germinated *G. intraradices* spores and found to be short-length chitin oligomers, CO-IV and CO-V. These compounds were shown to activate such symbiotic response (response typically activated by Nod factors) as nuclear Ca^{2+} spiking in the *M. truncatula* root epidermis (Genre et al., 2013; Sun et al., 2015). Production of these signal molecules was enhanced in the presence of strigolactones.

Because of the coenocytic nature of AM fungi and the absence of genetic tools, the genes determining the production of AM symbiotic signals remain unknown (Sanders and Croll, 2010). It is hypothesized that production of an array of different LCOs and COs by one AM fungi might explain their ability to form associations with a wide variety of plant species in which case different plants could recognize different signal molecules in the mixture (Oldroyd, 2013).

Signals released during RL symbiosis

To establish most rhizobial symbioses a set of bacterial genes is required (called *nod*, *nol*, or *noe* genes) which are activated by plant diffusible molecules (for example, flavonoids) secreted by the host plant roots (Hassan and Mathesius, 2012). For these Rhizobia, it is known that flavonoids or other signal molecules are recognized by bacterial NodD receptor proteins which then activate transcription of the other nodulation genes. Each *Rhizobium* species owns its individual set of nodulation genes determining its host-specificity (for example *nodE, F, H, L, P* and *Q*) and five *nod* genes which are common for all Rhizobia, *nodA*, *B*, *C*, *I* and *J*. These genes encode enzymes involved in the synthesis of the so called Nod factors, which were identified to be lipo-chitooligosaccharides (LCOs) (D'Haeze and Holsters, 2002). *NodA*, *B* and *C* are in charge of chitooligosaccharide backbone synthesis, whereas *nodI* and *J* are involved in LCO secretion. Nod factors produced by Rhizobia generally consist of 4-5 N-acetyl glucosamine (GlcNAc) residues connected via β1–4 -glycosidic bonds, with an N-acyl chain attached to the C2 of the non-reducing terminal sugar. Different Rhizobia strains produce Nod factors varying in their acyl chains structures (level of saturation and the length) and in the chemical substitutions on the sugar residues (such as methyl, fucosyl, acetyl or sulphate groups) (Dénarié et al., 1996; D'Haeze and Holsters, 2002) (Fig. 4B). Studies performed on bacterial mutants producing defective Nod factors have demonstrated that Nod factor structural individuality is crucial for the symbiotic association between bacteria and their host plants. For example, production of sulphated
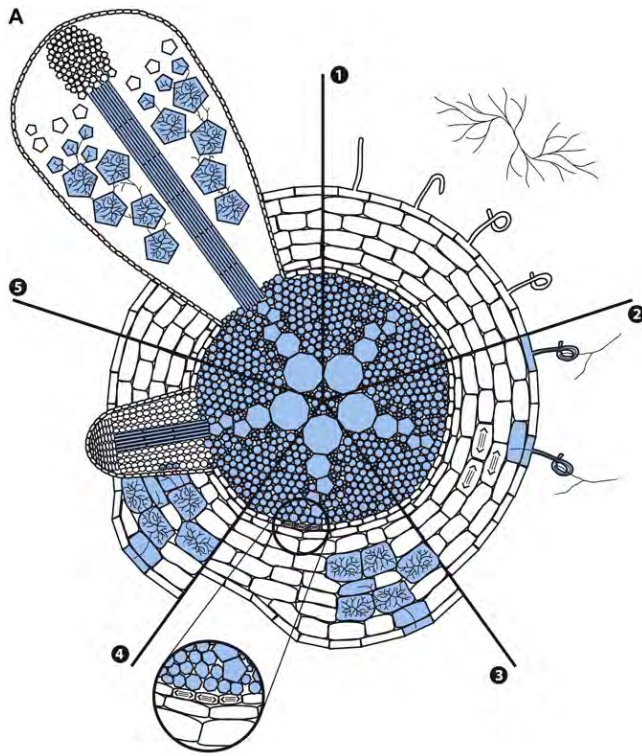
Fig.3 Steps in the development of actinorhizal symbiosis.

Symbiosis with Frankia is formed in several steps: Signal exchange between the actinorhizal plant and Frankia with following root hair deformation and infection (1); penetration of Frankia into a deformed root hair and elicitation of cortical cell divisions (2); infection of dividing cortical cells and formation of a prenodule (3). Simultaneously with prenodule, nodule primordium is formed by pericycle cell divisions. Frankia coming from the prenodule infects the nodule primordium (4). Formation of mature nodules (5). Adapted from (Peret, Swarup, Jansen *et al.*, 2007).

Nod factors by the *nodH* gene is the major determinant of host-specificity of *S. meliloti* for *Medicago truncatula*. In plants Nod factors applied at very low concentrations (10^{-12} M), were shown to trigger a number of symbiotic responses such as root hair curling, induction of early nodulin (ENOD) genes, calcium spiking, nodule primordium and lateral root formation.

Surprisingly a few symbiotic photosynthetic Rhizobia were reported to lack the genes required for Nod factor biosynthesis. The ability of these bacteria to colonize their host plants and form nodules suggests that these Rhizobia are either bypassing this signaling step or are producing signals other than LCO for symbiosis establishment (Giraud et al., 2007).

Signals released during AR symbiosis

It is believed that actinorhizal plants produce flavonoid signal compounds which being recognized by Frankia are provoking its growth toward the host root system (Hocher et al., 2011a). For the actinorhizal symbiosis it was shown that factors, inducing root hair deformation, were present in Frankia culture surpernatants (Popovici et al., 2010). Absence of *nod* genes in three sequenced Frankia genomes may suggest that actinorhizal symbiotic factors possess different structures than Nod factors produced by Rhizobia (Hocher et al., 2011a). However studies of other Frankia species need to be made to reinforce this conclusion.

Common Symbiotic Pathway

As mentioned earlier, genetic analyses of symbiotic mutants performed on model legumes *M. truncatula* and *L. japonicus* have revealed set of genes crucial for development of both the AM and RL symbioses. Proteins encoded by these genes form a signal transduction pathway, the so called common symbiotic pathway (CSP) (Fig.5) (Kouchi et al., 2010). Most of the CSP genes were also identified in *C. glauca* and *A. glutinosa*, two actinorhizal plant species, and some of these genes have been shown to be required for establishing the AR symbiosis, showing that AR symbiotic signaling also proceeds through the CSP (Gherbi et al., 2008, Hocher et al., 2011b).

One of the earliest plant symbiotic responses determined by the proteins of the CSP is the oscillation of cytosolic Ca^{2+} (Ca^{2+} spiking) appearing in the perinuclear region of root epidermal cells. It was shown that Ca^{2+} spiking is induced by Nod factors and both Myc LCOs and CO-IV produced by AM fungi and is also presumed to be stimulated by AR signal molecules (Liang et al., 2014; Genre et al., 2013; Hocher et al., 2011b). Based on the studies performed with different symbiotic mutants, genes of the CSP could be divided into two groups depending on their relation to Ca^{2+} spiking. The first group acts upstream of calcium oscillations and is believed to control the process of spiking. This group consists of the plasma membrane located leucine-rich repeat receptor kinase, LjSYMRK in *L. japonicus* or MtDMI2 in *M. truncatula* and cation channels located in the nuclear membrane, LjCASTOR and LjPOLLUX or MtDMI1. The exact mode of action is not yet defined for SYMRK/DMI2. However, interaction studies have led to a preliminary model which could explain the way this plasma membrane protein communicates with nuclear cation channels and coordinates

A.
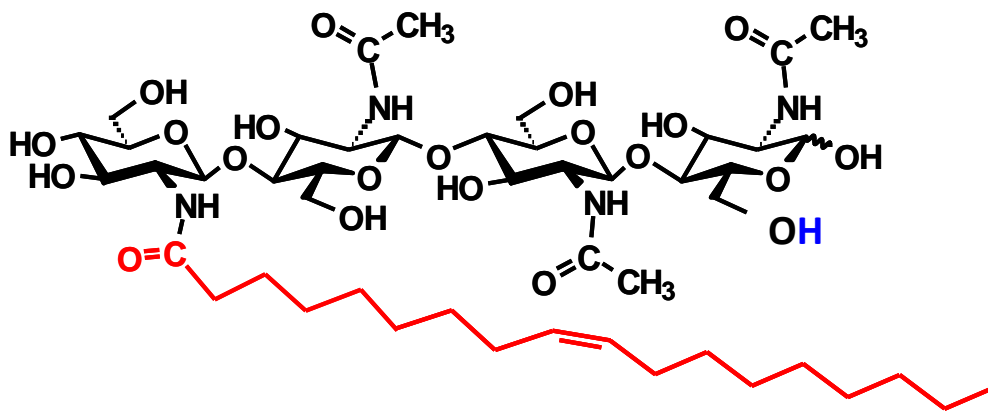
B.
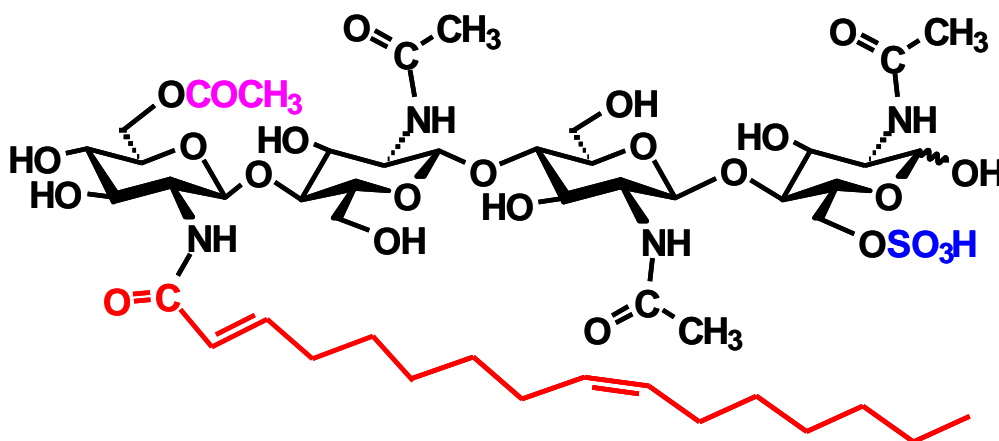
Fig.4 Chemical structures of Nod factors and Myc-LCOs.

(**A**) One of the major Myc-LCOs produced by *Rhizophagus irregularis* (LCO-IV (C18:1 Δ9)) which was shown to stimulate mycorrhization. (**B**) Major Nod factor produced by *Sinorhizobium meliloti* (LCO-IV (Ac, S, C16:2 Δ2,9)) crucial for the establishment of the symbiosis between *M. truncatula* and its symbiont.

calcium spiking. It was shown that SYMRK/DMI2 can interact with 3 hydroxy-3 methylglutaryl-CoA reductase (HMGR) (Kevei et al., 2007). This enzyme catalyzes a key step in the synthesis of mevalonic acid (mevalonate) a precursor molecule from the so called mevalonate biosynthetic pathway. This pathway gives a rise to multiple isoprenoid compounds including phytosteroids. It is hypothesized that association of DMI2 with HMGR may result in the activation of this enzyme and the production of isoprenoids, which could be involved in signal transduction between DMI2 and DMI1. Additionally SYMRK/DMI2 was shown to interact with a mitogen-activated protein kinase kinase (MAPKK- SIP2) that could also play a role in signal exchange between plasma membrane-associated DMI2 and nuclear membrane associated ion channels (Chen et al., 2012). Both HMGR and SIP2 were shown to play essential roles in the development of the RL symbiosis. Presumed to be controlled by DMI2, cation channels LjCASTOR/LjPOLLUX or MtDMI1 were shown to serve for regulating potassium flow and thus are expected not to be involved directly in calcium release. It is hypothesized that DMI1could trigger the opening of calcium channels or act as a counter ion channel compensating the charge produced during the movement of calcium. These calcium channels are not yet identified, however the first calcium pump involved in symbiotic calcium signaling, MCA8 was found for *M. truncatula* (Capoen et al., 2011). In *L. japonicus* two nucleoporins NUP85 and NUP133 were shown to be required for Ca^{2+} spiking although their mode of action is not yet understood (Saito et al., 2007).

Mutants in these common symbiotic genes are impaired in calcium spiking and are defective in AM and RL symbioses (Parniske, 2008).

Downstream of calcium spiking acts the second group of CSP genes which are involved in the perception of the calcium oscillations. This group consists of nucleus-localized calcium and calmodulin dependent protein kinase (CCaMK or MtDMI3). CCaMK /DMI3 gets activated by calcium which either can be bound directly to the EF hand motifs at the C terminus of the protein or in a complex with calmodulin (CaM) to the CaM-binding domain of CCaMK /DMI3. Activated CCaMK next phosphorylates a coil coiled protein LjCYCLOPS or MtIPD3, which acts as a transcriptional activator (Singh et al., 2014).

The components of the CSP are required for both RL and AM symbioses. Specificity for establishing each of these two mutualisms is believed to be determined both upstream and downstream of the CSP. Downstream of DMI3/IPD3 several transcription factors have been shown to be involved either primarily in nodulation, NSP2 and NSP1 (driving next expression of two additional transcription factors with nodulation specific functions NIN and ERN1) or mycorrhization, NSP2 and RAM1 (driving expression of the gene specific for mycorrhization, RAM2) (Oldroyd, 2013; Venkateshwaran et al., 2012). In addition, specificity for the rhizobial symbiosis is also conferred by a pathway that operates in parallel to the CSP, composed of genes specific for infection (such as PIR/NAP/CERBERUS). Cross-talk between the two pathways is ensured at the level of CYCLOPS/IPD3 (Madsen et al., 2010). The fact that mutants in the common SYM genes were still able to respond to the addition of Nod factors (rapid calcium influx and swelling of root-hair tips) suggested that these signal molecules were recognized by receptors placed upstream of the CSP.
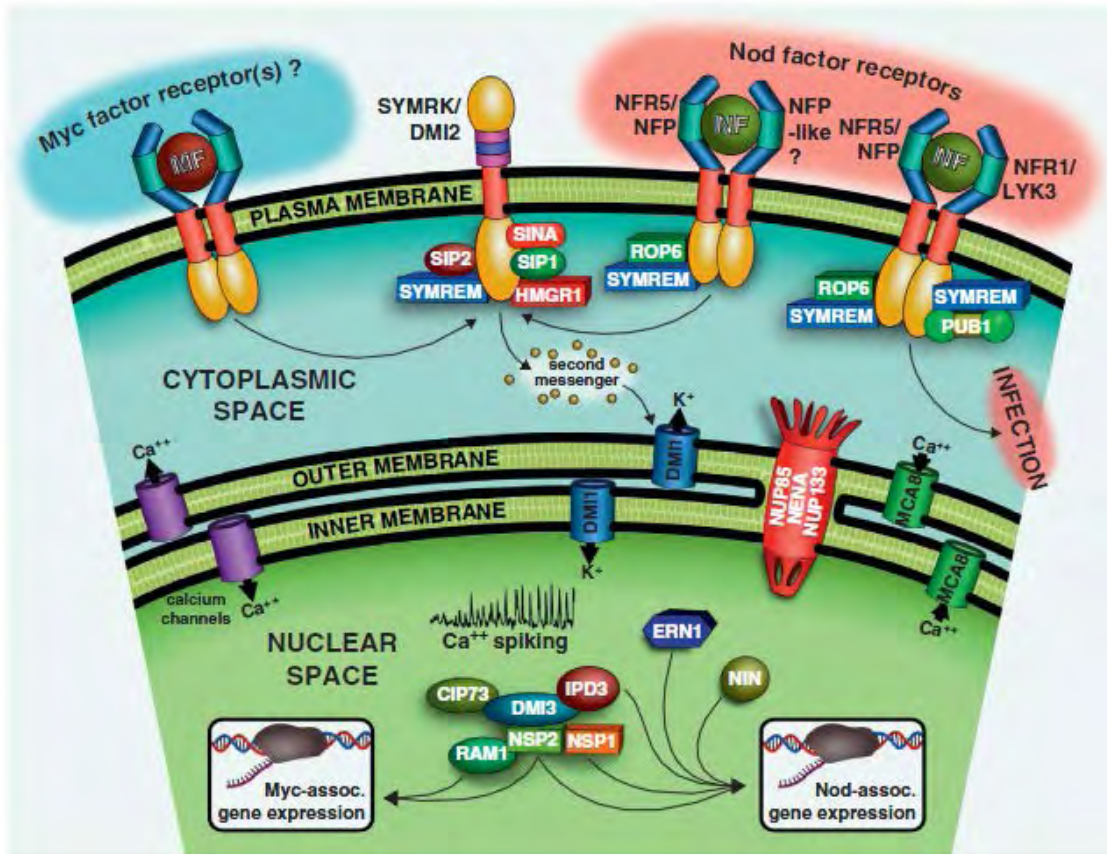
Fig.5 Model describing the receptors involved in LCO perception and the components of CSP.

This scheme proposed by (Venkateshwaran *et al.*, 2012) shows the perception of Nod factors by LjNFR5/MtNFP and LjNFR1/MtLYK3 in case of rhizobial symbiosis and unknown receptors for Myc-LCOs, the signal transduction through the plasma membrane localized LRR-receptor kinase, SYMRK/DMI2 the first component of CSP, and the downstream signaling to the nuclear ion channel CASTOR,POLLUX/DMI1 and calcium pump MCA8 which are triggering calcium spiking resulting in the activation of the calcium/calmodulin-dependent protein kinase, CCaMK /DMI3, which then coordinates the expression of symbiotic genes, determining either nodulation or mycorrhization (For detailed description see the text).

Through studies of *Medicago truncatula* and *Lotus japonicas* lysin-motif receptor-like kinases (LysM-RLKs) crucial for the rhizobial symbiosis were identified (Cullimore and Dénarié, 2003). This family of receptors has now also been implicated in the AM symbiosis and in pathogen responses as described below.

Perception of symbiotic signals by plant LysM RLKs

Forward genetic studies performed on *L. japonicus* symbiotic mutants impaired in Nod factor responses led to the identification of plasma membrane located Nod Factor Receptors, LjNFR1 and LjNFR5 (Madsen et al., 2003; Radutoiu et al., 2003). In *M. truncatula* synteny with a region in pea involved in Nod factor recognition identified a cluster of genes including MtLYK3, which is highly similar to LjNFR1 (Limpens et al., 2003). *M. truncatula* MtNFP was later identified from a Nod factor response mutant by homology to LjNFR5 (Arrighi et al., 2006). Later on similar symbiotic receptors were also identified for *Glycine max* (Indrasumunar et al., 2011) and *Pisum sativum* (Zhukov et al., 2008). Structurally these receptors belong to LysM-type receptor like kinases (LysM-RLKs) consisting of an extracellular domain with three Lysin motifs (LysM), which are known to bind GlcNAc containing compounds (Mesnage et al., 2014), a transmembrane region and an intracellular serine/threonine kinase-like domain. Lotus NFR5 and its orthologous protein from *Medicago*, NFP, lack the activation loop in their kinase domains and have been shown to possess so called dead kinases (Oldroyd, 2013; Madsen et al., 2011). In contrast NFR1 and LYK3 possess active kinases required for their symbiotic functioning and capable of auto and trans-phosphorylation (Fig.5) (Fig.6) (Madsen et al., 2011; Klaus-Heisen et al., 2011).

In accordance with symbiotic phenotypes, NFR1 and NFR5 are equally important for early Nod factor responses as well as rhizobial infection and nodulation. Identical mutant phenotypes determined by both receptors have led to the hypothesis of their hetero-oligomerization which was proposed to be required for Nod factor perception and downstream signaling. This suggestion is supported by the fact that transformation of *M. truncatula* with both NFR1 and NFR5 allows it to interact with *Mesorhizobium loti,* which normally nodulates *L. japonicus* (Radutoiu et al., 2007). Recent studies suggest that both NFR1 and NFR5 independently from each other bind Nod factors with nano-molar affinity (Broghammer et al., 2012). Similarly to *NFR5, NFP* mutants are impaired in all symbiotic responses to purified *Sinorhizobium meliloti* Nod factors, infection and nodule organogenesis (Ben Amor et al., 2003). *LYK3* mutants, being defective in proper root hair curling, infection threads formation and progression of CCD, still retain early symbiotic responses such as calcium spiking and root hair deformation, therefore differing from the NFR1 and NFP phenotypes. This suggests that LYK3 serves as an entry receptor for rhizobial infection, whereas NFP acts as a signaling receptor for early Nod factor responses, thus supporting the two-step model of Nod factor perception in *Medicago*, based on studies of *S. meliloti* mutants (Ardourel et al., 1994; Smit et al., 2007).

Despite NFP being predicted to associate with *S. meliloti* Nod factor by homology modeling
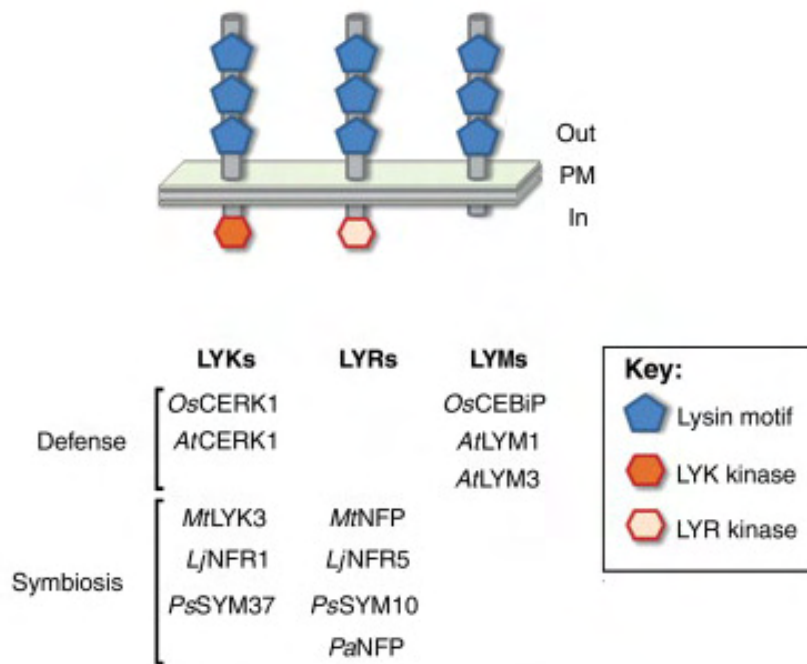
Fig.6 Schematic representation of plant lysin motif (LysM) proteins.

The main three groups of plant LysM proteins: the LysM Receptor Like Kinases (LysM-RLK) involved in both symbiosis and immunity possessing either an active kinase (LYKs) or a dead kinase (LYR); defense related GPI-anchored LysM proteins lacking intracellular kinase domains (LYMs). Abbreviations: PM, plasma membrane. Adapted from (Gust, Willmann, Desaki *et al.*, 2012).

and docking, (Mulder et al., 2006), to date no direct binding was demonstrated for Nod factors to either NFP or LYK3 (Bono et al. unpublished). The inability to bind LCO may suggest that NFP and LYK3 undergo hetero-oligomerization or complex formation with another receptor which is capable to bind LCOs. The existence of an additional yet unidentified Nod factor binding protein in *M. truncatula* was also suggested from a MtNFP/PsSYM10 domain swapping study showing that MtNFP/PsSYM10 do not discriminate sulphated and non-sulphated Nod factors (Bensmihen et al., 2011). A recently identified in *M. truncatula* LCO binding LysM RLK, LYR3 (Fliegmann et al., 2013) could be a good candidate for such a co-receptor (see chapter I).

Like NFR1 and NFR5, there is evidence that LYK3 and NFP functionally interact with each other. This is suggested from the hypersensitive response observed in case of their co-expression in *N. benthamiana* leaves (Pietraszewska-Bogiel et al., 2013). The recent demonstration that LYK3 and NFP hetero-oligomerization only occurs in specific nodule cells preparing for infection, has led to the suggestion that their interaction needs to be carefully regulated to avoid defense responses (Moling et al., 2014). The involvement of LYK3 in partner specificity is evident from studies in which plants with silenced LYK3 or weak LYK3 mutants (*hcl-4*) were shown to have reduced nodulation with *nodL* and *nodFE S. meliloti* mutants (Limpens et al., 2003; Smit et al., 2007). Interestingly in *M. truncatula* host specificity determined by LYK3 was suggested to be partly dependent on its interaction with an E3 ubiquitin ligase, PlantU-box protein 1 (PUB1), because RNAi *PUB1* plants were shown to be better nodulated by *nodL* and *nodFL* mutants in comparison to wild-type plants (Mbengue et al., 2010). In *M. truncatula* NFP has also been shown to play a role in plant immunity (Gough and Jacquet, 2013), which has led to the suggestion that it may play an adapter role in different protein complexes.

Neither NFR5 and NFP nor NFR1 and LYK3 are essential for mycorrhization. However Myc LCOs, produced by AM fungi, were shown to trigger symbiotic responses partially dependent on NFP (Maillet et al., 2011). Additionally a potential ortholog of NFR5/NFP from *P. andersonii* was shown to have a dual function and serve for both nodulation and mycorrhization (Op den Camp et al., 2011). Thus taken together the fact that AM fungi produce symbiotic signals which are recognized by the plants and trigger symbiotic responses, it is hypothesized that specific receptor possessing the ability of Myc LCOs perception should exist. The recent finding that *NFR1/LYK3* mutants are partially defective for mycorrhization, suggests that this receptor may act partially redundantly with other LysM-RLKs for this function (Zhang et al., 2015).

The production of lipo-chitooligosaccharides (Nod factors) by Rhizobia and their following recognition by plant LysM receptor like kinases (LysM-RLK) is proposed as a symbiotic mechanism appropriated by the legume/bacterial symbiosis from the AM association. This hypothesis is firstly supported by the ability of AM fungi to produce Myc-LCOs which are structurally close to Nod factors (Maillet et al., 2011) and secondly by the involvement of plant LysM-RLKs in mycorrhization. In *Parasponia andersonii,* a single gene, NFP, was shown to be necessary for the Parasponia

symbiosis with both Rhizobia and AM fungi (Op den Camp et al., 2011). Interestingly, in *M. truncatula* NFP although being involved in the recognition of the Myc-LCOs is however not essential for AM symbiosis formation (Maillet et al., 2011; Zhang et al., 2015). This may suggest that, in contrast to *Parasponia,* legumes have improved on their inherited AM symbiosis signaling machinery by evolving additional receptors specifically for the perception of Nod factor symbiotic signals. Indeed it has been suggested that the whole genome duplication event occurring approximately 55 mya in the legume family, could have given rise to additional receptors which became specialized for nodulation (Young et al., 2011).

The presence of at least 20 LysM-RLKs in legumes, suggest that this family has evolved for different functions.

Perception of chitooligosaccharides and other PAMPs

Beside perception of symbiotic signals LysM proteins were shown to be in involved in the recognition of several pathogen-associated molecular patterns (PAMPs) such as fungus-derived chitooligosacharides or bacteria- derived peptidoglycans.

The first LysM receptor for chitin, named OsCEBiP (*Oryza sativa* chitin elicitor binding protein), was identified from the plasma membrane of rice cells. By its structure this protein lacks an intracellular kinase domain and consists of an extracellular region with LysM domains, which is attached to the plasmamembrane by a GPI anchor. OsCEBiP was shown to bind chitin and to be essential for chitin responses since its silencing abolished plant defense responses to chitin and decreased plant resistance to pathogenic fungi (Kaku et al., 2006; Kishimoto et al., 2010). Recently a biochemical/structural approach has suggested that CEBiP molecules simultaneously bind to one chitin oligosaccharide, resulting in the dimerization of CEBiP. To transduce the chitin signal, a LysM-RLK called OsCERK1 (*Oryza sativa* chitin elicitor receptor kinase 1) was shown to be essential. This protein does not bind chitin but heterodimerizes with CEBiP, triggering OsCERK1 phosphorylation and activation of plant defense responses (Fig.6) (Shimizu et al., 2010; Hayafune et al., 2014).

Studies performed in *Arabidopsis thaliana* resulted in the identification of AtCERK1 (Miya et al., 2007), which is essential for chitin elicitor signaling. Unlike OsCERK1, the Arabidopsis protein binds chitin and crystallization studies have demonstrated that chitin gets accommodated by its second LysM domain (Liu et al., 2012) leading to homo-oligomerization. The affinity of AtCERK1 for chitin is quite low and recently another Arabidopsis LysM-RLK, AtLYK5 has been identified, possessing much higher affinity binding to chitin. Carrying an inactive kinase domain AtLYK5 has been shown to interact and trigger phosphorylation of AtCERK1, which then activates plant defense responses (Cao et al., 2014; Miya et al., 2007; Wan et al., 2008). A third *A. thaliana* LysM-RLK, AtLYK4, may act together or redundantly with AtLYK5, as absolute loss of chitin defense responses is obtained only through simultaneous mutation of AtLYK4 and AtLYK5 (Cao et al., 2014). Additionally chitin binding was demonstrated for the AtLYM2 protein which is closely related to OsCEBiP, however in Arabidopsis this protein is not essential for the activation of plant defense

responses but controls chitin triggered immunity at the level of the intercellular communication via plasmodesmata (Shinya et al., 2012; Faulkner et al., 2013).

Recently two *A. thaliana* LysM receptors, LYM1 and LYM3, were shown to bind directly bacterial peptidoglycan (PGN) and determine plant defense responses triggered by this elicitor (Willmann et al., 2011). Both LYM1 and LYM3 are structurally similar to OsCEBiP/AtLYM2 consisting of three LysM domains in the extracellular regions and lacking a kinase domain. Single *lym1* and *lym3* mutants were shown to have identical phenotypes possessing enhanced susceptibility to bacterial infection. This suggests that LYM1 and LYM3 are not functionally redundant and together are probably forming a PGN recognition complex. Interestingly AtCERK1 was shown to be also involved in PGN-triggered immunity being however unable to bind PGN. In the proposed model of PGN recognition LYM1 and LYM3 heterodimerize after PGN perception and then interact with AtCERK1 resulting in its activation and elicitation of plant defense responses.

In addition to LysM-RLKs plants carry many other RLKs (over 200 in Arabidopsis) which are evolutionarily related by possessing similar kinase domains, but in which the trans-membrane region is linked to different classes of ECDs (Shiu and Bleecker, 2001). Among them the best studied are two leucine- rich repeat receptors (LRR-RLKs) of *A. thaliana,* AtFLS2 receptor for bacterial flagellin (Chinchilla et al., 2006) and AtEFR receptor for bacterial elongation factor EF-TU (Zipfel et al., 2006). In case of FLS2 it was shown to bind bacterial flagellin-derived peptide ligand flg22 together with its co-receptor LRR-RLK AtBAK1. Perception of flg22 was shown to trigger FLS2 hetero-dimerization with BAK1 leading to FLS2 activation and subsequent appearance of plant defense responses (Sanchez-Vallet et al., 2015). A similar mechanism of ligand perception (elf18) with BAK1 as a co-receptor was demonstrated for AtEFR receptor (Roux et al., 2011).

Binding of specific elicitors to their ECDs can be used for the creation of chimeric proteins which are allowing to enlarge the number of biological responses which could be triggered by particular signal molecules. Thus, for example, several chimeric receptors were created by exchanging the ECDs between the AtCERK1, EFR and FLS2 proteins (De Lorenzo et al., 2011; Wang et al., 2014) (see chapter II).

Objectives of the thesis

As described in the introduction, perception of LCO signal molecules plays a crucial role in the rhizobial symbiosis and is thought to be also required for the establishment of the mycorrhizal symbiosis. To date two genetically identified receptors NFP and LYK3 were clearly shown to be involved in LCO perception, however neither appears to bind these signal molecules directly. Together with the unknown mode of LCO perception, the biochemical functioning of LYK3 and NFP is unclear.

Recently identified with a biochemical approach, the *M. truncatula* LYR3 protein possesses high affinity binding to Nod factors and Myc-LCOs versus COs, thus it is presumed to have a specific symbiotic function. However, to date its biological role in the two symbioses remains unclear. Also it is not known whether orthologs of LYR3 are present in other legume species and if the LCO binding ability is conserved among these orthologs.

Thus, to improve existing knowledge about the biological and biochemical functioning of NFP, LYK3 and LYR3 the following specific objectives were addressed during my PhD project.

1. **To analyze Nod and Myc- LCO binding to MtLYR3 orthologs from different legume species.**

   This objective addresses whether LCO binding ability is conserved among *M. truncatula* LYR3 protein orthologs from different legume species (*Pisum sativum, Glycine max, Phaseolus vulgaris, Lotus japonicus*) including *Lupinus angustifolius* which is blocked in mycorrhization. This together with the investigation of LYR3 binding specificity towards Nod and Myc LCOs should result in better understanding of the role that the LYR3 protein could play in the rhizobial and mycorrhizal symbioses.
   Furthermore biochemical characterization of LCO binding to LYR3 aiming to understand mode of LCO perception will be performed.

2. **To study if LCO binding by LYR3 might be used for the induction of plant responses in non-legumes.**

   By using a domain-swapping approach, chimeric receptors will be created consisting of the LYR3 extracellular domain fused to the kinase domain belonging to receptors involved in plant defense. Through expression in model plants, the ability of the chimeric receptors to trigger particular defense responses after LCO perception will be examined. This will demonstrate the possibility of using LYR3 to create new applications for LCO.

3. **To study activation by LCOs of NFP and LYK3, using phosphorylation as an activation sign.**

   Playing crucial roles in the rhizobial symbiosis and being partially involved in Myc-LCO

responses and the mycorrhizal symbiosis respectively, NFP and LYK3 are still poorly understood in terms of their relations with LCO. Here we propose to investigate LCO perception by NFP and LYK3 through detection of their phosphorylation after symbiotic treatments.

Chapter I

Molecular Basis of Lipo-chitooligosaccharide Recognition by the Lysin Motif Receptor-like Kinase LYR3 in Legumes

Molecular Basis of Lipo-chitooligosaccharide Recognition by the Lysin Motif Receptor-like Kinase LYR3 in Legumes*

Nikita Malkov[#$1], Judith Fliegmann[#$], Charles Rosenberg[#$], Virginie Gasciolli[#$], Antonius CJ Timmers[#$], Julie Cullimore[#$], Jean-Jacques Bono[#$2]

From [#]INRA, Laboratoire des Interactions Plantes-Microorganismes (LIPM), UMR441, 31326 Castanet-Tolosan, France

[$]CNRS, Laboratoire des Interactions Plantes-Microorganismes (LIPM), UMR2594, 31326 Castanet-Tolosan, France

*Running title: *Lipo-chitooligosaccharide binding to LYR3 in legumes*

To whom correspondence should be addressed: Jean-Jacques Bono, Laboratoire des Interactions Plantes Micro-organismes (LIPM), UMR CNRS-INRA 2594/441, 24 Chemin de Borde-Rouge – Auzeville, 31326 Castanet-Tolosan Cedex, France, Fax: +33-561285061; Tel: +33-561285050; E-mail: Jean-Jacques.Bono@toulouse.inra.fr

_____
___

Background: Medicago Lysin Motif Receptor-Like Kinase LYR3 is a high-affinity binding protein for lipo-chitooligosaccharidic (LCOs) symbiotic signals.

Results: LYR3 from other legumes except lupin bind LCOs and domain swapping/mutagenesis reveals regions required for binding.

Conclusion: Residues in LysM3 of LYR3 play a crucial role in LCO recognition.

Significance: Elucidating the LCO binding mechanisms helps to understand how plants discriminate friends producing LCOs, from foes.

ABSTRACT

In *Medicago truncatula*, the lysin motif (LysM) receptor-like kinase LYR3 has been recently identified as a high affinity binding protein for lipo-chitooligosaccharides (LCOs), i.e. the Nod factors and Myc-LCO signals produced by symbiotic Rhizobia bacteria and arbuscular mycorrhizal fungi respectively. In this work, LYR3 from other legume species has been cloned and characterized in terms of affinity and specificity for the Myc-LCOs and the Nod factors produced by different Rhizobial symbionts. All the LYR3 orthologs, except those from two *Lupinus* species, where no LCO binding could be detected, exhibited binding characteristics similar to those of the Medicago protein: a high affinity for LCO but not for chitooligosaccharides, and no strong selectivity towards the chemical substitutions of the Nod factors which are important for the specific recognition of the rhizobial symbionts. Swapping experiments between each of the three LysMs of the extracellular domain of the *M. truncatula and Lupinus angustifolius* LYR3 proteins revealed the crucial role of the third LysM in LCO binding. Further site directed mutagenesis on this domain identified residues involved in high affinity binding. These studies suggests that LCO recognition by LYR3 might differ from that of chitin perception by structurally-related LysM receptors identified in Arabidopsis and rice, for which ligand binding relies primarily on the second lysin motif.

_____
_

In plant-microbe interactions, lipo-chitooligosaccharides (LCOs)[3], namely rhizobial Nod factors and Myc-LCOs produced by arbuscular mycorrhizal (AM) fungi, are important signaling molecules for establishing two major agricultural and ecological root endosymbioses. Nod factors are essential for the establishment of the nitrogen-fixing symbiosis with legumes, whereas Myc-LCOs stimulate mycorrhization of higher plants (1). Nod factors and Myc-LCOs are LCOs consisting of a chitin backbone made of 4 or 5 β-1,4-linked *N*-acetylglucosamine (GlcNAc) units, in which the nonreducing terminal unit is de *N*-acetylated and *N*-acylated by a fatty acid. Chemical

substitutions on both reducing and non-reducing ends and the length and degree of unsaturation of the fatty acid chain characterize the Nod factors produced by each rhizobial strain and are important determinants of host legume specificity (2). To date only one AM fungus has been studied and it is not clear how the lower diversity of LCOs (3) and the production of related short chain chitooligosaccharides (COs) (4), are involved in the wide host range of these fungi. Beside the symbiotic signals, longer chain COs composed of 6 to 8 GlcNAc units, originating from the cell wall of pathogenic fungi, are involved in plant immunity (5).

How structurally-related LCO/CO signals are perceived, allowing plants to discriminate different friends and foes, is an important question. A major breakthrough has been achieved by the identification of plant lysin motif (LysM)-containing proteins, such as extracellular receptor-like proteins (LYMs) and trans-membrane receptor-like kinases (LysM-RLKs), termed LYKs (LysM domain-containing RLK) or LYRs (LYK-related), as key components of CO and LCO perception (6,7). All these proteins contain three LysMs, each consisting of 40-50 amino acids, separated by linker regions containing two Cys-X-Cys motifs. For chitin and COs, LysM-RLKs (AtCERK1, AtLYK4 and AtLYK5) and a LYM protein (OsCEBiP) have been shown to bind these GlcNAc-containing signals and to be involved in defense responses in Arabidopsis and rice respectively (8-14). Structural studies provided further evidence that the second lysin motif (LysM2) of AtCERK1 and OsCEBiP mediates interaction with the GlcNAc residues (15,16).

Recently, a biochemical approach has identified the LysM-RLK LYR3 of the legume *Medicago truncatula* as a high affinity LCO-binding protein (17). This protein is highly selective for the LCO structure since it exhibited a high affinity (K_d in the nanomolar range) for Nod factors and Myc-LCOs but not for COs (K_d in the micromolar range). Here we report the characterization of LYR3 orthologs in other legumes. We found that, among the tested legumes, only the lupin ortholog was unable to bind LCOs. In order to better understand the molecular basis of LCO recognition, we developed a chimeric gene and domain-swapping approach to pinpoint the role of individual lysin motifs in ligand binding.

EXPERIMENTAL PROCEDURES

Cloning and transient expression of LYR3 from different legumes - BLAST searches in different genomic databases (http://blast.ncbi.nlm.nih.gov/; http://www.kazusa.or.jp/; http://www.phytozome.org/) using the MtLYR3 sequence were performed to identify putative orthologs in different legume species. Candidate genes were then examined by micro-synteny analysis. Based on the sequences available in the databases for the different plant species, specific primers were designed and all the putative orthologous genes were amplified using Phusion high fidelity DNA polymerase (New England Biolabs, 2000 units/ml) and genomic DNA from the following plant lines as template: *Pisum sativum* cv. Cameor, *Lotus japonicus* Gifu B-129-S9, *Phaseolus vulgaris* G19883, *Glycine max* cv. Williams 82, *Lupinus angustifolius* cv. Turkus, *Lupinus atlanticus* GM083B. The genes were then cloned via Gateway technology into pENTR, sequenced, and phylogenetic analysis of the sequences was performed (http://www.phylogeny.fr). The genes were transferred into binary vectors to create fusions with *YFP*. The proteins were then expressed in *Nicotiana. benthamiana* leaves and verified after 3-4 days by fluorescent microscopy. Membrane fractions were prepared from extracts of expressing leaves and equal quantities of 15-25 ug membrane proteins per lane were separated by SDS-PAGE and the LYR3 proteins were checked by immunoblot detection using anti-GFP antibodies (amsbio, 1/7000). The detailed procedure for the cloning, expression and analysis of LYR3 is described in (17).

Production of the LYR3 chimeric proteins and HCA analysis - All the chimeric proteins were cloned by using the Golden Gate technology. Fragments containing single LysM domains were amplified using primers specifically designed for Golden Gate reaction, containing *Bsa*I restriction sites and compatible cohesive ends. The Cys-X-Cys motifs delineated the ends of the LysM1 and LysM2 domains such that the LysM1 domain contained the N-terminal signal peptide (SP) and flanking region and the LysM3 domain contained the flanking region up to the predicted trans-membrane (TM) domain. All internal *Bsa*I restriction sites detected inside of the fragments to be combined were eliminated by site-directed mutagenesis. Fragments of LysM3 containing point mutations were obtained either by site-directed mutagenesis or by custom DNA synthesis. Chimeric proteins were assembled from the single LysM containing fragments as well as YFP tagged NFP (Nod Factor Perception) trans-membrane TM and intracellular kinase domain (NFP/YFP chimera) into the pCAMBIA2200 binary vector as

previously described (17), and transiently expressed in *N. benthamiana* leaves.

HCA was performed using the dedicated program (http://mobyle.rpbs.univ-paris-diderot.fr/).

Confocal microscopy – Disks of transformed leaves were de-aerated with a 10 ml syringe filled with water and mounted in water on a microscope slide. Image series covering the entire depth of the lower epidermis were taken with a Leica SP2 confocal microscope with the 514 laser line for excitation and an emission window from 525 to 580 nm, using a 40x0.8 water immersion objective. Images are presented as maximum projections covering at least half of the total depth of the lower epidermis.

Ligands and binding assays – NodRlv-IV(Ac, C18:4Δ2,4,6,11) was isolated from the bacterial supernatant of *R. leguminosarum* LPR5045 (pIJ1089) (18) and purified by reverse-phase HPLC on a C18 column as described in (19). Myc-LCOs and other LCOs were described in (3,19,20). LCO-V(C18:1Δ11, Me-Fuc) was a gift of Novozymes BioAg, Inc (Milwaukee, Wisconsin, USA).

Nod factor binding assays were performed as described in (17), using membrane fractions (containing 10–100 µg protein) isolated from the different LYR3 and LYR3 chimera expressing leaves and 0.4–2 nM of ^{35}S-LCO (LCO-IV(C16:2Δ2,9, ^{35}S). At least two replicate extracts were analysed with three binding assays and the standard error of the mean (SEM) was calculated. The specific binding activity of the expressed proteins was normalized by densitometry scanning of western blots.

RESULTS

Identification of LYR3 orthologs in legumes - In *M. truncatula NFP* and *LYR3* are located as an inverted tandem repeat on chromosome 5 (21,22). BLAST searches in different genomic databases using the MtLYR3 sequence identified the closest homologs. The putative orthologous genes in *P. sativum*, *L. japonicus*, *P. vulgaris*, *G. max*, *L. angustifolius* and *L. atlanticus* were then selected, where possible, by microsynteny analysis. This was particularly useful to choose two, probably homoeologous genes on chromosomes 1 and 11 from allotetraploid *G. max* (23). The deduced protein sequences showed high levels of identity ranging from 64 to 95% for the entire proteins and from 71 to 96% for their extracellular domains (Fig. 1*A*). The phylogenetic analysis confirmed that these genes were the orthologs of

MtLYR3, with PsLYR3 being the closest one (Fig. 1*B*).

LYR3 orthologs in legumes, except in lupin, exhibit LCO binding properties - All the MtLYR3 orthologs were expressed in *Nicotiana benthamiana* leaves as YFP fusions, *via A. tumefaciens* infiltration. After 3-4 days, the YFP fluorescence was detected as expected in the plasma membrane, suggesting that all the proteins were properly folded, processed and correctly localized. Fig. 2*A* shows the expression of PsLYR3 and LanLYR3 as representatives of the set of proteins. Immunoblot analysis of membrane extracts prepared from expressing *N. benthamiana* leaves reported in Fig. 2*B*, showed that the different LYR3 orthologs were well expressed.

The affinity of the LYR3 orthologs for LCOs was then determined by radioligand binding experiments using a ^{35}S-LCO (LCO-IV(C16:2Δ2,9, ^{35}S)). This compound corresponds to the Nod factor produced by *Sinorhizobium meliloti* (NodSm factor) and was previously used to characterize MtLYR3 (17). Except for the orthologs of the two lupin species, where no binding was detectable, all the other orthologs showed clear binding activity that was further characterized. Scatchard analysis of saturation binding experiments revealed the presence of a single class of binding sites for each LYR3 protein, exhibiting a high affinity (K_d) for the ^{35}S-LCO. The affinities for the ^{35}S-LCO, reported in Table I, showed that they were in the same order of magnitude as that of MtLYR3 (K_d = 25 nM). In order to characterize the selectivity of the binding of the different orthologs, competition experiments were performed with various LCOs including Myc-LCOs (Myc-LCO-IV(C16:0, S); Myc-LCO-IV(C16:0); Myc-LCO-IV(C18:1Δ9, S)) (3) or synthetic and natural Nod factors corresponding to those produced by the symbionts of *P. sativum* (NodRlv-IV(Ac, C18:4Δ2,4,6,11)), *P. vulgaris* (NodRt-V(Me, C18:1Δ11)) and *G. max* (LCO-V(C18:1Δ11, MeFuc)) (24). CO-V was used as a competitor to determine the selectivity of recognition of LCOs *vs* COs. As reported in Table I and as previously observed for MtLYR3 (17), all the tested orthologs showed a high selectivity for the lipo-chitooligosaccharidic structure, since CO-V was a poor competitor of ^{35}S-LCO binding (K_i > 10 µM). None of the orthologs discriminated the chemical substitutions of the Nod factors involved in the specific recognition between Rhizobia and their host plants. For example the NodRlv-IV(Ac, C18:4Δ2,4,6,11), with a poly-unsaturated fatty

acid representing the major determinant of host specificity for *P. sativum* (25), had a comparable affinity for all the LYR3 orthologs. LYR3 orthologs also exhibited a high affinity for the Myc-LCOs which was comparable to that for the Nod factors. However, the affinity of the two *G. max* homoeologues for the Myc-LCO-IV(C16:0) was lower compared to that of the other legumes. Considering all the data reported in Table I, the affinity for the LCOs appeared to increase with either increasing the length of the acyl chain from 16 to 18 or that of the oligochitin backbone from IV to V, suggesting that a LCO-V (C18) structure could be a common feature for high-affinity binding of LCOs to the LYR3 proteins. The absence of any detectable binding of *L. angustifolius* (LanLYR3) and *L. atlanticus* (LatLYR3) LYR3 proteins was unexpected considering the overall level of homology of the extracellular domain within the legume orthologs (Fig. 1).

LysM3 is required for high affinity binding to LCOs - We took advantage of the lack of LCO binding to LanLYR3 to better understand the molecular basis of LCO recognition by MtLYR3. For this purpose we swapped the LysMs between MtLYR3 and LanLYR3 to determine their role in high-affinity binding to LCOs. Golden Gate cloning was used to obtain the individual LysMs and associated flanking regions of MtLYR3 and LanLYR3 (Fig.3*A*). They were then assembled in different combinations to construct eight chimeric extracellular domains (ED) where each LysM of LanLYR3 was replaced by the corresponding one of MtLYR3. These constructs were all made as NFP/YFP chimeras to facilitate expression and detection (17).

The eight chimeric proteins were produced in *N. benthamiana* leaves and all of them showed some localization in the plasma membrane as observed by confocal microscopy for LLM, MMM, MML or LLL taken as examples (inset Fig. 3*B*). The membrane fractions prepared from the expressing leaves were then probed by immunoblot to determine the level of expression of each chimeric protein, before testing for their LCO-binding ability. The results reported in Fig. 3*B* showed that all the chimeras were well expressed, but only four, including that with the reconstituted ED of MtLYR3 (MMM), were able to bind the ^{35}S-LCO. The other three chimera which bound the ^{35}S-LCO all possessed the LysM3 of MtLYR3 and either the LysM1 and the LysM2 of LanLYR3 (LLM) or the LysM1 of LanLYR3 and the LysM2 of MtLYR3 (LMM) or vice-versa (MLM). To examine whether the MtLysM3 and/or its flanking region confers high

affinity binding, two additional chimeras were made: one with the LanLysM3 flanked by the linker regions of MtLysM3 (LLmLm), and the other one, with MtLysM3 flanked by the linker regions of LanLysM3 (LLlMl). Analysis of these chimeras demonstrated that MtLysM3, and not its flanking regions, plays a critical role in Nod factor binding, since LLmLm remained inactive like LLL, whereas LLlMl gained binding activity (Fig. 3*B*).

Scatchard plots deduced from saturation experiments for the reconstituted ED of MtLYR3 (MMM) and the chimeric proteins LLM, LMM and MLM revealed the presence of a single class of binding site. The affinities (K_d) of these different binding proteins for the ^{35}S-LCO, reported in Fig. 3*B*, showed that they were comparable to that of MtLYR3 (17). All the chimeras showed a similar specificity for LCOs, since a concentration of up to 2 µM of CO-V did not compete for ^{35}S-LCO binding (data not shown).

To determine if the ligand recognition only depended on the third lysin motif, chimeras consisting of an ED containing MtLysM3 alone or MtLysM1 followed by MtLysM3 in tandem were produced. As revealed by confocal images of *N. benthamiana* expressing leaves, the resulting YFP-tagged proteins were mis-localized, suggesting a problem of protein folding (data not shown). The membrane fractions prepared from the expressing leaves did not show any binding activity.

Several amino acids, including Y-228 in LysM3 are critical for LCO binding - To further characterize the molecular basis of LCO recognition by LYR3 proteins, point mutations were introduced in the LysM3 of LanLYR3 with the flanking regions of MtLysM3 (LLmLm) or in the LysM3 of MtLYR3 with the flanking regions of LanLysM3 (LLlMl) in order to obtain either a gain or a loss of binding activity. A first set of point mutations was designed by targeting W_{196}, L_{222} and Y_{228}, based on the numbering of the sequence of MtLYR3, which are highly conserved in the LysM3 of LYR3 proteins exhibiting LCO-binding activity but are not present in LanLysM3 (Fig. 4*A* upper panel). As shown (Fig. 4*A*), the substitution $Y_{228}Q$ in the ED of MtLysM3 completely abolished the binding activity of the chimeric protein LLlMl, while the other substitutions, $W_{196}G$ and $L_{222}M$, did not provoke any change. However, none of the reverse substitutions in the LysM3 of LanLYR3 conferred binding activity, suggesting that residues in addition to Y_{228} are required.

MtLYR3 and LanLYR3 share 84% and 74% identity for LysM1 and LysM2

respectively. Their LysM3 domains are less conserved with only 70% identity (with 15 amino acids different). Moreover, hydrophobic cluster analysis (HCA), revealed a different pattern of structural features for the LysM3 of LanLYR3 compared to that of MtLYR3 (Fig. 4*B*). Therefore, mutations were introduced in the sequence of LanLysM3 ($G_{196}W$, $D_{197}G$, $T_{211}F$, $N_{219}T$, $M_{222}L$, $N_{224}Q$, $Q_{228}Y$) in order to mimic MtLYR3 in terms of HCA pattern and conserved residues present in LYR3 proteins exhibiting high affinity LCO-binding (Fig. 4*B*). The mutated protein produced in *N. benthamiana* leaves was correctly addressed to the plasma membrane and showed a binding activity corresponding to an affinity (K_d) of 111 nM for the ^{35}S-LCO, as determined by the Scatchard plot analysis of a saturation experiment (Fig. 4*C*). Therefore the introduced mutations in LanLysM3 to mimic MtLysM3, resulted in a clear gain of binding activity for LanLYR3 even if the affinity of the mutated protein did not fully reach that of LLlMl (K_d = 36 nM).

DISCUSSION

In our search for LCO binding proteins using a biochemical approach, we have recently identified in *M. truncatula* the LysM-RLK LYR3 as a high affinity LCO-binding protein. The affinity of LYR3 for Nod factors and Myc-LCOs was similar and in the nM range, in contrast to the μM affinities for COs of different degrees of polymerization corresponding to signals produced by either pathogens or AM fungi (17). In the present work LYR3 orthologs have been identified in a set of nitrogen fixing legumes (Fig. 1) including the other model legume *L. japonicus* and legumes of agronomical interest, among them, lupin, a rare example of a legume species, being a non-host for AM fungi (26). We showed that all the MtLYR3 orthologs, except those from the two lupin species, are high affinity LCO-binding proteins. The binding was specific for the LCO structure (Nod factors and Myc-LCOs) since the affinity for COs was over 500-fold less than for the best LCO (Table I). However, no selectivity was observed towards the different substitutions of the Nod factors involved in host-specific recognition (27), suggesting that LYR3 does not play a particular role in the recognition of the specific Nod factors produced by rhizobial symbionts. The binding characteristics of LYR3 are more in line with either a generic role in the symbiosis with Rhizobia or a role in the AM symbiosis. This latter role is further suggested by the observation that LYR3 from lupins, which does not form the

AM symbiosis, lacks LCO binding activity. However, transcriptomic and genomic data indicate that several genes important for the establishment of the mycorrhizal symbiosis, such as *RAM2* are missing in lupins (28). Thus the loss of binding to LYR3 in lupins is unlikely to be the sole cause of the lack of mycorrhization in these species but could be one of many changes that occurred following the loss of selective pressure for the functioning of the AM symbiosis.

The lack of binding activity of the lupin orthologs, which share 75% identity in the ED with the other orthologs that bind LCOs (Fig. 1), gave the opportunity to address the question of the role of the individual lysin motifs in LCO recognition by the LYR3 proteins. Analysis of chimeric LysM domain-swapped proteins revealed the importance of LysM3 for high affinity binding (Fig. 3). Indeed, swapping the LysM3 of LanLYR3 by the corresponding one of MtLYR3 resulted in a gain of binding activity, whereas LysM1 and LysM2 were interchangeable between LanLYR3 and MtLYR3 provided that MtLysM3 was present in the chimeras.

Docking studies and structural analyses of plant LysM proteins have shown that a single LysM is able to accommodate a Nod factor or CO (15-17,29-31). For AtCERK1 and OsCEBiP, the second lysin motif physically interacts with the GlcNAc residues (15,16). For the LysM effector Ecp6 of the fungal pathogen *Cladosporium fulvum*, crystal structure analysis established that chitin binding was achieved by two binding sites, one in LysM2 with an affinity in the micromolar range and a second one in a groove between LysM1 and LysM3, exhibiting a picomolar affinity (32). Our attempts to examine whether LCO binding to LYR3 requires either LysM1 or LysM2 in addition to LysM3 were inconclusive. Chimeric proteins, containing either the LysM3 of MtLYR3 alone or in a tandem repeat following LysM1, were not correctly addressed to the plasma membrane and thus the lack of binding to these proteins may be due to incorrect folding and processing, which is known to affect the biological activity of LysM-RLKs (33).

Site-directed mutagenesis performed in LysM3, allowed Y_{228} to be identified as a critical residue for LCO recognition, since $Y_{228}Q$ substitution in the ED of MtLysM3 completely abolished the binding activity (Fig. 4). Gain of function studies suggest that this Y residue must be in a particular structural context to allow LCO recognition. The lack of conservation of this

residue in the CO binding sites of AtCERK1 or Ecp6 may suggest that it plays a specific role in the recognition of LCOs. This would be consistent with differences in the mode of binding of asymmetrical LCOs, compared to symmetrical COs (15,16, 32). LCO recognition by LYR3 could involve the LysM3 to accommodate the acyl chain in an accessory binding site close to a site for the oligosaccharidic backbone, similar to the mechanism described for the binding of a glycolipid to an extended binding site of a C-type lectin (34). Our aim now is to solve the structure of the ED of MtLYR3 in combination with a LCO in order to map the ligand-binding site and to better understand the role of the different lysin motifs in LCO binding.

REFERENCES

1. Gough, C., and Cullimore, J. (2011) Lipo-chitooligosaccharide signalling in endosymbiotic plant-microbe interactions. *Mol Plant Microb Interact* **24**, 867-878
2. Dénarié, J., Debellé, F., and Rosenberg, C. (1992) Signaling and host range variation in nodulation. *Annu Rev Microbiol* **46**, 497-531
3. Maillet, F., Poinsot, V., André, O., Puech-Pages, V., Haouy, A., Gueunier, M., Cromer, L., Giraudet, D., Formey, D., Niebel, A., Martinez, E. A., Driguez, H., Bécard, G., and Dénarié, J. (2011) Fungal lipochitooligosaccharide symbiotic signals in arbuscular mycorrhiza. *Nature* **469**, 58-63
4. Genre, A., Chabaud, M., Balzergue, C., Puech-Pagès, V., Novero, M., Rey, T., Fournier, J., Rochange, S., Bécard, G., Bonfante, P., and Barker, D. G. (2013) Short-chain chitin oligomers from arbuscular mycorrhizal fungi trigger nuclear Ca^{2+} spiking in *Medicago truncatula* roots and their production is enhanced by strigolactone. *New Phytol* **198**, 190-202
5. Shibuya, N., and Minami, E. (2001) Oligosaccharide signalling for defence responses in plant. *Physiological and Molecular Plant Pathology* **59**, 223-233
6. Gust, A. A., Willmann, R., Desaki, Y., Grabherr, H. M., and Nürnberger, T. (2012) Plant LysM proteins: modules mediating symbiosis and immunity. *Trends Plant Sci* **17**, 495-502
7. Antolín-Llovera, M., Petutsching, E. K., Ried, M. K., Lipka, V., Nürnberger, T., Robatzek, S., and Parniske, M. (2014) Knowing your friends and foes – plant receptor-like kinases as initiators of symbiosis or defence. *New Phytol* **204**, 791-802
8. Cao, Y., Liang, Y., Tanaka, K., Nguyen, C. T., Jedrzejczak, R. P., Joachimiak, A., and Stacey, G. (2014) The kinase LYK5 is a major chitin receptor in *Arabidopsis* and forms a chitin-induced complex with related kinase CERK1. *eLife* **3:e03766**
9. Kaku, H., Nishizawa, Y., Ishii-Minami, N., Akimoto-Tomiyama, C., Dohmae, N., Takio, K., Minami, E., and Shibuya, N. (2006) Plant cells recognize chitin fragments for defense signaling through a plasma membrane receptor. *Proc Natl Acad Sci USA* **103**, 11086-11091
10. Miya, A., Albert, P., Shinya, T., Desaki, Y., Ichimura, K., Shirasu, K., Narusaka, Y., Kawakami, N., Kaku, H., and Shibuya, N. (2007) CERK1, a LysM receptor kinase, is essential for chitin elicitor signaling in *Arabidopsis*. *Proc Natl Acad Sci USA* **104**, 19613-19618
11. Wan, J., Zhang, X.-C., Neece, D., Ramonell, K. M., Clough, S., Kim, S.-y., Stacey, M. G., and Stacey, G. (2008) A LysM receptor-like kinase plays a critical role in chitin signaling and fungal resistance in *Arabidopsis*. *Plant Cell* **20**, 471-481
12. Iizasa, E., Mitsutomi, M., and Nagano, Y. (2009) Direct binding of a plant LysM receptor-like kinase, LysM RLK1/CERK1, to chitin *in vitro*. *J Biol Chem* **285**, 2996–3004
13. Petutschnig, E. K., Jones, A. M. E., Serazetdinova, L., Lipka, U., and Lipka, V. (2010) The Lysin motif receptor-like kinase (LysM-RLK) CERK1 is a major chitin-binding protein in *Arabidopsis thaliana* and subject to chitin-induced phosphorylation. *J Biol Chem* **285**, 28902-28911
14. Wan, J., Tanaka, K., Zhang, X.-C., Son, G. H., Brechenmacher, L., Nguyen, T. H. N., and Stacey, G. (2012) LYK4, a Lysin motif receptor-like kinase, is important for chitin signaling and plant innate immunity in Arabidopsis. *Plant Physiol* **160**, 396-406
15. Liu, T., Liu, Z., Song, C., Hu, Y., Han, Z., She, J., Fan, F., Wang, J., Jin, C., Chang, J., Zhou, J.-M., and Chai, J. (2012) Chitin-induced dimerization activates a plant immune receptor. *Science* **336**, 1160-1164
16. Hayafune, M., Berisio, R., Marchetti, R., Silipo, A., Kayama, M., Desaki, Y., Arima, S., Squeglia, F., Ruggiero, A., Tokuyasu, K., Molinaro, A., Kaku, H., and Shibuya, N. (2014) Chitin-induced activation of immune signaling by the rice receptor CEBiP relies on a unique sandwich-type dimerization. *Proc Natl Acad Sci USA* **111**, 404-413
17. Fliegmann, J., Canova, S., Lachaud, C., Uhlenbroich, S., Gascardi, V., Pichereaux, C., Rossignol, M., Rosenberg, C., Cumener, M., Pitorre, D., Lefebvre, B., Gough, C., Samain, E., Fort, S., Driguez, H., Vauzeilles, B., Beau, J.-M., Nurisso, A., Imberty, A., Cullimore, J., and Bono, J.-J. (2013) Lipo-chitooligosaccharidic symbiotic signals are recognized by LysM Receptor-Like Kinase LYR3 in the legume *Medicago truncatula*. *ACS Chem Biol* **8**, 1900-1906

18. Spaink, H. P., Bloemberg, G. V., Van Brussel, A. A. N., Lugtenberg, B. J., van der Drift, K. M., Haverkamp, J., and Thomas-Oates, J. E. (1995) Host specificity of *Rhizobium leguminosarum* is determined by the hydrophobicity of highly unsaturated fatty acyl moieties of the Nodulation Factors. *Mol Plant Microb Interact* **8**, 155-164

19. Gressent, F., Drouillard, S., Mantegazza, N., Samain, E., Geremia, R. A., Canut, H., Niebel, A., Driguez, H., Ranjeva, R., Cullimore, J., and Bono, J. J. (1999) Ligand specificity of a high-affinity binding site for lipo-chitooligosaccharidic Nod factors in *Medicago* cell suspension cultures. *Proc Natl Acad Sci USA* **96**, 4704-4709

20. Rasmussen, M. O., Hogg, B., Bono, J. J., Samain, E., and Driguez, H. (2004) New access to lipo-chitooligosaccharide nodulation factors. *Org Biomol Chem* **2**, 1908-1910

21. Kim, D. H., Parupalli, S., Azam, S., Lee, S.-H., and Varshney, R. K. (2013) Comparative sequence analysis of nitrogen fixation-related genes in six legumes. *Frontiers in Plant Science* **4**, 1-8

22. Arrighi, J.-F., Barre, A., Ben Amor, B., Bersoult, A., Soriano, L. C., Mirabella, R., de Carvalho-Niebel, F., Journet, E.-P., Ghérardi, M., Huguet, T., Geurts, R., Dénarié, J., Rougé, P., and Gough, C. (2006) The *Medicago truncatula* lysin motif-receptor-like kinase gene family includes *NFP* and new nodule-expressed genes. *Plant Physiol* **142**, 265-279

23. Schmutz, J., Cannon, S. B., Schlueter, J., Ma, J., Mitros, T., Nelson, W., Hyten, D. L., Song, Q., Thelen, J. J., Cheng, J., Xu, D., Hellsten, U., May, G. D., Yu, Y., Sakurai, T., Umezawa, T., Bhattacharyya, M. K., Sandhu, D., Valliyodan, B., Lindquist, E., Peto, M., Grant, D., Shu, S., Goodstein, D., Barry, K., Futrell-Griggs, M., Abernathy, B., Du, J., Tian, Z., Zhu, L., Gill, N., Joshi, T., Libault, M., Sethuraman, A., Zhang, X.-C., Shinozaki, K., Nguyen, H. T., Wing, R. A., Cregan, P., Specht, J., Grimwood, J., Rokhsar, D., Stacey, G., Shoemaker, R. C., and Jackson, S. A. (2010) Genome sequence of the palaeopolyploid soybean. *Nature* **463**, 178-183

24. D'Haeze, W., and Holsters, M. (2002) Nod factor structures, responses, and perception during initiation of nodule development. *Glycobiology* **12**, 79R-105

25. Spaink, H. P., Sheeley, D. M., van Brussel, A. A., Glushka, J., York, W. S., Tak, T., Geiger, O., Kennedy, E. P., Reinhold, V. N., and Lugtenberg, B. J. (1991) A novel highly unsaturated fatty acid moiety of lipo-oligosaccharide signals determines host specificity of *Rhizobium*. *Nature* **354**, 125-130

26. Oba, H., Tawaray, K., and Wagatsuma, T. (2001) Arbuscular mycorrhizal colonization in Lupinus and related genera. *Soil Science and Plant Nutrition* **47**, 685-694

27. Dénarié, J., Debellé, F., and Promé, J. C. (1996) Rhizobium lipo-chitooligosaccharide nodulation factors: signaling molecules mediating recognition and morphogenesis. *Annu Rev Biochem* **65**, 503-535

28. Delaux, P.-M., Varala, K., Edger, P. P., Coruzzi, G. M., Pires, J. C., and Ané, J.-M. (2014) Comparative phylogenomics uncovers the impact of symbiotic associations on host genome evolution. *PLoS Genet* **10**, e1004487

29. Mulder, L., Lefebvre, B., Cullimore, J., and Imberty, A. (2006) LysM domains of *Medicago truncatula* NFP protein involved in Nod factor perception. Glycosylation state, molecular modeling and docking of chitooligosaccharides and Nod factors. *Glycobiology* **16**, 801-809

30. Ohnuma, T., Onaga, S., Murata, K., Taira, T., and Katoh, E. (2008) LysM domains from *Pteris ryukyuensis* chitinase-A: a stability study and characterization of the chitin-binding site. *J Biol Chem* **283**, 5178-5187

31. Radutoiu, S., Madsen, L. H., Madsen, E. B., Jurkiewicz, A., Fukai, E., Quistgaard, E. M., Albrektsen, A. S., James, E. K., Thirup, S., and Stougaard, J. (2007) LysM domains mediate lipochitin-oligosaccharide recognition and Nfr genes extend the symbiotic host range. *EMBO J* **26**, 3923-3935

32. Sánchez-Vallet, A., Saleem-Batcha, R., Kombrink, A., Hansen, G., Valkenburg, D.-J., Thomma, B., P. H. J, and Mesters, J., R. (2013) Fungal effector Ecp6 outcompetes host immune receptor for chitin binding through intrachain LysM dimerization. *eLife* **2:e00790**

33. Lefebvre, B., Klaus-Heisen, D., Pietraszewska-Bogiel, A., Hervé, C., Camut, S., Auriac, M.-C., Gasciolli, V., Nurisso, A., Gadella, T. W. J., and Cullimore, J. (2012) Role of N-glycosylation sites and CXC motifs in trafficking of *Medicago truncatula* Nod Factor Perception protein to the plasma membrane. *J Biol Chem* **287**, 10812-10823

34. Taylor, M. E., and Drickamer, K. (2014) Convergent and divergent mechanisms of sugar recognition across kingdoms. *Curr Opin Struct Biol* **28**, 14-22

FOOTNOTES

[2]To whom correspondence should be addressed. Fax: +33-561285061; Tel: +33-561285050; E-mail: Jean-Jacques.Bono@toulouse.inra.fr

[3]The abbreviations used are : LCOs, lipochitooligosaccharides; AM, arbuscular mycorrhizal; GlcNAc, *N*-acetylglucosamine; COs, chitooligosaccharides; LysM, lysin motif; LYM, extracellular receptor-like proteins; LysM-RLK, lysin motif receptor like kinase; LYK, LysM domain-containing RLK; LYR, LYK-related; AtCERK1, *Arabidopsis thaliana* chitin elicitor receptor kinase 1; OsCEBiP, *Oryza sativa* chitin elicitor binding protein; cv, cultivar; HCA, hydrophobic cluster analysis; TM, trans-membrane; SP, signal peptide; ED, extracellular domain

TABLE I: Affinity (K_d) of the LYR3 orthologs for LCOs (Nod factors and Myc-LCOs) and COs.

The nomenclature used shows the degree of polymerization of the GlcNAc backbone (IV or V) and in parenthesis the modifications at the non-reducing end including the acyl chain, followed by those at the reducing end. LCOs are synthetic molecules, Nod factors are biologically produced LCOs.

Compound	K_d (nM with SEM) of the LYR3 proteins				
	PsLYR3	PvLYR3	LjLYR3	GmLYR3-01	GmLYR3-11
LCO-IV(C16:2Δ2 Δ 9, S)	31 +/- 4.8	40 +/- 3.5	33 +/- 3.4	32 +/- 2.2	64 +/- 5.1
Myc-LCO-IV(C16:0, S)	24 +/- 3.2	17 +/- 2.6	11 +/- 2.4	18 +/- 2.8	32 +/- 4.9
Myc-LCO-IV(C16:0)	50 +/- 8.8	23 +/- 6.9	42 +/- 2.5	71 +/- 8.8	140 +/- 29
Myc-LCO-IV(C18:1Δ9, S)	16 +/- 1.6	13 +/- 2.6	9 +/- 2.0	12 +/- 2.0	20 +/- 3.5
NodRlv-IV(Ac, C18:4Δ2,4,6,11)	14 +/- 2.0	29 +/- 4.8	10 +/- 1.9	20 +/- 3.5	16 +/- 2.8
NodRt-V(Me, C18:1Δ11)	21 +/- 3.5	20 +/- 1.6	10 +/- 2.5	13 +/- 0.7	14 +/- 2.2
LCO-V(C18:1Δ11, MeFuc)	7 +/- 2.9	11 +/- 2.8	7 +/- 1.2	14 +/- 2.2	17 +/- 1.1
LCO-V(C18:1Δ11)	7 +/- 0.9	29 +/- 3.7	9 +/- 2.0	17 +/- 1.8	35 +/- 3.6
LCO-V(C18:1Δ11, S)	11 +/- 2.1	9 +/- 0.8	8 +/- 1.4	6 +/- 1.2	18 +/- 2.4
CO-V	$>10^3$	$>10^3$	$>10^3$	$>10^3$	$>10^3$

Figure 1

A

	MtLYR3	PsLYR3	LjLYR3	PvLYR3	GmLYR3-01	GmLYR3-11	LanLYR3	LatLYR3
MtLYR3	-	80.6	69.3	66.4	67.6	67.1	63.6	67.6
PsLYR3	89.7	-	67.0	65.3	67.2	67.1	62.4	64.7
LjLYR3	77.6	76.4	-	67.9	73.0	72.0	66.8	69.6
PvLYR3	75.9	76.4	72.4	-	82.5	81.8	66.9	70.5
GmLYR3-01	79.9	82.2	77.6	85.1	-	94.6	68.7	71.5
GmLYR3-11	79.9	81.6	76.4	83.3	96.0	-	68.6	70.6
LanLYR3	74.7	75.9	73.6	74.1	75.3	74.7	-	86.2
LatLYR3	73.0	72.4	73.6	71.8	74.1	73.0	89.7	-

B
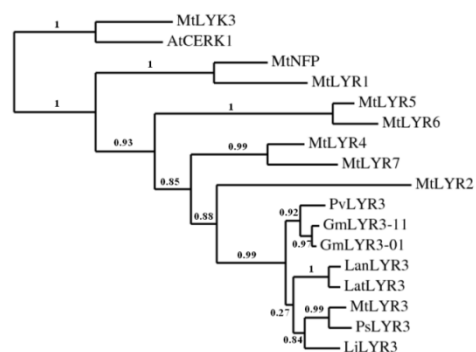
FIGURE 1. Similarity between legume LYR3 proteins. A, percentage of identity between the LYR3 orthologs at the level of the entire protein (in grey) or the extracellular domain. B, phylogenetic tree of the LYR proteins of *M. truncatula*, showing the orthology of the legume LYR3 proteins with MtLYR3. MtLYK3 and AtCERK1, representatives of the LYK group of LysM-RLKs, were used as outgroup. The branches show the bootstrap values. The LYR3 proteins are named with the first letters of the genus and species: *Ps= Pisum sativum, Lj = Lotus japonicus, Pv = Phaseolus vulgaris, Gm = Glycine max, Lan = Lupinus angustifolius, Lat = Lupinus atlanticus, At = Arabidopsis thaliana.*

Figure 2
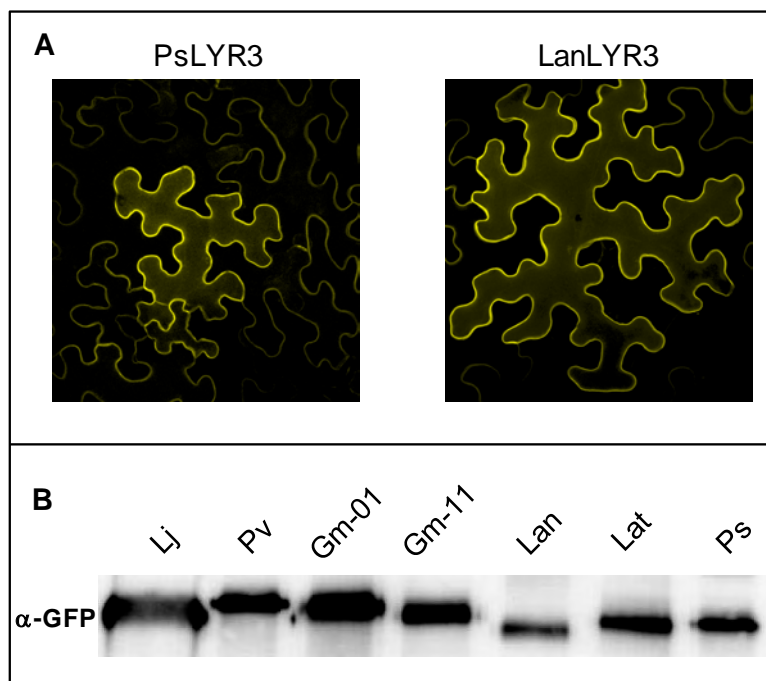
FIGURE 2. Expression of LYR3 orthologs in *N. benthamiana* leaves. A, confocal images of epidermal cells showing the plasma membrane localization of PsLYR3 and LanLYR3 YFP-tagged proteins. B, immunodetection of YFP-tagged LYR3 orthologs in membrane fractions, using anti-GFP antibodies. Nomenclature as in legend to Figure 1.

Figure 3
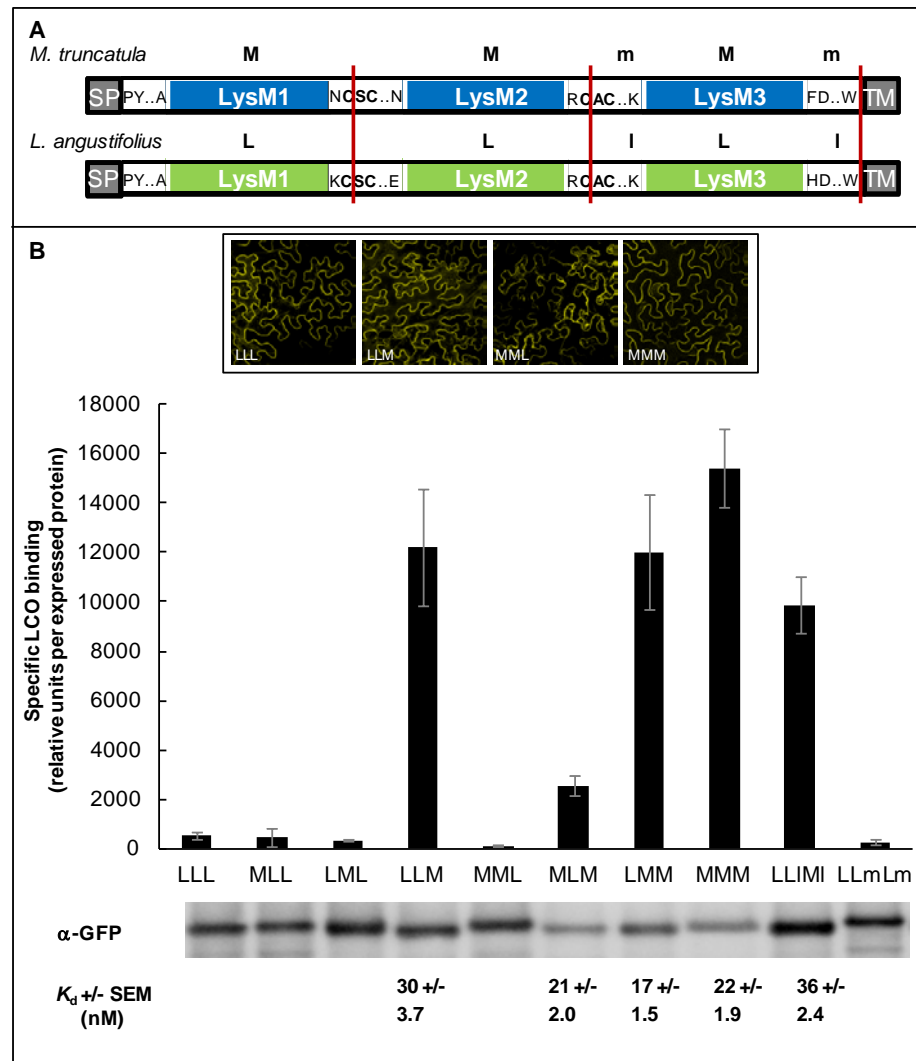
FIGURE 3. Analysis of LCO binding to *M. truncatula* and *L. angustifolius* LysM domain- swapped LYR3 proteins. A, schematic representation of the extracellular domains showing positions of borders and amino acids at the end of each individual module of the MtLYR3 (M) and LanLYR3 (L) proteins, used for domain swapping. The third module is shown subdivided into flanking regions (m or l) and LysM domain (M or L). Signal peptide (SP) and trans-membrane domain (TM) are shown. B, specific binding activity (with SEM) of the protein chimera with ED consisting of swapped LysM domains between MtLYR3 and LanLYR3, showing the importance of the LysM3 domain. The modules are ordered from LysM1 to LysM3. Immunodetection of the chimeric proteins in membrane fractions of *N. benthamiana* leaves and themodynamic parameters of the LCO interaction, affinity (K_d with SEM) is shown beneath. nd = not determined. Inset: confocal images of epidermal cells of *N. benthamiana* leaves expressing chimeric proteins, which either show LCO-binding activity (LLM, MMM), or not (LLL, MML).

Figure 4
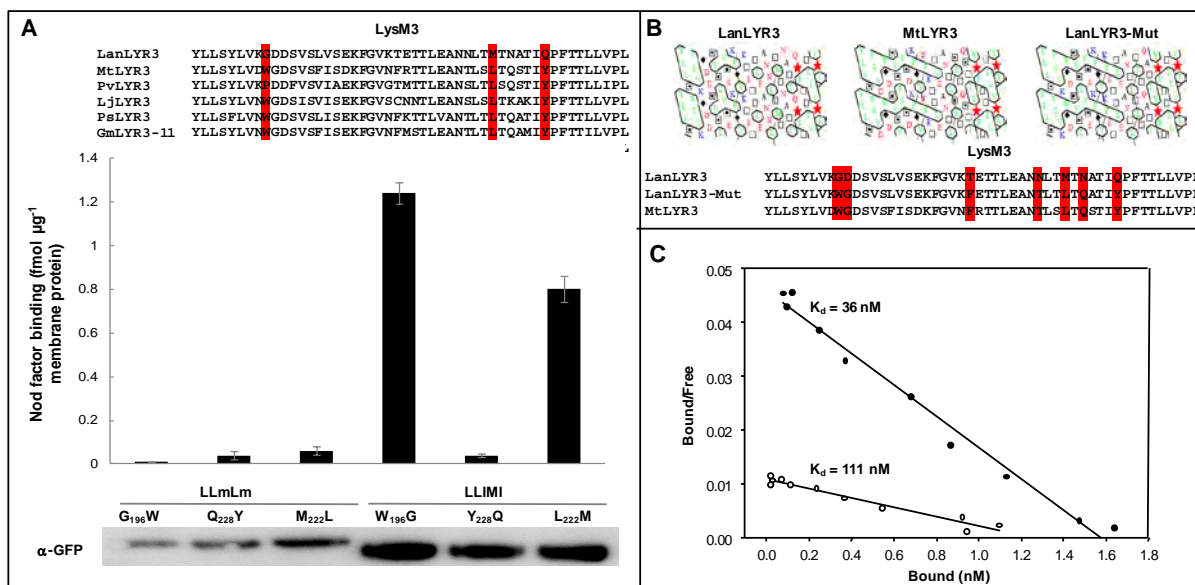
FIGURE 4. Identification of amino acid residues in LysM3 of MtLYR3, involved in high affinity LCO-binding. A, upper panel: sequence alignment of LYR3 proteins showing three highly conserved residues not present in LanLYR3. Lower panel: specific binding activity (with SEM) of the chimeric proteins LLmLm and LLlMl carrying single point mutations in the identified LysM3 residues, showing the importance of MtLYR3 Y_{228} by loss of function. Immunodetection of the proteins in membrane extracts of *N. benthamiana* leaves is shown beneath. B, HCA plots of the LysM3 of MtLYR3, LanLYR3, and of LanLYR3-Mut, which contains point mutations targeting conserved residues of LCO-binding proteins or shaping the HCA pattern to that of MtLYR3. C, Scatchard plot analysis of LCO binding to LLlMl (●) and LanLYR3-Mut (o), showing that mimicking the MtLYR3 HCA pattern in LanLYR3-Mut leads to gain of binding.

Chapter II

Use of the LYR3 extracellular domain in chimeric receptors for potential biotechnological applications

Introduction

As described in the previous chapter, the LysM-RLK LYR3 was shown to be conserved as a LCO binding protein in different legume species. LCOs have been used since 2004 in the agricultural sector to stimulate plant growth and development, resulting in better yield and thus serving as positive regulators. From the side of new applications it was attractive to investigate whether LYR3 and its capability to bind LCO could be used to enlarge the spectrum of LCO application by, for instance, engineering its ability to provoke plant defense responses. For this study it was decided to use an approach based on the creation of chimeric proteins. The general idea was to create chimeric receptors which would consist of the extracellular domain (ECD) of LYR3 fused to the kinase domain (KD) of one of the defense-related RLKs. It was expected that high affinity binding of LCO by the ECD of LYR3 would lead to the activation of the chimeric protein kinase followed by the elicitation of defense responses. The relevance of this approach was recently demonstrated in the study performed for two *Lotus japonicus* symbiotic receptors NFR1 and NFR5 whose extracellular domains were combined with the kinase of AtCERK1, an *Arabidopsis thaliana* receptor essential for chitin signaling (Wang et al., 2014). By co-expression in *cerk1-2 A. thaliana* plants, NFR1/CERK1 and NFR5/CERK1 chimeric receptors were shown to trigger a number of defense responses after their activation with 100 µM LCO. As the CERK1 kinase was shown to stay functional in these chimeric receptors, the kinase of CERK1 was chosen for the creation of LYR3 chimeric receptors. Two approaches were used for this work. In the first approach, an already existing transgenic *A. thaliana cerk1* line expressing aequorine (Wan et al., 2012) was used in stable transformation with LYR3/CERK1 constructs, therefore allowing the early defense response of cytosolic calcium influx to be used to detect the activation of LYR3/CERK1 chimeras with LCO. Secondly, as stable transformation of the *A. thaliana* cerk1, aequorine line was expected to be time-consuming, an approach of transient expression of chimeric proteins in the leaves of *Nicotiana benthamiana* was used in order to provide a faster means to analyze activation with LCO and measurement of defense responses in this heterologous system.

Another *A. thaliana* defence receptor EFR was selected as the second candidate protein whose kinase could be fused to the ECD of LYR3. Defining recognition of bacterial elongation factor EF-TU, EFR has been used several times in the composition of chimeric receptors (Zipfel et al., 2006; Albert et al., 2010; De Lorenzo et al., 2011). For instance, kinase of EFR being fused to the ECD of WAK1, the *A. thaliana* receptor for oligogalacturonides (OGs), was shown to stay biologically active and trigger the defence responses in *N. benthamiana* leaves after treatment with OGs (Brutus et al., 2010). Thus by analogy with WAK1/EFR and OGs it was expected that expressed in *N. benthamiana* LYR3/EFR chimeric receptors would be responsive to LCO. The genome of *Nicotiana* spp. does not contain *EFR*, however transient expression of this receptor was shown to be sufficient to trigger emission of ethylene after treatment with the EF-TU derived peptide elicitor, elf-18 (Zipfel et al., 2006). Accordingly, for our study, the appearance of stress ethylene in response to LCO was selected to be used as the sign of LYR3/EFR activation.

For creation of both CERK1 and EFR containing chimeras two LYR3 proteins were selected, originating either from *Medicago truncatula* (MtLYR3) or from *Glycine max* (GmLYR3). In this way LYR3 binding and activation specificity could be studied through monitoring the differences in the intensity of the stress responses after the treatment of chimeras with the LCOs preferentially recognized by the *M. truncatula* or *G. max* proteins.

Experimental procedures

Genetic constructions and N. benthamiana transient transformation.

Generation of chimeric constructions by using Golden Gate technology and subsequent *Agrobacterium* transformation and transient expression of chimeric proteins in the leaves of *N. benthamiana* was performed as described in chapter I.

Stable transformation of A. thaliana cerk1 plants expressing aequorine.

Stable transformation of *A. thaliana* was performed by using the floral dip method (Clough and Bent, 1998). *Agrobacterium tumefaciens* strains (GV3101) harboring sequences encoding chimeric proteins were grown for 2 days at 28°C on selective YEB agar plates. Next *Agrobacterium* were scratched from the plates and resuspended in 10 ml YEB liquid medium. The bacteria were incubated for four hours at 28°C and these pre-cultures were used to inoculate 250 ml of liquid culture. Grown overnight at 28°C up to an OD_{600}=1,5, the liquid cultures were centrifuged at 8000 rpm for 10min at room temperature. Pelleted down bacteria were next resuspended in 5% sucrose in water in order to reach a final OD_{600}=1. The resulting solutions were supplemented with Silwett L77 at 100 μl/L concentration. For each stable transformation five *A. thaliana* plants in the beginning of their florification stage (approx. five weeks old) were used. The first flowering shoots were previously cut to induce the formation of additional inflorescences. During the transformation plants were dipped and gently agitated in the bacterial suspension for 10 seconds. After short drying the treated plants were covered with a plastic film and held away from direct light for 24 hours. Afterwards plastic covers were removed and plants were cultivated in the greenhouse for a full life cycle up to the appearance of seeds.

Measurement of aequorin luminescence.

Seeds obtained from the *A. thaliana* plants stably transformed with chimeric constructions were surface-sterilized in ethanol solution supplemented with hypochlorite (95% ethanol and 0,26% hypochlorite) and grown on MS agar plates for 14 days at 25°C with 16h/8h day/night cycle. Grown plantlets were screened for the presence of red fluorescence under Leica MZ6 stereomicroscope. Selected fluorescent plants were next incubated overnight in 2.5 μM coelenterazine (Calbiochem, Bad Soden, Germany) water solution. Bioluminescence was measured in the digital luminometer (Lumat LB9507; Berthold, Bad Wildbad, Germany) for the samples consisting of five plantlets. Samples were treated with the elicitors within the first three minutes after being placed in the

luminometer. Luminescence was monitored for 10-20 minutes by recording relative light units every second. At the end of each measurement the total amount of aequorin was determined by adding 500 μL of lysis buffer (10 mM CaCl2, 2% Nonidet P-40, and 10% ethanol) to the samples. Luminescence data was transformed into cytosolic Ca^{2+} concentration using the equation established by (Allen et al., 1977).

Measurement of ethylene.

For ethylene measurements, 5mm disks were cut out from *N. benthamiana* agroinfiltrated leaves and incubated overnight in water, with their abaxial side turned up. Next, samples consisting of five disks were placed in sealed 10-mL flasks containing 2 mL H_2O or elicitor solutions and incubated with agitation for 2 hours. For some of the experiments disks were first infiltrated with water or elicitors and then exposed as described above. To analyze emission of ethylene 1 mL gas samples were withdrawn with a syringe from the flasks and injected into an Agilent 7820A gas chromatograph (Felix et al., 1999). Obtained data was treated with Agilent ChemStation offline software.

Western blotting

Immuno-detection of the proteins was performed as described in the previous chapter by using anti-HA-HRP (Roche, 1:2000) antibodies.

Results

Stable transformation of cerk1 Arabidopsis thaliana plants expressing aequorine, with LYR3/AtCERK1 chimeric constructions and selection of transformants.

Stable transformation was performed for the chimeric proteins consisting of the ectodomains of MtLYR3 or GmLYR3 proteins and the kinase domain of the *A. thaliana* CERK1 receptor. Each chimera was designed in two modifications according to the type of its trans-membrane (Tm) region which was either originating from LYR3 (LYR3Tm) or from CERK1 (TmCERK1). All proteins were fused at their C-termini to the HAST tag and their expression was driven by the 35S promoter.

In addition to the p35S:GmLYR3/TmCERK1-HAST, p35S:GmLYR3Tm/CERK1-HAST, p35S:MtLYR3/TmCERK1-HAST, p35S:MtLYR3Tm/CERK1-HAST constructions, plants were also transformed with a p35S:CERK1/TmCERK1-HAST construction (reconstituting *AtCERK*) and with the pCAMBIA2200 vector (empty vector) in which all genetic constructions were cloned. Transformation of *A. thaliana cerk1* plants was done with *Agrobacterium tumefaciens* bacteria carrying the 6 different genetic constructions. After the transformation, plants (F0 generation) were grown to produce the seeds which were then germinated (F1 generation) and screened for the presence of the T-DNA. Screening was based on the detection of red fluorescence determined by the DsRed reporter gene present in the pCAMBIA2200 binary vector. No plants transformed with p35S:GmLYR3Tm/CERK1-HAST, p35S:MtLYR3/TmCERK1-HAST, p35S:MtLYR3Tm/CERK1-HAST and p35S:CERK1/TmCERK1-HAST constructions were found. However, several fluorescent
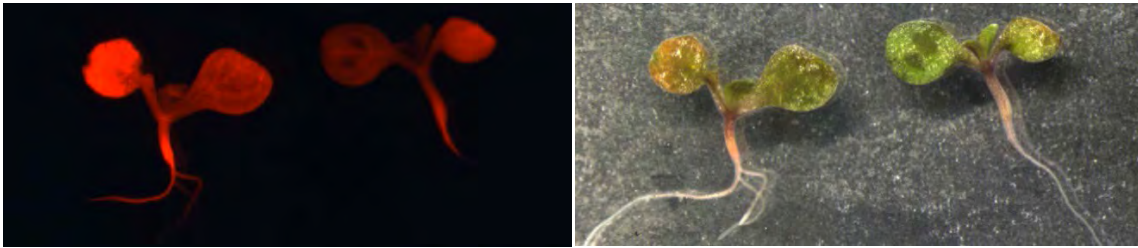
Fig.1 Selection of the stably transformed *A. thaliana* plants by the detection of DsRed fluorescence.

Two seedlings expressing the DsRed protein obtained from the plant transformed with the GmLYR3/TmCERK1 chimera are shown.
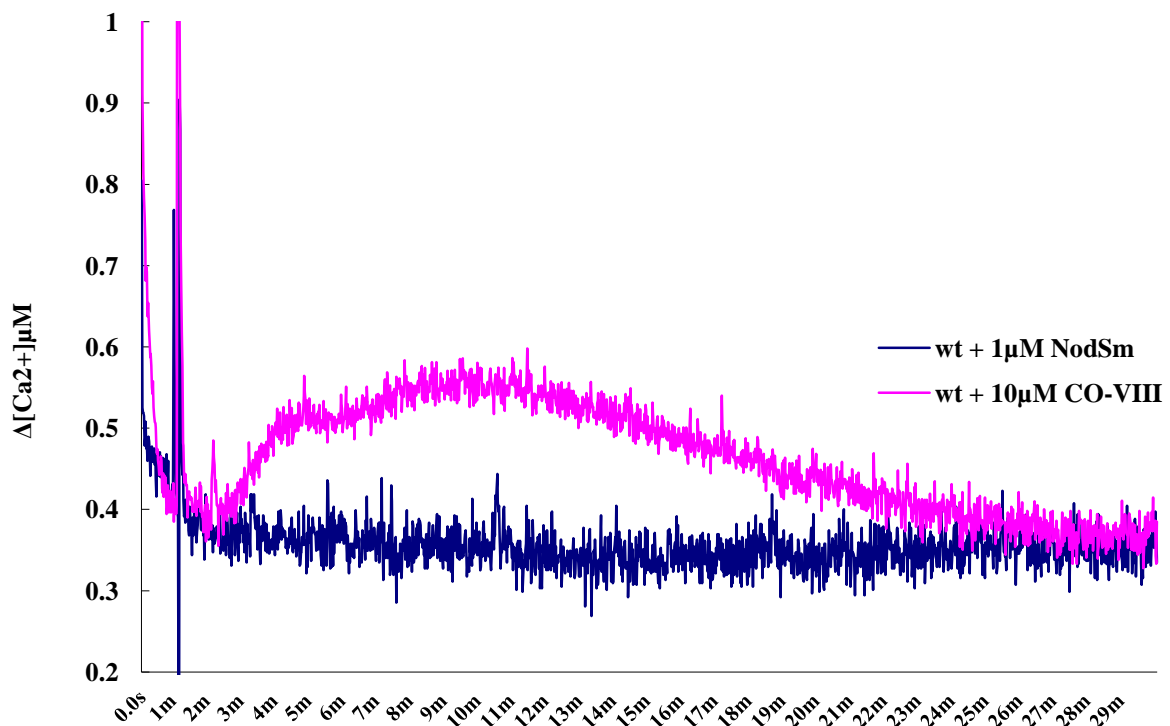
Fig.2 Changes in free calcium concentration in the cytosol of wild type col-0 *A. thaliana* plants after their treatment with LCO-IV(S,C16:2Δ2,9) or CO-VIII.

For each measurement five 14 days old *A. thaliana* plantlets expressing aequorine were treated with either 1μM LCO-IV (Ac, S, C16:2Δ2, 9) or 10μM CO-VIII. Strong Ca response was detected only for chito-octamer treatment.

60

plants were found among the p35S:GmLYR3/TmCERK1-HAST and empty vector transformants. The ratio between the number of selected fluorescent plants and total amount of analyzed plants (3 fluorescent for approx. 600 analyzed in case of p35S:GmLYR3/TmCERK1-HAST) suggested that the efficiency of transformation was less than 0.5%. As the ubiquitin promoter was driving expression of the DsRed protein, fluorescence was observed in both roots and shoots of the selected plants (Fig.1). These, few selected transformed plants were grown to produce seeds which were then germinated and analyzed under the fluorescent microscope. As expected for genetic segregation, the majority of the observed plants (80%) (F2 generation) appeared to be fluorescent.

Calcium response to Nod factors or CO-VIII of wild type A. thaliana and transgenic plants expressing GmLYR3/TmCERK1 or GmLYR3Tm/CERK1

The cytosolic calcium influx in response to LCO was first studied for wild type *A. thaliana* plants. Five14-days old *A. thaliana* plantlets, stably expressing aequorin, were treated either with 1µM *Sinorhizobium meliloti* Nod factor (LCO-IV (Ac, S, C16:2 Δ2, Δ9)) or 10µM chito-octamer (CO-VIII). Two elicitor independent rapid calcium responses, evoked, probably by mechanical stress, were detected within the first two minutes of measurement for all analyzed samples. Longer lasting calcium influx was observed for the plants treated with CO-VIII, whereas addition of LCO did not trigger a calcium response (Fig.2). Obtained results were suggesting that wild type *A. thaliana* plants are insensitive to LCO and thus could be used for studies of LCO specific activation of defense responses.

One of the transgenic lines possessing the strongest fluorescence and expected to express GmLYR3/TmCERK1 chimeric protein was used to study the calcium influx in response to LCO. With that aim five 14-days old seedlings were treated with either H_2O or 1 µM LCO-IV (Ac, S, C16:2 Δ2, 9). Each treatment was performed in triplicate. Both curves obtained in this experiment were containing smooth shoulders decreasing to the basal level within the first three minutes of measurement and so far were looking different to the curves observed with the wild type *A. thaliana* plants. Appearance of the shoulders was probably caused by a slight modification in the measurement procedure which led to the alignment of the two peaks corresponding to the mechanical stress. However, starting from the 3 minutes time point up to the end of measurement no calcium influx was detected either for H_2O or for LCO treated samples (Fig.3). With the aim to check the level of GmLYR3/TmCERK1chimeric protein expression, western blotting detection was performed in the crude extracts obtained from the fluorescent plants (data not shown). No immunoreactive signals that could correspond to the whole protein or its degradation product were detected. Analysis of two other transgenic lines revealed that they were also lacking expression of the chimeric receptor.

The obtained results suggested that in spite of the presence of the DsRed protein, the protein of interest GmLYR3/TmCERK1 was absent in the selected transgenic plants. As the initially performed transformation did not result in the creation of transgenic lines stably expressing LYR3/CERK1 chimeric proteins it was decided to repeat the transformation of *A. thaliana cerk1*plants with all chimeric constructions.
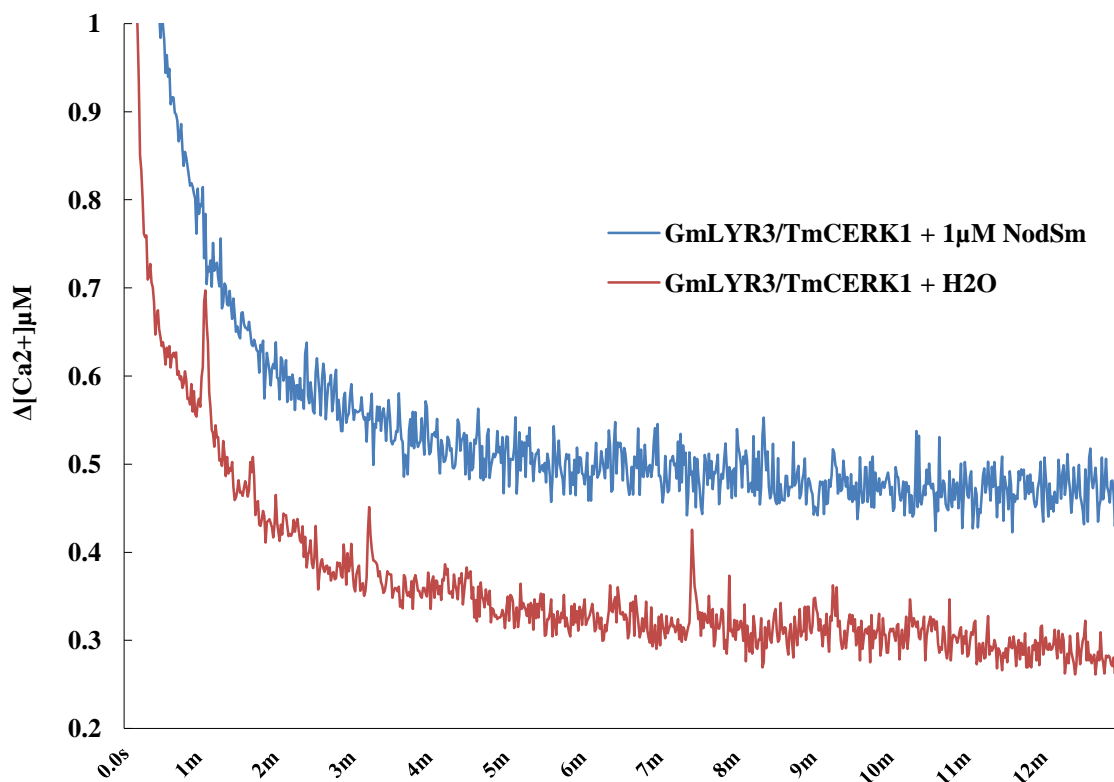
Fig.3 Changes in free calcium concentration in the cytosol of the *A. thaliana* plants transformed with the GmLYR3/TmCERK1 chimeric receptor.

Five 14 days old fluorescent plantlets were treated with 1μM LCO-IV(S,C16:2Δ2,9). Measurements were repeated three times with different seedlings and resulted in the absence of LCO dependent stress Ca response.
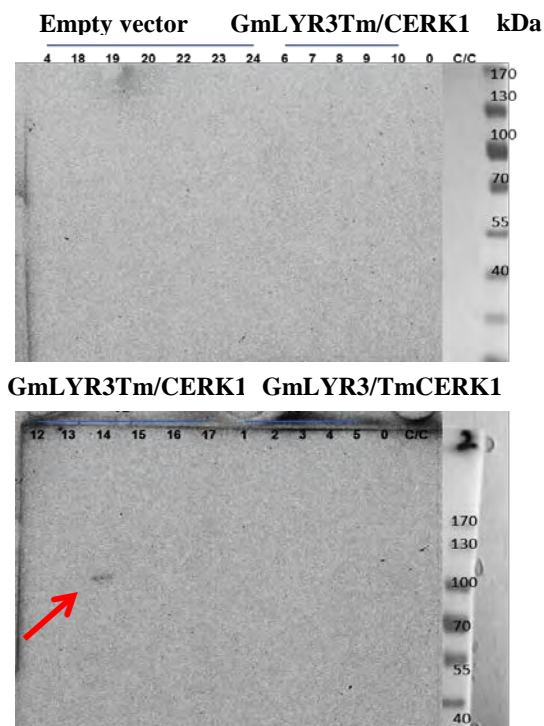
Fig.4 Immunodetection of the chimeric proteins in crude extracts from *A. thaliana* plants stably transformed with empty vector and GmLYR3Tm/CERK1, GmLYR3/TmCERK1 constructions.

For each transgenic line crude extracts were prepared from three 14 days old *A. thaliana* plantlets. Detection of chimeric proteins was performed with anti-HA-HRP antibodies. Faint band corresponding to the GmLYR3Tm/CERK1 (110 kDa) protein was observed only in one line, number 14.

Screening of transformed plants was realized through detection of red fluorescence, as described above. A few fluorescent plants (efficiency of transformation was as low as in previous experiment) were found among the p35S:GmLYR3Tm/CERK1-HAST, p35S:GmLYR3/TmCERK1-HAST and empty vector transformants. Each selected line was cultivated up to the F2 generation. To check the chimeric protein expression several F2 red fluorescent plants were analyzed by western blotting for each of the transgenic lines. The faint signal corresponding to the GmLYR3Tm/CERK1protein was detected only for one out of 18 analyzed lines (Fig.4). Plants belonging to this line were used to measure the calcium response after LCO treatment. Several modifications were introduced in the new experiment. As the studied chimera contained the GmLYR3 extracellular domain the *Sinorhizobium meliloti* Nod factor was replaced with the LCO produced by the soybean symbiont, *Bradyrhizobium japonicum* (LCO-V (Fuc, Me, C18:1)).The measurement was performed in a similar way to (fig.1) in case the LCO would trigger an early calcium response of short duration. The LCO concentration was decreased from 1 µM to 200 nM to be in agreement with the nM range affinity of the LYR3 proteins for the LCO. As a positive control wild type plants were treated with 1 µM CO-VIII. Measurement performed for the plantlets expressing GmLYR3Tm/CERK1 protein resulted in the absence of calcium influx after their treatment with H_2O or 200 nM LCO-V (Fuc, Me, C18:1). A strong calcium response was observed after addition of 1 µM CO-VIII to the wild type plants (Fig.5). Thus, according to the obtained data, GmLYR3Tm/CERK1 chimeric receptor expressed in *A. thaliana* stayed inactive in the presence of LCO.

Transient expression of LYR3/CERK1 chimeric proteins in the leaves of N. benthamiana.

As stable transformation of *A. thaliana* did not work for the majority of the chimeric constructions, together with the absence of LCO dependent calcium response in the transgenic plants containing the GmLYR3Tm/CERK1 construct, it was decided to use an alternative strategy for the LYR3/CERK1 activation study. The four LYR3/CERK1 chimeric proteins, the reconstituted CERK1 protein and the empty vector control were expressed in the leaves of *N. benthamiana,* in order to study their activation with LCO in this simpler system.

To produce the proteins, leaves of the plants were infiltrated with the same *Agrobacterium tumefaciens* bacteria as used for stable *A. thaliana* transformation. At 44 hours after infiltration (hai) in the leaves transformed with the p35S:GmLYR3/TmCERK1-HAST, p35S:GmLYR3Tm/CERK1-HAST, p35S:MtLYR3/TmCERK1-HAST and p35S:MtLYR3Tm/CERK1-HAST constructions the symptoms of hypersensitive response (HR) were detected. The observed HR was manifested by the number of water soaked lesions on the abaxial side of the leaf. At 48 hai rare areas of shiny water soaked lesions were observed in the leaves transformed with the p35S:CERK1/TmCERK1-HAST construction, whereas the leaves expressing Mt and GmLYR3/CERK1 chimeric proteins were flaccid and some necrotic desiccated zones were detected (Fig.6). Chimeric proteins with the trans-membrane region of LYR3 were triggering similarly strong HR as the chimera with the CERK1 Tms (data not shown). At this time point the quantification of HR was performed (Fig.7). All LYR3/CERK1
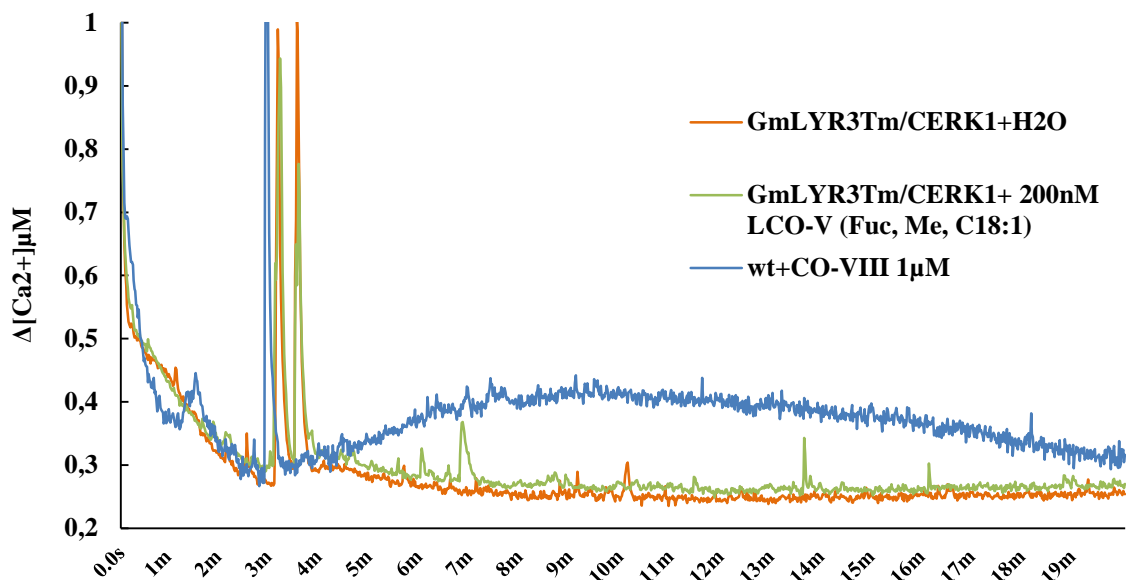
Fig.5 Changes in free calcium concentration in the cytosol of the wild type *A. thaliana* plants and plants expressing the GmLYR3Tm/CERK1 chimeric receptor.

Five 14 days old *A. thaliana* plantlets expressing aequorine and GmLYR3Tm/CERK1 chimeric protein were treated with either 200nM LCO-V (Fuc, Me, C18:1) or 1μM CO-VIII. Strong Ca response was detected only in case of chito-octamer treatment.
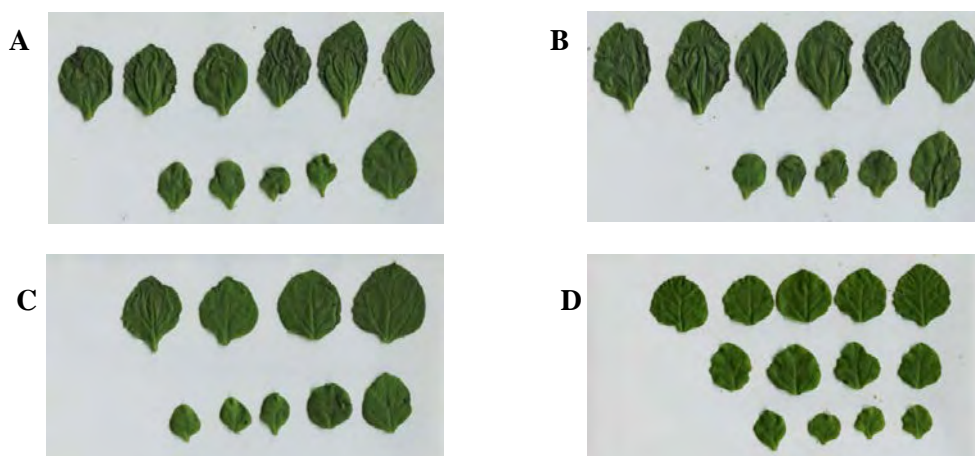
Fig.6 Visualization of the HR symptoms observed at 48 hai in the tobacco plants expressing LYR3/AtCERK1 chimeric proteins or native CERK1 receptor.

A- Plants expressing GmLYR3/TmCERK1, the leaves are faded and their desiccation has started; **B**- Plants expressing MtLYR3/TmCERK1, the HR is identic to the one observed for GmLYR3/TmCERK1; **C**- Plants expressing CERK1/TmCERK1, the leaves are not possessing flaccidity or desiccation; **D**- Plants expressing empty vector, no stress symptoms. Chimeric proteins with the trans-membrane region of LYR3 were triggering similarly strong HR as the presented chimeras.

chimeras triggered equally strong HR which was much stronger than in plants expressing the chimera reconstituting the native CERK1. At the last observations, performed at 72 hai, leaves expressing LYR3 chimeric receptors were consisting mainly of necrotic and desiccated tissue. Leaves expressing the reconstituted CERK1 receptor at this time point were fully covered with water soaked lesions, however lacking any necrosis or desiccation. No HR symptoms were observed at any time point for the plants transformed with the empty vector.

With the aim to check the expression levels of the chimeric proteins, *N. benthamiana* transformation was repeated and samples for western blotting were collected at 36 hai, before the appearance of the first HR symptoms. Relatively weak bands of equal intensity were detected with anti-HA antibodies for the two GmLYR3 chimeric receptors and the one reconstituting CERK1 (Fig.8).

Since for the two GmLYR3/CERK1 chimeric proteins no differences in terms of their expression or triggered HR were observed it was decided to perform the LCO activation treatment for only one chimeric protein, namely GmLYR3/TmCERK1. Plants expressing this chimeric receptor were infiltrated with H_2O or 1 μM LCO-V (Fuc, Me, C18:1) at 24 hai. Similar treatment was performed for the plants expressing the CERK1/TmCERK1 receptor. Both plants expressing LYR3 chimeric protein and reconstituted CERK1were also treated with 10 μM CO-V with the aim to check whether the CO would lead to the reduction of HR, according to a recently published inhibitory effect of this ligand on CERK1 activation (Liu, Liu, 2012). Quantification of the HR performed at 48 hours after bacterial infiltration resulted in the detection of equal stress response in the plants expressing GmLYR3/TmCERK1 protein treated with LCO-V (Fuc, Me, C18:1), CO-V or water (Fig.9). However the HR observed in this experiment was slightly reduced in comparison to the previous experiment. A decrease in the cell death response was observed for the plants expressing the chimera reconstituting native CERK1 receptor, but only specifically after treatment with CO-V (not with LCO).

Expression and evaluation of LCO binding activity of the LYR3/EFR chimeric proteins.

Chimeric constructions were prepared consisting of the *Medicago* or soybean LYR3 extracellular domains with their own TM regions or the TM region of EFR fused to the kinase domain of EFR. These chimeras, plus a chimera reconstituting native EFR and the empty vector control were expressed in *N. benthamiana* leaves. At 72 hai crude extracts obtained from leaves transformed with LYR3/EFR constructs were analyzed by western blotting (Fig.10A). All the LYR3/EFR chimeric proteins showed comparable and high levels of expression. In comparison to LYR3/EFR, the EFR/TmEFR protein was expressed to a lower degree. Equilibrium binding experiments with the LCO-IV (^{35}S,C16:2Δ2,9) ligand, performed on the membrane fraction extracted from the leaves, revealed a high binding activity for the chimera consisting of soybean ECD and EFR transmembrane and kinase regions - GmLYR3/TmEFR (Fig.11). The binding activity of the MtLYR3/EFR proteins was much lower and in case of the other chimeras was not greater than the background levels observed for the empty vector control and for the chimera reconstituting native EFR. With the aim to check the
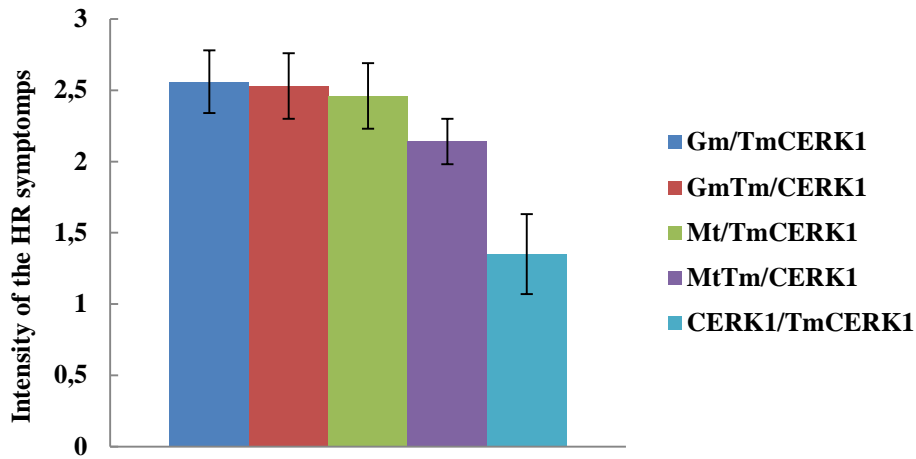
Fig.7 Quantification of the HR in the leaves of *Nicotiana benthamiana* plants expressing LYR3/AtCERK1 chimeric proteins and native CERK1 receptor.

Each chimeric protein was expressed in five *N. benthamiana* plants for 48 hours when the quantification of the HR was done. The intensity of the stress symptoms was measured by using the scale: 0-no stress symptoms, 1- first symptoms, rare water soaked lesions; 2-strong symptoms, generalized water soaked lesions, leaf flaccidity; and 3- necrosis and desiccation of the leaf. All LYR3/AtCERK1 chimeras triggered equally strong HR which was larger than in the plants expressing the chimera reconstituting native CERK1.
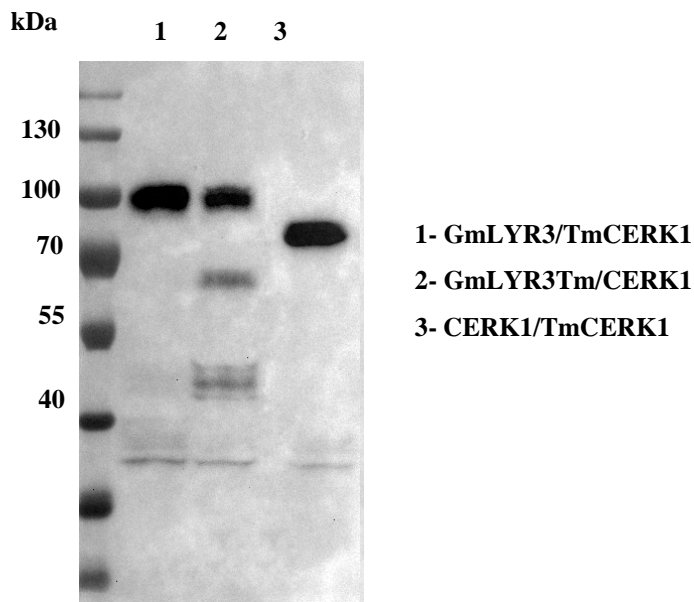
1- GmLYR3/TmCERK1

2- GmLYR3Tm/CERK1

3- CERK1/TmCERK1

Fig.8 Immunodetection of the chimeric proteins in crude extracts from *N. benthamiana leaves.*

N. benthamiana samples for western blotting were collected at 36 hai. Polypeptides corresponding to GmLYR3/TmCERK1(100 kDa), GmLYR3Tm/CERK1(100 kDa) and CERK1/TmCERK1(80 kDa) chimeric proteins were detected with anti-HA-HRP antibodies.

66

level of the chimeric proteins expression in the membrane extracts, western blotting was performed (Fig.10B). Strong degradation probably explaining the lack of binding was observed for GmLYR3Tm/EFR, however, all other chimeras were present in similar high levels.

From these results the chimera possessing the strongest binding activity i.e. GmLYR3/TmEFR was chosen for further studies together with the EFR reconstituting chimera as a control.

***Measurement of ethylene production in the leaves of N. benthamiana expressing LYR3/EFR chimeric proteins after their treatment with NodSm factor.***

For the stress ethylene measurements leaves of *N. benthamiana* were infiltrated with *A. tumefaciens* carrying p35S:GmLYR3/TmEFR-HAST, EFR/TmEFR-HAST or empty vector constructions. At 72 hai 5 mm diameter leaf disks were dissected out from the infected leaves and incubated over-night in water to eliminate ethylene evoked by the mechanical stress. Stimulation of ethylene production was performed at 86 hai. With that aim samples (five leaf disks per sample) expressing GmLYR3/TmEFR or EFR/TmEFR proteins were incubated for 2 hours in water containing 1 µM LCO-IV (S, C16:2Δ2,9), 5 µM elf18 or H_2O. Similar treatments were performed for the sample transformed with the empty vector. Ethylene measurements showed an absence of ethylene emission in the GmLYR3/TmEFR sample after treatment with 1 µM LCO, 5 µM elf18 or water (Fig.12A). For the EFR/TmEFR sample a noticeable ethylene signal (4,4 pMol/mg/h) was detected only after treatment with 5µM elf18. No ethylene was produced in the empty vector sample after its treatment with different elicitors.

Absence of ethylene production in response to LCO treatment could be explained by the inability of Nod factor, due to its physico-chemical properties, to penetrate the cutine of epidermal cells to reach the cell plasma membrane where the activation of GmLYR3/TmEFR chimeric receptor should happen. With the aim to improve LCO penetration the experiment was repeated, except that the activation of the chimeric receptors was attempted by pressure infiltration of 1 µM LCO-IV (S, C16:2Δ2,9), 5 µM elf18 or water to the abaxial side of the leaf disks. Additionally a GmLYR3/TmEFR leaf sample was treated in a similar way to the previous experiments but with an increased concentration of 10 µM NodSm factor to exclude the possibility that the previously used 1 µM concentration was insufficient for this receptor activation. The measurements showed an absence of ethylene emission by the GmLYR3/TmEFR sample after its infiltration with water, 5 µM elf18 or 1 µM LCO. Treatment with 10 µM LCO also did not lead to ethylene production (Fig.12B). For the EFR/TmEFR sample an ethylene response (4,3 pMol/mg/h) was detected specifically with 5 µM elf18. No ethylene was detected for the empty vector sample. A rise in the basal ethylene level was observed for all infiltrated samples. In this case ethylene emission was probably evoked by the mechanical stress due to the injection of elicitors.
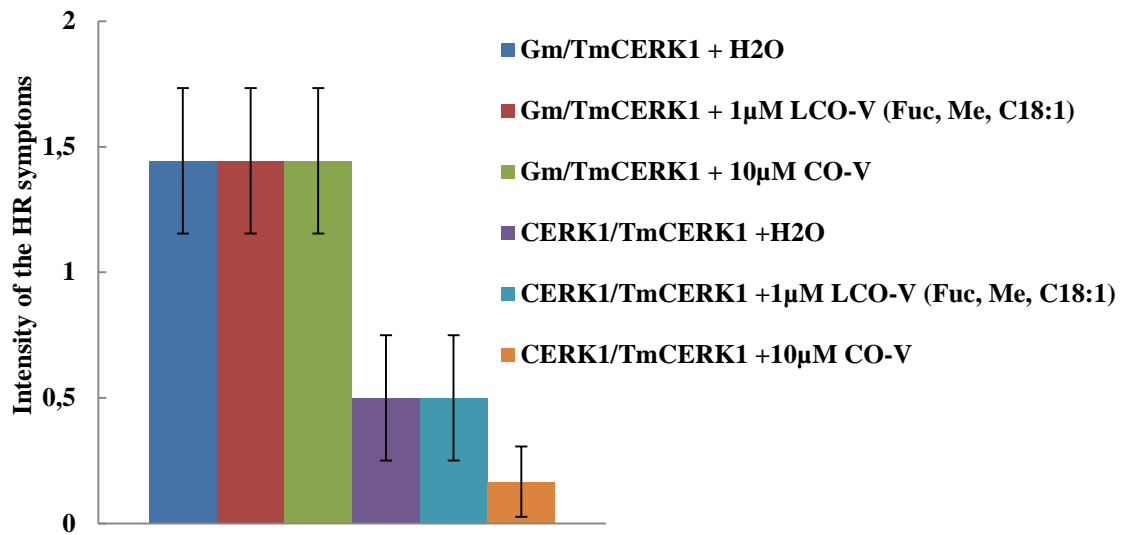
Fig.9 Quantification of the HR after treatment of *N. benthamiana* plants expressing chimeric receptors with LCO-V (Fuc, Me, C18:1) or CO-V.

Quantification of the HR at 48hai was done by using the same scale (from 0 to 3) as indicated in fig.7 and resulted in a general weakening of stress symptoms in comparison to the one observed previously probably due to an additional infiltration of the plants with the ligands. Strong HR insensitive to the treatments with 10µM CO-V or 1µM LCO-V (Fuc, Me, C18:1) was observed for the plants expressing GmLYR3/TmCERK1. Chimera reconstituting native CERK1 was triggering weaker cell death symptoms which were reduced after its treatment with CO-V.
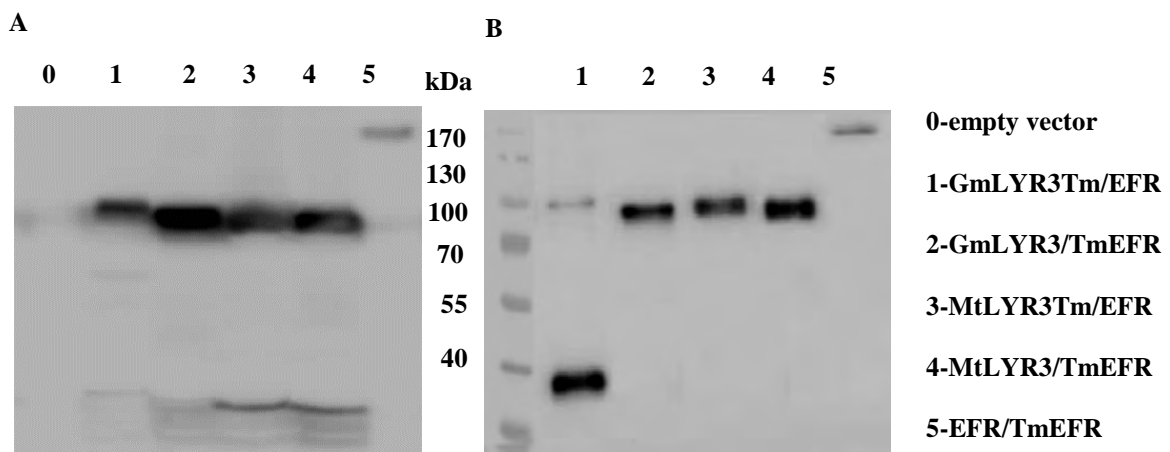
Fig.10 Detection of GmLYR3 and MtLYR3/EFR and EFR/TmEFR chimeric proteins in the crude extracts and microsomal fractions obtained from *N. benthamiana* leaves at 72 hai.

Polypeptides corresponding to the chimeric receptors were detected with anti-HA-HRP antibodies in the extracts obtained from the transformed tobacco leaves (**A**) and membrane fractions (**B**) which were used for the binding experiments. In both crude extract and membrane fraction EFR/TmEFR protein was less abundant in comparison to LYR3/EFR chimeras. GmLYR3Tm/EFR protein was strongly degraded in microsomal fraction.

68

Measurement of ethylene production in the leaves of N. benthamiana expressing AtCERK1/TmEFR chimeric protein after their treatment with CO-VIII.

A study of ethylene production, triggered by the AtCERK1/TmEFR chimeric receptor after its treatment with CO-VIII, was used to clarify whether the absence of LCO dependent ethylene production observed for GmLYR3/TmEFR protein could be caused by the physico-cgemical properties of LCO. CO-VIII being less hydrophobic than LCO should have less difficulties in passing the plant cell wall and activating membrane located receptor. To test this hypothesis an AtCERK1/TmEFR chimeric protein was constructed and expressed in the leaves of *N. benthamiana* and a leaf sample was prepared as described above and treated for 2 hours in the presence of 10 µM CO-VIII or with water. As the positive control, transient expression of EFR/Tm/EFR receptor and its treatment with 5 µM elf18, 10 µM CO-VIII or water was performed. In the subsequent measurements no ethylene was detected for the AtCERK1/TmEFR sample after treatment with CO-VIII or water. A strong ethylene response (5,8 pmol/mg/h) was observed in the EFR/Tm/EFR sample specifically following treatment with 5 µM elf18 (Fig.12C).

Measurement of ethylene production in the leaves of N. benthamiana co-expressing GmLYR3/TmEFR and GmLYR3/TmBAK1 chimeric proteins after treatment with NodSm factor.

In *vivo* perception of bacterial PAMP (elf18) by EFR leads to its hetero-dimerization with another *A. thaliana* receptor BAK1 and this is crucial for EFR activation and signal transduction (Roux, Schwessinger, 2011).We therefore decided to investigate ethylene emission in response to LCO treatment in leaf samples co-expressing the GmLYR3/TmEFR chimeric protein with a protein consisting of the soybean LYR3 extracellular region and *A. thaliana* BAK1 trans-membrane region and kinase domain, GmLYR3/TmBAK1. Once the corresponding genetic construction was cloned, co-expression as well as separate expression of GmLYR3/TmBAK1 and GmLYR3/TmEFR was performed. Additionally proteins reconstituting EFR (EFR/TmEFR) and BAK1 (BAK1/TmBAK1) were co-expressed and expressed independently from each other in the *N. benthamiana* leaves.

At 40 hai, HR symptoms, represented by a number of small areas with water soaked lesions, were observed on the abaxial side of the leaves expressing the BAK1/TmBAK1 receptor alone and co-expressing BAK1/TmBAK1 together with EFR/TmEFR. Four hours later at 44 hai similar symptoms were detected in leaves co-expressing GmLYR3/TmEFR and GmLYR3/TmBAK1. At this time point weaker symptoms were observed in the leaves expressing EFR/TmEFR protein (Fig.13). At 72 hai leaves expressing BAK1/TmBAK1, BAK1/TmBAK1 together with EFR/TmEFR and GmLYR3/TmEFR together with GmLYR3/TmBAK1 showed HR symptoms of similar intensity represented by the shiny water soaked lesions fully covering the abaxial side of the leaves. Leaves expressing the EFR/TmEFR protein, at this time point, demonstrated a much less intensive HR. During the complete time period no stress symptoms were detected in the leaves expressing either GmLYR3/TmEFR or GmLYR3/TmBAK1 chimeric proteins alone. Therefore, in the next experiment aiming to measure an ethylene response activation by LCO, all the samples were harvested at 48 hai
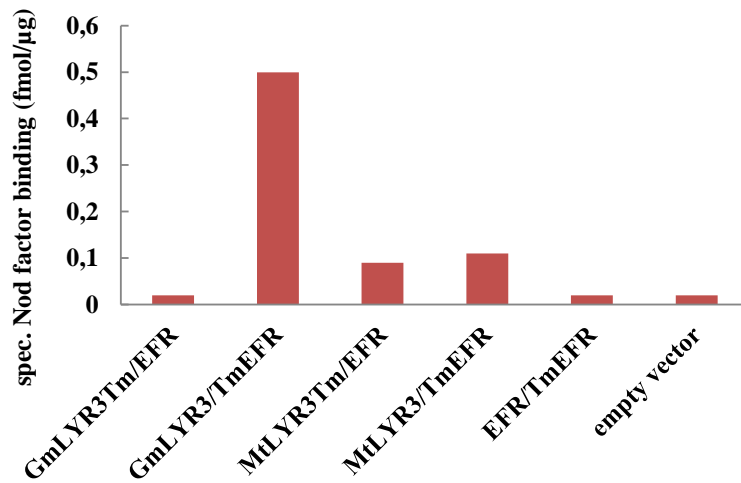
Fig.11 Specific binding of LCO-IV(^{35}S,C16:2Δ2,9) to the GmLYR3 and MtLYR3/EFR chimeric proteins.

Specific binding was measured for 25μg of membrane proteins obtained from transformed *N. benthamiana* leaves and resulted in the detection of strong binding for the GmLYR3/TmEFR, comparable to the binding observed for native GmLYR3 protein. For two MtLYR3/EFR receptors binding was strongly reduced. No binding to LCO-IV (^{35}S,C16:2Δ2,9) was detected for the GmLYR3Tm/EFR, EFR/TmEFR and empty vector.
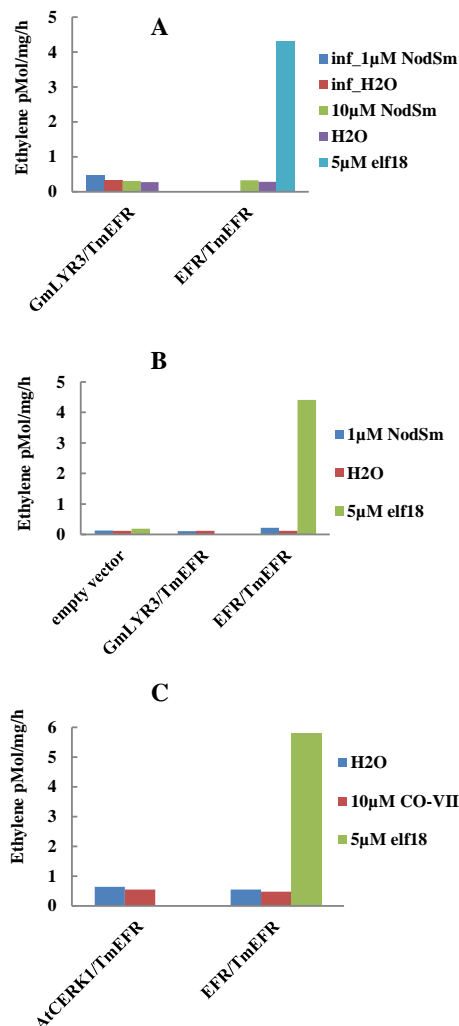
Fig.12 Induction of ethylene biosynthesis with different elicitors in *N. benthamiana* leaves expressing GmLYR3/TmEFR, EFR/TmEFR and AtCERK1/TmEFR chimeric proteins.

Emission of ethylene was analyzed in *N. benthamiana* samples at 86 hai (five 5mm leaf disks per sample/3 repetitions) and resulted in the detection of signal only in case of EFR/TmEFR treatment with 5μM elf18 (**A**). Improved treatments, via LCO infiltration (inf) or with more concentrated LCO did not lead to the LCO dependent ethylene emission (**B**). No ethylene response was detected either after AtCERK1/TmEFR chimeric receptor treatment with CO-VIII (**C**).

70

and not at 72 hai to try to avoid the HR. However, despite this earlier harvesting, at the moment of ethylene measurement corresponding to a 72 hai time point, strong HR symptoms were present in the leaves expressing BAK1/TmBAK1, BAK1/TmBAK1 + EFR/TmEFR, GmLYR3/TmEFR + GmLYR3/TmBAK1 and to a lower degree in leaves expressing EFR/TmEFR. Measurement of ethylene elicitation showed an absence of the gas emission in response to water, 1 µM LCO-IV (S, C16:2Δ2,9) or 5 µM elf 18 in all samples expressing alone or co-expressing GmLYR3/TmEFR and GmLYR3/TmBAK1 chimeras. Surprisingly no ethylene response was observed for one out of two positive controls, BAK1/TmBAK1 + EFR/TmEFR after treatment with 5 µM elf 18. Emission of ethylene was detected only for the EFR/TmEFR sample treated with 5µM elf18 (data not shown).

Since most of the samples showed stress symptoms that could have negatively affected the functionality of the chimeric proteins, the experiment was repeated by shifting the harvesting time to 24 hours (24 hai) and the time of ethylene measurement to 48 hai. To check whether all proteins were enough expressed at 48 hai, western blot analysis at this time point was performed. Immuno-reactive signals at molecular masses corresponding to those of the chimeric proteins, 150 kDa for EFR/TmEFR, 90 kDa for BAK1/Tm/BAK1, 100 kDa for GmLYR3/TmEFR and 110 kDa for GmLYR3/TmBAK1 were detected in the relevant samples (Fig.14). In the case of GmLYR3/TmEFR and GmLYR3/TmBAK1 co-expression, despite the close molecular mass of the two proteins the more extended shape of the main band (100 kDa-110 kDa) and the presence of the minor bands corresponding to both GmLYR3/TmEFR and GmLYR3/TmBAK1 validated the co-expression of the two proteins. Following treatment of the leaf samples with water, 1 µM LCO-IV (S, C16:2Δ2,9) or 5 µM elf 18 an ethylene response was detected for both positive controls expressing either EFR/TmEFR chimeric protein alone (0.73 pMol/mg/h) or co-expressing EFR/TmEFR together with BAK1/TmBAK1(0.72 pMol/mg/h) after treatment with 5 µM elf18 (Fig.15). Absence of ethylene production in response to LCO or elf 18 treatments was observed for BAK1/TmBAK1, GmLYR3/TmEFR or GmLYR3/TmBAK1samples. Interestingly the basal levels of ethylene were increased in all samples expressing chimeric proteins containing the BAK1 kinase i.e. BAK1/TmBAK1, BAK1/TmBAK1 + EFR/TmEFR, and GmLYR3/TmBAK1 in comparison to the ethylene backgrounds observed for the other chimeras (EFR/TmEFR and GmLYR3/TmEFR). A very strong ethylene response was detected for the sample co-expressing the GmLYR3/TmEFR and GmLYR3/TmBAK1 chimeric proteins, but this was independent of LCO treatment as it occurred after either water (1.31 pmol/mg/h) or 1 µM LCO-IV (S, C16:2 Δ29) (1.45 pmol/mg/h) treatment.

Measurement of ethylene production in response to NodSm factor in the leaves of N. benthamiana co-expressing GmLYR3/TmEFR and GmLYR3/TmBAK1 chimeric proteins pretreated with CO-IV and in the leaves co-expressing MtLYR3/TmEFR and GmLYR3/TmBAK1.

One of the explanations for the strong non-specific ethylene response and HR observed in the plants co-expressing GmLYR3/TmEFR and GmLYR3/TmBAK1 could be auto-activation of the EFR kinase due to ligand-independent hetero-dimerization between GmLYR3/TmBAK1 and
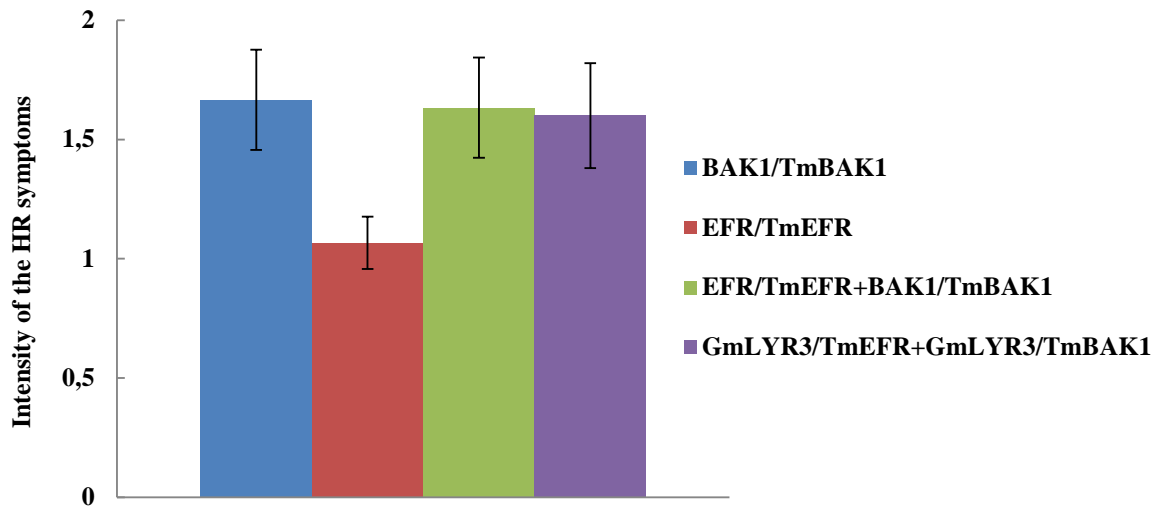
Fig.13 Quantification of the HR in the leaves of *N. benthamiana* plants expressing alone or co-expressing GmLYR3/TmEFR and GmLYR3/TmBAK1 chimeric proteins as well as native EFR and BAK1 receptors.

Quantification was performed at 44 hai. HR was observed in five *N. benthamiana* plants for each chimeric protein or proteins combination. Intensity of the stress symptoms was measured by using the same scale as before (0-no stress symptoms, 1- first symptoms, rare water soaked lesions; 2-strong symptoms, generalized water soaked lesions, leaf flaccidity; and 3- necrosis and desiccation of the leaf) and resulted in detection of equally strong HR for BAK1/TmBAK1, EFR/TmEFR+BAK1/TmBAK1 and GmLYR3/TmEFR+GmLYR3/TmBAK1 whereas EFR/TmEFR was triggering weaker stress symptoms.
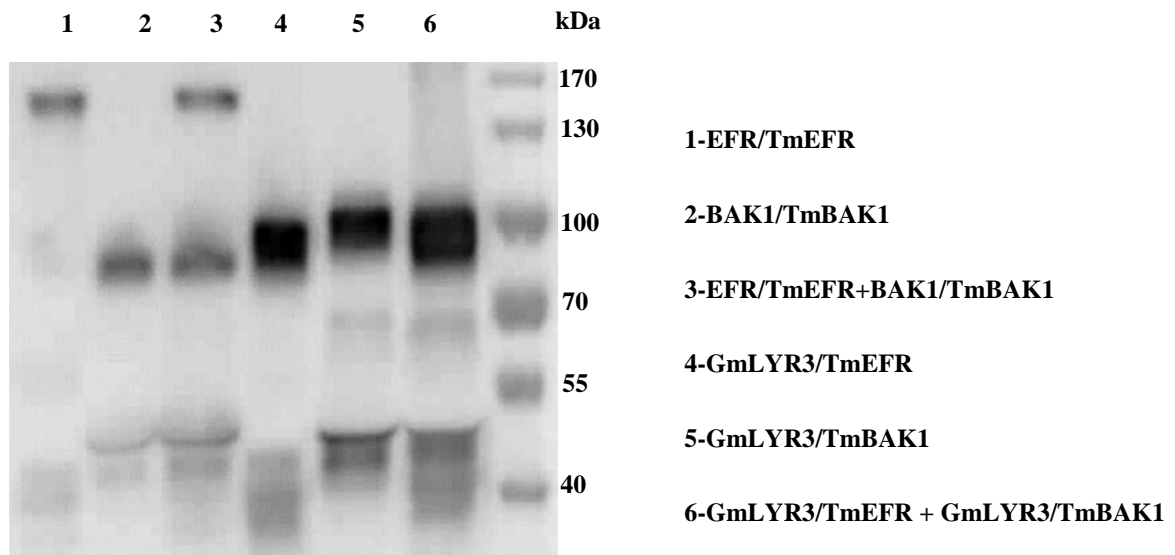
Fig.14 Immunodetection of single or co-expressed GmLYR3/TmEFR and GmLYR3/TmBAK1 chimeric proteins and native EFR and BAK1 in the crude extracts from *N. benthamiana* leaves.

Polypeptides corresponding to all chimeric receptors and their combinations were detected with anti-HA-HRP antibodies in crude extracts obtained from *N. benthamiana* leaves at 48 hai.

GmLYR3/TmEFR. The stability of such dimers could be strengthened by the homo-dimerization between the two identical GmLYR3 extracellular domains of these chimeras. Based on these assumptions two modifications which could interfere with the chimeric proteins hetero-dimerization or stability of formed dimers were tested.

Firstly plants co-expressing GmLYR3/TmBAK1 and GmLYR3/TmEFR were pretreated with CO-IV. This pre-treatment was proposed because of the recently shown negative effect of a short CO (CO-V) on CERK1 oligomerization and binding, and because of the known ability of LYR3 to bind CO-IV with low affinity ($KI < 10\mu M$) (Fliegmann et al., 2013).The aim was to reduce or eliminate the HR symptoms by interrupting homo-dimer formation and before further ligand-induced ethylene measurements. Leaves of the plants expressing GmLYR3/TmBAK1 and GmLYR3/TmEFR chimeric receptors were infiltrated with 10µM CO-IV at 24 hai. The HR quantification done at 48 hai and 74 hai resulted in the absence of any effect of CO-IV on the HR which was equally strong for treated and untreated plants (data not shown). The measurement of ethylene was therefore not done because of this cell death response.

In the second experiment GmLYR3/TmBAK1 was co-expressed with MtLYR3/TmEFR instead of GmLYR3/TmEFR. It was expected that the ligand independent dimerization between these two proteins would be less stable due to the number of differences present in MtLYR3 and GmLYR3 extracellular domains. Chimeric proteins MtLYR3/TmEFR with GmLYR3/TmBAK1 and GmLYR3/TmEFR with GmLYR3/TmBAK1were co-expressed in the tobacco leaves for 48 hours and HR was quantified. The results showed a two-fold reduction in the cell death response for the MtLYR3/TmEFR and GmLYR3/TmBAK1 protein couple in comparison to co-expressed GmLYR3/TmEFR and GmLYR3/TmBAK1 (Fig.16). Since less HR was observed in the case of MtLYR3/TmEFR and GmLYR3/TmBAK1 co-expression, an experiment aimed at measuring the ethylene response activation with LCO in this sample was performed. Samples from transgenic *N. benthamiana* leaves expressing GmLYR3/TmEFR, MtLYR3/TmEFR, GmLYR3/TmBAK1 and co-expressing EFR/TmEFR with BAK1/TmBAK1, GmLYR3/TmEFR with GmLYR3/TmBAK1 and MtLYR3/TmEFR with GmLYR3/TmBAK1 were harvested (at 24hai) and treated (at 48 hai) with water, 1 µM LCO-IV (Ac, S, C16:2 Δ2, Δ9) or 5 µM elf 18. Western blotting detection performed at this time point suggested that the chimeric proteins were equally well expressed in both single and co-transformed leaves (Fig.17). A relatively strong ethylene response (0.72 pmol/mg/h), triggered by 5 µM elf 18, was detected in the control sample co-expressing EFR/TmEFR with BAK1/TmBAK1 (Fig.18). No gas emission was observed in response to the treatment with elicitors in GmLYR3/TmEFR, MtLYR3/TmEFR and GmLYR3/TmBAK1 samples. A strong elicitor independent ethylene response (1.2-1.8 pmol/mg/h) was detected in the sample co-expressing GmLYR3/TmEFR and GmLYR3/TmBAK1 chimeric proteins. Non-specific emission of ethylene to a lower degree was observed for the sample co-expressing MtLYR3/TmEFR and GmLYR3/TmBAK1 (0,3-0,5 pmol/mg/h). No clear, specific LCO induction of the ethylene response was seen for these two samples.
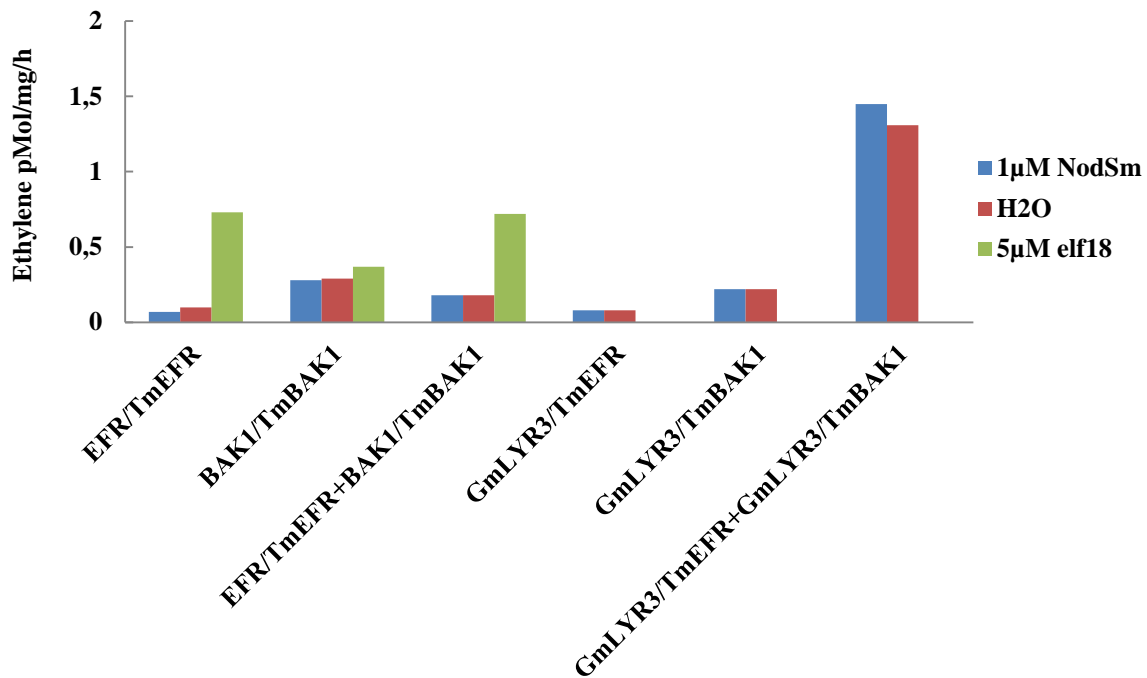
**Fig.15 Induction of ethylene biosynthesis with different elicitors in *N. benthamiana* leaves expressing alone or co-expressing GmLYR3/TmEFR and GmLYR3/TmBAK1 chimeric proteins as well as native BAK1 and EFR receptors.**

Emission of ethylene was analyzed in *N. benthamiana* samples at 48 hai (five 5mm leaf disks per sample/3 repetitions) and resulted in the detection of ethylene response after elf18 treatment in the samples containing native EFR and strong ligand independent response in case of GmLYR3/TmEFR and GmLYR3/TmBAK1 co-expression.
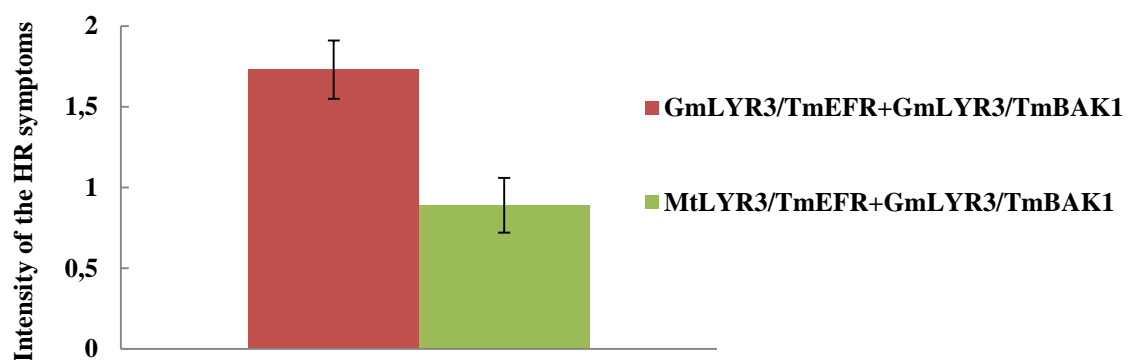
Fig.16 Quantification of the HR in the leaves of *N. benthamiana* plants co-expressing GmLYR3/TmEFR with GmLYR3/TmBAK1 and MtLYR3/TmEFR with GmLYR3/TmBAK1.

Quantification was performed at 48hai and resulted in the detection of much reduced HR in case of MtLYR3/TmEFR co-expression with GmLYR3/TmBAK1.

74

To exclude the possibility that the co-expression of LYR3 containing chimeras could negatively influence their ability to bind LCO, equilibrium binding for all chimeric receptors and their co-expressed combinations was performed. Strong binding of LCO-IV(35S,C16:2Δ2,9) was detected in leaf membrane extracts for all individual LYR3 containing chimeras and for co-expressed chimeric proteins, GmLYR3/TmEFR with GmLYR3/TmBAK1 and MtLYR3/TmEFR with GmLYR3/TmBAK1 (Fig.19).

Conclusions and discussion.

Results obtained in this study have shown that col-0 *A. thaliana* plants expressing aequorine do not activate a stress calcium response after treatment with NodSm factor (LCO-IV (S, C16:2Δ29)) in contrast to CO-VIII, suggesting that LCO is unable to trigger this defense response in *A. thaliana*. Thus, *A. thaliana* is a good heterologous system to study whether LCO binding to LYR3 chimera can lead to LCO dependent calcium responses (Fig.2).

In the experiments with plants stably expressing LYR3/CERK1 chimeric proteins we faced several problems which affected the obtained results. Firstly, due to low efficiency of transformation no red fluorescent plants considered as transformed and expected to express the chimeric proteins were obtained for the MtLYR3/TmCERK1, MtLYR3Tm/CERK1 and CERK1/TmCERK1 constructions. Secondly, among the few fluorescent transformants found for GmLYR3/TmCERK1 and GmLYR3Tm/CERK1 only in one plant expression of the GmLYR3Tm/CERK1 protein was confirmed by immuno-detection (Fig.4). Absence of chimeric proteins in all other fluorescent plants could point to the chimeric genes being silenced or to problems of their co-integration with the fluorescent marker into the genome of *A. thaliana*. Lack of calcium influx observed after the treatment of transgenic plants expressing the GmLYR3Tm/CERK1 protein with *B. japonicum* Nod factor suggests that this chimeric receptor remained inactive in the presence of LCO (Fig.5). However, the low level of this protein expression could have been insufficient for defense response activation and therefore we cannot exclude the possibility that stronger expression of GmLYR3Tm/CERK1 would trigger calcium influx in response to LCO. Additionally it should be noted that the trans-membrane region originating in this chimeric protein from the GmLYR3 receptor might not be optimal for either LCO binding (see Fig. 11) or the activation of the CERK1 kinase. Several studies have shown that chimeric protein activation works better if the kinase domain is fused to its native Tm (Brutus et al., 2010).

Summarizing the above observations, stable transformation of *A. thaliana* plants with all chimeric proteins carrying different trans-membrane regions and with positive CERK1/TmCERK1 control should be repeated by introducing such modifications in the transformation procedure which would improve its efficiency. Also because of the limited expression observed for GmLYR3Tm/CERK1 driven by the 35S promoter the use of stronger promoters providing better expression in *A. thaliana* should be considered. To exclude the possibility of gene silencing, genetic
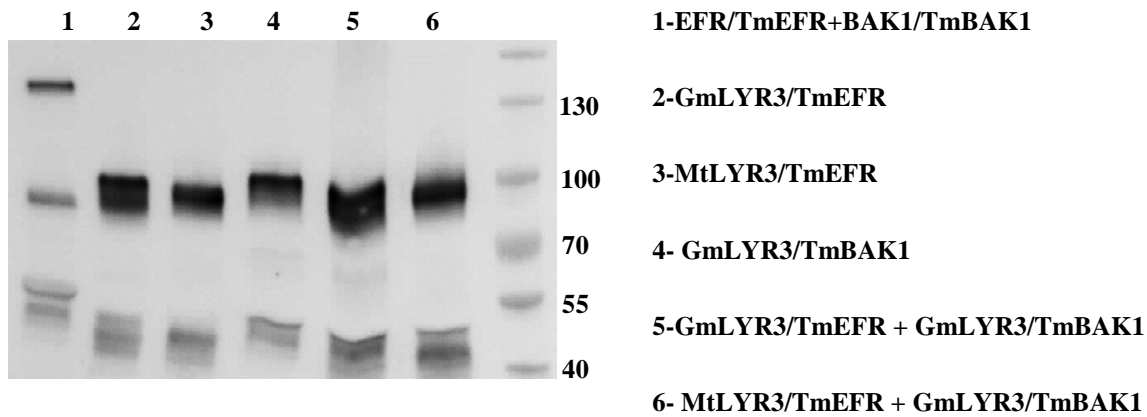
Fig.17 Immunodetection of single or co-expressed GmLYR3/TmEFR and GmLYR3/TmBAK1 or MtLYR3/TmEFR and GmLYR3/TmBAK1 chimeric proteins as well as native EFR and BAK1 receptors in the crude extracts from *N. benthamiana* leaves.

Polypeptides corresponding to all chimeric receptors and their combinations were detected with anti-HA-HRP antibodies in crude extracts obtained from *N. benthamiana* leaves at 48 hai.
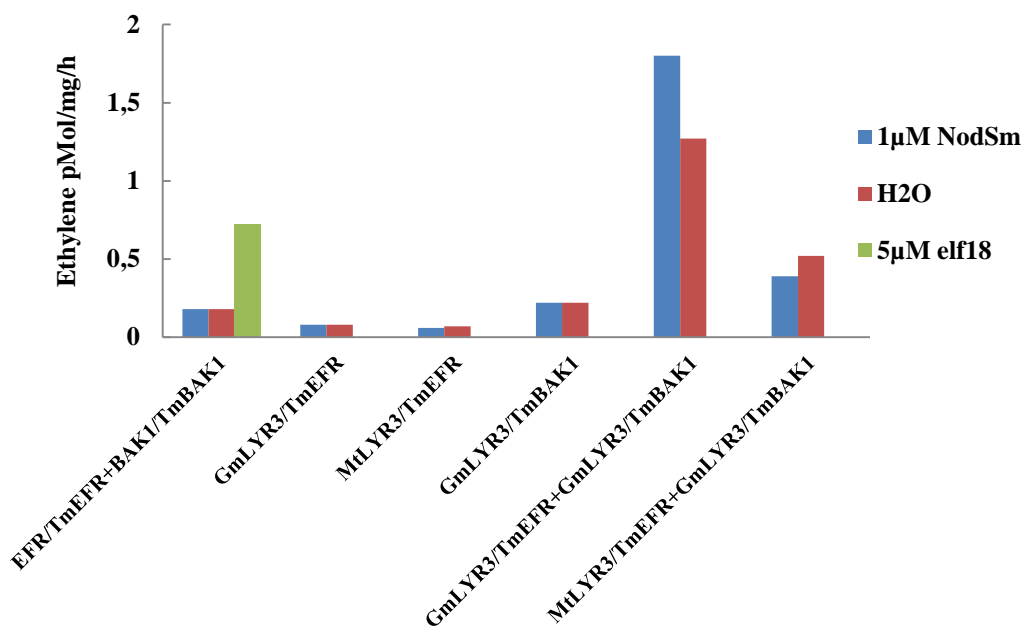
Fig.18 Induction of ethylene biosynthesis with different elicitors in *N. benthamiana* leaves expressing alone or co-expressing GmLYR3/TmEFR and MtLYR3/TmEFR with GmLYR3/TmBAK1 chimeric proteins as well as native BAK1 and EFR receptors.

Emission of ethylene was analyzed in *N. benthamiana* samples at 48 hai (five 5mm leaf disks per sample/3 repetitions) and resulted in the detection of ethylene response after elf18 treatment in the sample co-expressing EFR and BAK1 proteins. Strong ligand independent response was observed in case of GmLYR3/TmEFR and GmLYR3/TmBAK1 co-expression. Similar but much reduced non-specific ethylene production was detected in the sample co-expressing MtLYR3/TmEFR and GmLYR3/TmBAK1 chimeric proteins.

76

constructions for new transformation could be supplemented with the gene encoding P19, the siRNA binding protein (Lakatos et al., 2004).

Strong cell death response triggered by heterologous production of LYR3/CERK1 and CERK1/TmCERK1 proteins in the leaves of *N. benthamiana* points to the auto-activation of the chimeras after their expression in this system (Fig.6, 7). In the case of CERK1/TmCERK1, this observation is in agreement with previously reported ligand independent oligomerization of CERK1 driven by the 35S promoter in *A. thaliana* (Liu et al., 2012) or induction of defense-like responses in case of *CERK1* overexpression in *N. benthamiana* leaves (Pietraszewska-Bogiel et al., 2013). According to the immuno-detection results, the LYR3/CERK1 and CERK1/TmCERK1 proteins were very strongly and equally expressed in the *N. benthamiana* leaves, which probably led to their homooligomerization and subsequent activation of the CERK1 kinase up to a level sufficient to trigger the cell death response (Fig.8). However it is notable that the HR triggered by CERK1/TmCERK1 was much weaker than the stress response observed in the case of LYR3/CERK1 expression. This could point to better homodimerization of the LYR3/CERK1 chimeras, resulting in the reinforcement of their auto-activation. As the MtLYR3 protein has recently been shown to form homodimers in *N. benthamiana* leaves (J. Fliegmann and A. Jauneau, unpublished data) it could be expected that the LYR3/CERK1 chimeras are additionally stabilized by the homodimerization between Mt or Gm LYR3 ectodomains.

The absence of changes in the intensity of HR symptoms observed after pretreatment of plants expressing GmLYR3/TmCERK1 protein with LCO-V (Fuc, Me, C18:1) or CO-V suggests that both elicitors in the given conditions were not able to affect the biological activity of the chimeric protein. In contrast CO-V partially inhibited the stress responses triggered by the CERK1/TmCERK1 protein, supporting previously published data suggesting that binding of this ligand leads to the interruption of CERK1 dimerization which is required for its active state (Fig.9) (Liu et al., 2012).

Thus, the study of defense responses triggered by LYR3/CERK1 chimera in response to LCO would need, to use a weaker promoter to lower their transient expression in *N. benthamiana* in order to avoid an autoactivation leading to HR in absence of ligand, which is in contrast to the suggestions made for improving the expression of the same proteins in stable transformants of *A. thaliana*.

Concerning the EFR chimera, the absence of ethylene production in response to LCO-IV (S, C16:2Δ2,9) treatment observed for the GmLYR3/TmEFR chimera, together with the strong ethylene response detected for the weaker expressed EFR/TmEFR protein after its treatment with elf18, suggests that the GmLYR3/TmEFR chimeric receptor is not sensitive to and could not be activated by LCO (Fig.12A). The ability to bind LCO, validated for the GmLYR3/TmEFR protein in equilibrium binding experiments with LCO-IV(^{35}S,C16:2Δ2,9), suggests that the problem is not with intrinsic ligand binding by the GmLYR3/TmEFR protein (Fig.11). The lack of ethylene response after GmLYR3/TmEFR chimera treatments, designed to improve access of LCO (infiltration or exposure with LCO at 10 µM concentration), points to the problem not being either due to ligand accessibility
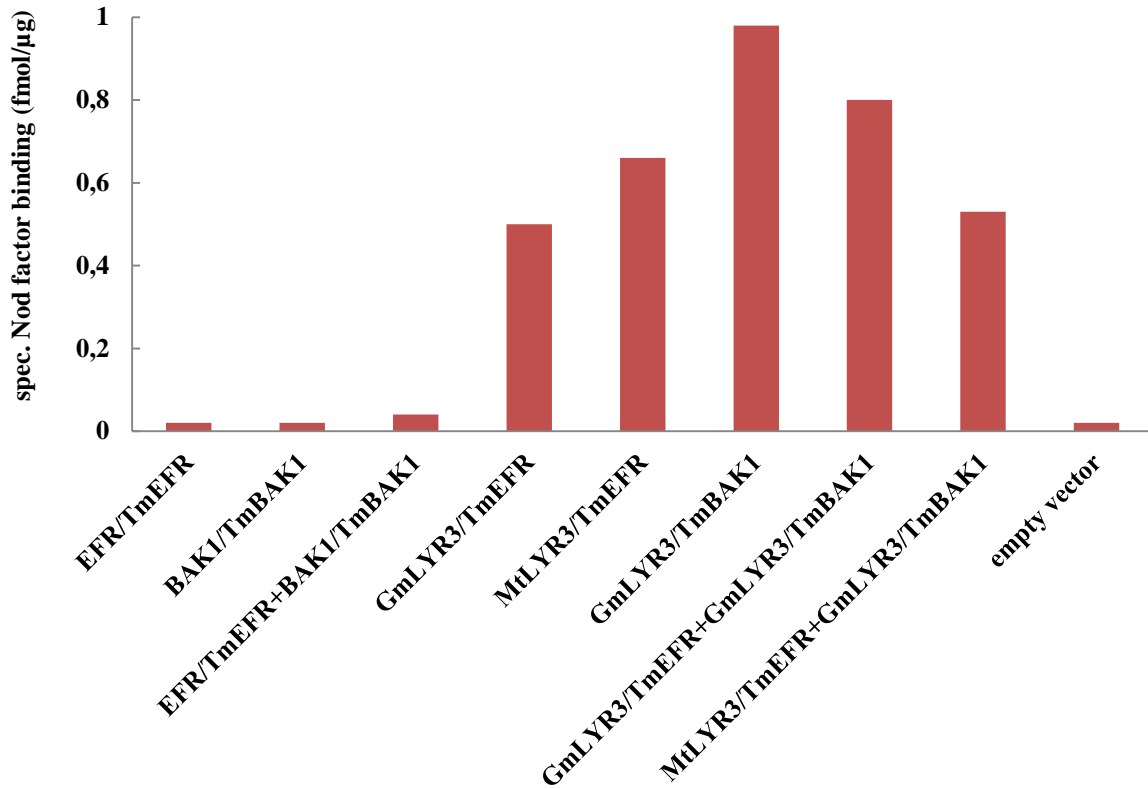
Fig.19 Specific binding of LCO-IV(^{35}S,C16:2Δ2,9) to the GmLYR3/TmEFR and MtLYR3/TmEFR chimeric proteins expressed alone or co-expressed with GmLYR3/TmBAK1. Specific binding was measured for 25µg of membrane proteins obtained from transformed *N. benthamiana* leaves (48hai) and resulted in the detection of strong binding for all LYR3 containing proteins and their combinations. No binding was detected for single or co-expressed EFR/TmEFR and BAK1/TmBAK1 receptors as well as for empty vector.

(Fig.12B). The inability of the AtCERK1/TmEFR chimeric protein to be activated with CO-VIII, suggests a problem in the activation of the EFR kinase in these LysM-EFR constructs (Fig.12C).

To try to improve the activation of the EFR kinase and the ethylene response, the co-receptor BAK1 was used, as it has previously been shown to be required for EFR responses in *A. thaliana* (Roux, Schwessinger, 2011). Co-expression of BAK1 with EFR did not lead to an improvement in elf18-dependent ethylene production and with GmLYR3/TmEFR, GmLYR3/TmBAK1 led to a strong HR and constitutive ethylene response (Fig.13, 15). This could suggest an EFR kinase activation, probably caused by its ligand-independent dimerization with the kinase of BAK1. Attempts to reduce this constitutive ethylene response, by treatment with CO-IV, failed (Fig.15, 18) suggesting that dimerization of these chimeric receptors could not be interrupted in a similar way as was demonstrated for CERK1 with CO-V. However the response was partly reduced for co-expression with GmLYR3/TmBAK1, when GmLYR3/TmEFR was replaced with MtLYR3/TmEFR (Fig.16,18), demonstrating that LYR3/TmEFR-TmBAK1 dimerization is at least partially determined by GmLYR3 ECDs homodimerization. However even in these conditions, no LCO dependent ethylene production was observed. Since overexpression of the chimeric proteins is likely to be the main reason for their ligand-independent interaction it could be expected that weaker expression may solve the problem of LYR3/TmEFR and LYR3/TmBAK1 proteins nonspecific dimerization, leaving the opportunity for LCO, which was shown to bind to both chimeric receptors (Fig.19), to participate in EFR kinase activation.

Thus, summarizing the observations made for both LYR3/TmCERK1 and LYR3/TmEFR chimeric proteins it could be concluded that the LYR3 protein possesses the potential to be used as a part of chimeric receptors, as some LYR3 chimera retained LCO binding activity when coupled with different Tm and kinase domains. There appears to be a need to control carefully the expression of the chimeric proteins to avoid constitutive activation of the kinase domains so that their biological activity can be controlled by the ligand. Further study of the LYR3 protein, especially investigation of its LCO binding mechanisms and the control of oligomerization, would help to design more efficient chimeric proteins containing the LYR3 ECD and responsive to LCO.

Chapter III

Activation of symbiotic LysM-RLKs by phosphorylation

Introduction

This chapter describes the study of NFP and LYK3 activation in the epidermis of *Medicago truncatula* roots after their treatment with *Sinorhizobium meliloti* or purified Nod factor from this bacterium.

Two *M. truncatula* LysM-RLKs NFP and LYK3 required for nodulation and Nod factor responses were chosen as the objects of this study since both of them are involved in LCO perception (Arrighi et al., 2006; Smit et al., 2007). In the case of NFP its LysM domains were predicted to bind LCOs by homology modeling and docking with Nod factor (Mulder et al., 2006) whereas LYK3 was shown to be involved in the specific recognition of Nod factor chemical decorations (Smit et al., 2007). However, in our conditions no direct binding of LCOs to NFP and LYK3 was detected. It was thus decided to study indirectly the interaction of these receptors with symbiotic molecules by detecting their activation after the symbiotic treatments. We found it advantageous to work with the proteins located in the epidermis since in this case their activation could be studied in the cells directly in contact with the symbiotic signal molecules.

To investigate the activation of symbiotic receptors in this specific tissue several tools could be used. One of them is to observe symbiotic responses triggered by the studied receptor after its activation. For NFP its symbiotic activity in the epidermis was recently investigated (Rival et al., 2012). In this study promoter pLeEXT1 originating from tomato was used to express *NFP* in the epidermal tissue of *M. truncatula*. Firstly using a pLeEXT1:GUS construction this promoter was shown to be expressed specifically in epidermal cells but not in the cortex of *Medicago* roots. Hairy root transformation of *nfp* mutant plants with the pLeEXT1:NFP construction resulted in complementation for early symbiotic responses such as *ENOD11* gene expression and cortical cell division (CCD) in these plants after their treatment with *Sinorhizobium meliloti*. In this chapter we describe similar experiment performed to study LYK3 symbiotic activity in the epidermis of *M. truncatula* roots.

The second tool to study receptor activation originates from the known phenomenon that ligand perception by a RLK often leads to the phosphorylation of its kinase domain. This very common posttranslational modification often plays a crucial role in the activation and biological functioning of the proteins. For example, AtCERK1, a LysM-RLK of *Arabidopsis thaliana*, was shown to be specifically phosphorylated after chitooligosaccharide (CO) perception and this, in turn, was necessary for the activation of defense responses (Petutschnig et al., 2010). One of our proteins of interest, LYK3, possesses 60% identity and is phylogenetically close to AtCERK1, so it may be activated by LCO in a similar way as AtCERK1 with CO. Therefore ligand-induced phosphorylation of LYK3 might be used to detect its interaction with Nod factor. By analogy with LYK3 we also investigated in our study the phosphorylation induced by ligand perception for NFP.

To detect the phosphorylation it was decided to use a novel approach called Phos-tag™ SDS-PAGE. Phosphorylation can lead to the retardation of protein migration during SDS-PAGE. Recently it was shown that this retardation can be enhanced by applying the selective phosphate-binding tag

molecule, Phos-tag™ (Tomida et al., 2008). Phos-tag™ represents an acrylamide pendant molecule holding a phosphate binding site which consists of two Zn^{2+} or Mn^{2+} ions and is able to bind phosphorylated forms of tyrosine, serine and threonine. Addition of Phos-tag™ to the acrylamide gel, followed by SDS-PAGE, causes a decrease of the migration speed and strong retardation of the phosphorylated proteins in comparison to their non-phosphorylated forms due to the temporary trapping of the phosphate groups by the evenly diffused Phos-tag™ molecules anchored in the gel.

For the reason that NFP possesses a dead kinase (Arrighi et al., 2006), in the event of detection of its phosphorylation, the study would be extended to the identification of the protein kinase that phosphorylates NFP. Such question could be answered by the expression and further analysis of NFP phosphorylation in plants mutated in the kinase genes chosen as the candidates for NFP phosphorylation. Two receptors LYK3 and DMI2 possessing active kinases and participating in the same symbiotic processes as NFP are the most expected candidates for NFP trans-phosphorylation. This assumption especially makes sense in the light of the studies done for NFP (NFR5), LYK3 (NFR1) and DMI2 (SYMRK) orthologs in *L. japonicus* in which NFR1 was shown to be able to phosphorylate NFR5 in *vitro* (Madsen et al., 2011) whereas SYMRK was able to interact with NFR5 when co-expressed in *N. benthamiana* leaves (Antolín-Llovera et al., 2014). Generation of a hypersensitive response observed during NFP and LYK3 co-expression in *N. benthamiana* also points to the possibility of interaction (direct or indirect) between these two receptors (Pietraszewska-Bogiel et al., 2013).

It was decided also to study LYR3 phosphorylation by LYK3. This receptor, described in the previous chapter, owns, like NFP, an inactive kinase and thus it would require another protein kinase for its phosphorylation. A recent study (J. Fliegmann, unpublished) has shown that LYK3 interacts with LYR3 and so may serve as the protein kinase for LYR3 phosphorylation. Therefore the phosphorylation status of NFP and LYR3 was examined in wild-type plants and also in *DMI2* and *LYK3* mutants in order to determine the potential role of DMI2 and LYK3 in this process.

Experimental procedures

Plant growth conditions

Generation and growth of A. rhizogenes transformed plants:

Seeds of the *Medicago truncatula* wild type plants (A17) and EMS Nod⁻ mutants (*lyk3-1* (*hcl-1*)) and *dmi2-1*) (Catoira et al., 2000; Catoira et al., 2001) were scarified with concentrated sulfuric acid for five minutes and then surface sterilized with 12% sodium hypochlorite for 2 minutes. Next, sterilized seeds were vernalized for two days on 1% agar plates at 4°C and germinated in the dark at 25°C for three days. For *A. rhizogenes* transformation five days old seedlings were transferred to Fahraeus agar plates (15g/l agar, $MgSO_4$-0.5 mM, KH_2PO_4-0.7 mM, Na_2HPO_4-0.8 mM, Fe-EDTA-0,02 mM and microelements $MnCl_2$, $CuSO_4$, $ZnCl_2$, H_3Bo_3, Na_2MoO_4 each at 0.1 µg/l concentration, after autoclaving supplemented with sterile $CaCl_2$-1 mM, NH_4NO_3 – 5 mM and Kanamycin -20 µg/ml)

where the tips of the roots of the plantlets were cut off with a sterile razor. Place of the cut was treated with *Agrobacterium rhizogenes* strain ARqua1 ($_{OD600}$=0.03) carrying on the pCambia2202 plasmid the pLeEXT1:LYK3-FLAG, p35S:LYK3-FLAG, pLeEXT1:NFP-FLAG or pLeEXT1:LYR3-HAST constructions together with the kanamycin resistance gene. For generation of transgenic roots plants were grown for two weeks at 25°C with 16h/8h day/night cycle and then moved either to sepiolite solid media in the case of *lyk3-1* complementation experiments or to an aeroponic system in the case of NFP and LYR3 phosphorylation studies in *lyk3-1* and *dmi2-1* mutants.

Plants transferred to sepiolite were first grown for two weeks in 5ml pipette tips and after for one week in mini-pots of 50ml volume. During the cultivation, plants were watered with liquid Fahraeus medium, supplemented with 1 mM NH_4NO_3. Two days before the symbiotic treatment the sepiolite pots were washed with water and equilibrated in nitrogen deficient Fahraeus medium.

In the aeroponic system, plants were grown for one month with nutrient medium ($CaCl_2$-2 mM, $MgSO_4$-0.25 mM, K_2SO_4-0.5 mM, K_2HPO_4-3.8 mM, KH_2PO_4-1.7 mM Fe-EDTA-0,05 mM NH_4NO_3-5 mM and microelements $MnSO_4$-10.6 µM, $CuSO_4$-3.2 µM, $ZnSO_4$-0.7 µM, H_3Bo_3-30 µM, Na_2MoO_4-1 µM). Three days before harvesting the aeroponic medium was replaced with water and in one hour with aeroponic medium lacking NH_4NO_3.

Growth conditions for experiments with stably transformed plants:

Seeds of *M. truncatula* plants stably expressing pLeEXT1:LYK3-FLAG or pLeEXT1:NFP-FLAG constructions were sterilized and germinated in the similar way as was described for the plants used for *A. rhizogenes* transformations. Five days old seedlings were transferred from Fahraeus agar plates to the aeroponic system and grown for one month in the presence of the nitrogen source. Three days before symbiotic treatments the medium was replaced with water for one hour and then with the aeroponic medium lacking a nitrogen source.

Symbiotic treatments

For the lyk3-1 complementation experiment:

Wild-type *Sinorhizobium meliloti* strain GMI6526 harboring the pXLGD4 plasmid with a constitutively-expressed ß-galactosidase (LacZ) gene was grown for three days at 28°C on tryptone yeast agar medium (TY) containing 6 mM $CaCl_2$ and 10 µg/ml tetracycline. Grown bacteria were resuspended in water and used to inoculate five weeks old plants in mini-pots (2 mL of an OD_{600} = 0.1per plant). After inoculation half of the plants were grown for 6 days and the other half for 21 days.

For the NFP activation experiments:

Wild-type *Sinorhizobium meliloti* strain GMI6526 was grown on TY agar plates at 28°C for two days. Grown bacteria were used to inoculate 10 ml of LB medium (NaCl-10 g/l, yeast extract-5 g/l, bacto-tryptone- 10 g/l). Overnight (o/n) grown 10 ml liquid bacterial culture was used as a pre-culture to produce 200 ml liquid culture. Grown o/n 200 ml liquid culture was diluted to an OD_{600}= 0.4

and cultivated for five more hours in the presence of luteolin at 5 μM concentration. Next, the bacteria were spun down at $4x10^3$g, resuspended in sterile water and added to the aeroponic medium, reaching a final concentration of $2x10^7$ bacteria/ml. One month old plants stably expressing the pLeEXT1:NFP-FLAG construction were incubated with the bacteria for two hours in the aeroponic system after which time their roots were harvested, frozen in liquid nitrogen and ground to a powder.

For the LYK3 activation experiment:

Plants, stably expressing pLeEXT1:LYK3-FLAG construction and grown for one month in aeroponic system, were treated with purified Nod factor (LCO-IV (Ac, S, C16:2 Δ2, Δ9)) from *Sinorhizobium meliloti* (Roche et al., 1991). During the treatment the roots of the transgenic plants were soaked for 20 minutes in water containing 10^{-8} M Nod factor. After the treatment roots were harvested, frozen in liquid nitrogen and ground to a powder.

Staining and microscopy methods

Histochemical staining for β-galactosidase activity provided by the pXLGD4 plasmid in *S. meliloti* was performed as described previously (Ardourel et al., 1994). To prepare the sections, root fragments were embedded in 4% agarose solution and cut into 50 μm-thick slices with the vibratome (Leica VT1000S). Root fragments as well as sections were observed with Zeiss Axioplan2 imaging microscope.

Standard and Phos-tag SDS-PAGE

To avoid the de-phosphorylation of the studied proteins, extracts were treated with two phosphatase inhibitors Na_3VO_4 (1 mM) and NaF (10 mM). During both normal and Phos-tag™ SDS-PAGE proteins were separated on 9% acrylamide gels. Phos-tag™ gel was supplemented with 25 μM Phos-tag™ and 50 μM $MnCl_2$. After migration, proteins were transferred onto nitrocellulose membranes and detected with antibodies coupled to horseradish peroxidase (HRP): anti-GST-HRP (GE Healthcare, 1:10,000), anti- rabbit -phospho-Thr (Invitrogen, 1:1000) in combination with anti-rabbit-coupled HRP (Millipore, 1:25,000), anti-FLAG-HRP (Sigma, 1:5000) and anti-HA-HRP (Roche, 1:2000).

Sample extraction and fractionation

Fractionation of sample extracts was performed using a SIGMA 3K18 centrifuge or an Optima MAX-E Ultracentrifuge. Frozen root powder was resuspended in the extraction buffer (25 mM Tris-HCl buffer pH 8.5, 0.47 M sucrose, 10 mM EDTA, 10 mM dithiothreitol, protease inhibitor cocktail (4-(2-aminoethyl) benzenesulfonyl fluoride hydrochloride (AEBSF), antipain, leupeptin, aprotinin, pepstatin, chymostatin) or in the same buffer lacking EDTA and centrifuged for 10 minutes to obtain the $3x10^3$ g supernatant fraction. To obtain the $20x10^3$g or $45x10^3$g supernatant fractions the $3x10^3$ g supernatant was centrifuged for 40 minutes at these centrifugal forces. The pellets obtained after this
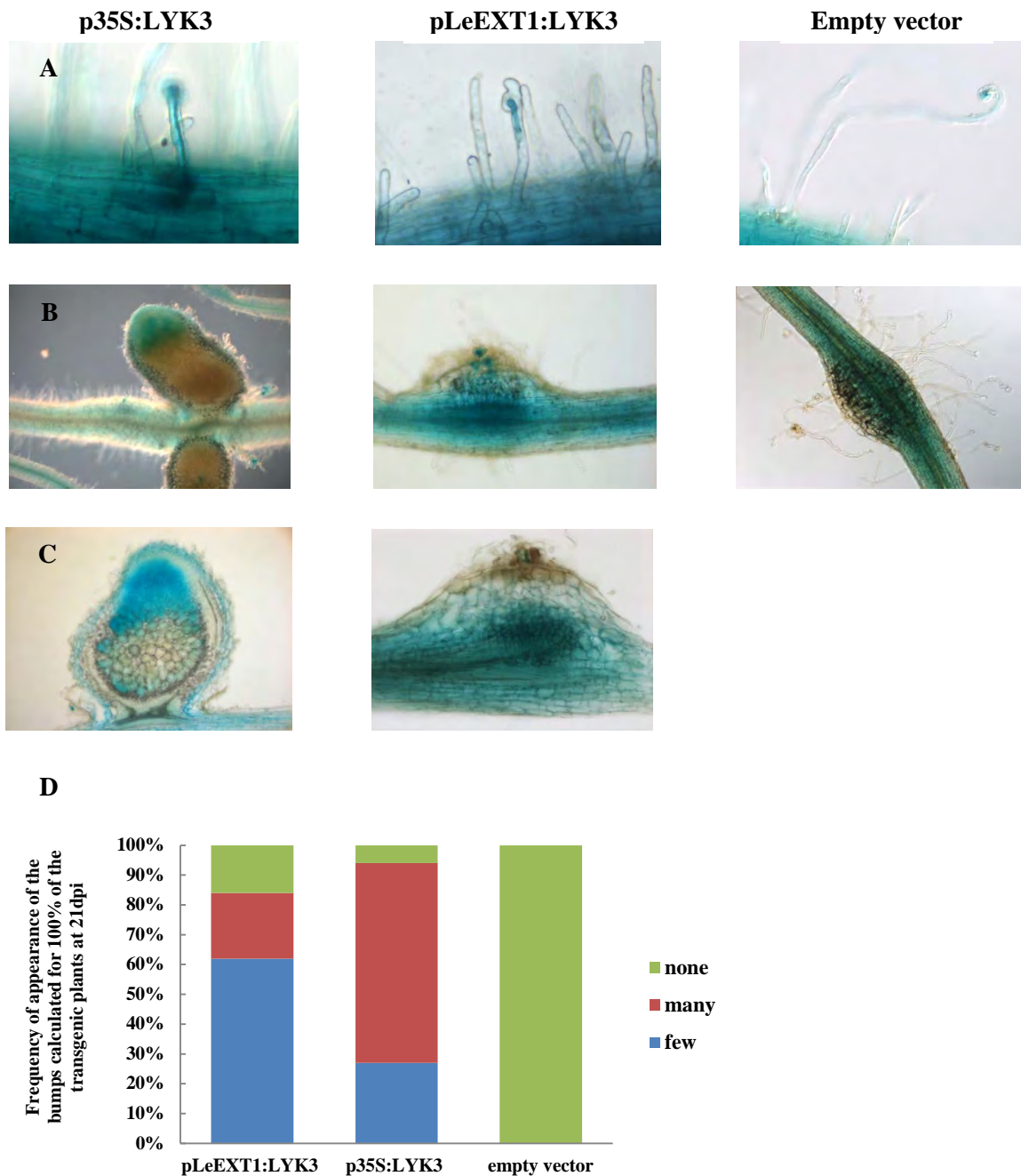
Fig.1 Results of *lyk3-1* complementation with pLeEXT1:LYK3-FLAG.

(**A**) Microscopy of mutant *lyk3-1* plants transformed with p35S:LYK3, pLeEXT1:LYK3 and empty vector at 6 dpi with *S. mileloti.* For both plants transformed with p35S:LYK3 or pLeEXT1:LYK3 initiation of infection thread formation was observed. (**B**) Microscopy of similar transformants at 21 dpi- fully developed nodules were detected for the plants complemented with p35S:LYK3, whereas plants transformed with pLeEXT1:LYK3 were owning the bumps. (**C**) Sections of the nodules validating their normal morphology and the bumps showing the arrest of infection thread on the level of epidermis. (**D**) Quantification of nodules and bumps in p35S:LYK3, pLeEXT1:LYK3 and empty vector transformants.

90

centrifugation corresponding to the 20×10^3g or 45×10^3g membrane fractions were resuspended in the binding buffer (25 mM Na-cacodylate buffer pH 6.0, 0.25 M sucrose, 1 mM MgCl$_2$, 1 mM CaCl$_2$, protease inhibitor cocktail) and centrifuged for another 10 minutes at 20×10^3g or 45×10^3g respectively. The obtained pellets were resuspended in the binding buffer.

Results

Study of LYK3 symbiotic activity in the epidermis of Medicago truncatula roots.

To study LYK3 biological activity in the epidermal tissue we performed an experiment similar to the one which was recently done for NFP (Rival et al., 2012) and described in the introduction. Hairy root transformation of *lyk3-1* mutant plants with the pLeEXT1:LYK3 construction was done, using *Agrobacterium rhizogenes*. The control plants were transformed with either empty vector pCambia2202 (in which *LYK3* was originally cloned) or with *LYK3* expressed from the constitutive 35S promoter (p35S:LYK3). Both LYK3 proteins were tagged at their C-termini with the 3xFLAG tag. After the regeneration of transformed roots on the selective medium, plants were inoculated with the wild-type strain of *Sinorhizobium meliloti* harboring the ß-galactosidase gene on the pXLGD4 plasmid (strain GMI6526). Transgenic roots were analyzed at 6 and 21 days after inoculation (dai) by histochemical staining based on ß-galactosidase activity and further observed under the stereomicroscope. At 6 dai several symbiotic responses, namely tight root hair curls with entrapped bacteria and the beginning of infection thread (IT) formation, were detected for the plants transformed with either pLeEXT1:LYK3 or p35S: LYK3 (Fig.1A). Plants transformed with the empty vector showed root hair deformation and formation of some loose root hair curls whereas no infection threads were detected. Observations done at 21dai (Fig.1B) resulted in the detection of several developed infection threads which were reaching the sub-epidermal cell layer and the occurrence of few bumps on the roots of majority of the plants transformed with pLeEXT1:LYK3 (Fig.1D). Next, the bumps were embedded and microtome sectioned with the aim to check whether they were infected by *Rhizobium*. For all analyzed samples, infection threads were shown to be arrested immediately after reaching the base of the epidermal cell, being, therefore, unable to invade and infect the cortical cell layers forming the bump (Fig.1C). Fully developed pink nodules and many bumps were observed for the plants transformed with p35S:LYK3 (Fig. 1B/C). Further sectioning confirmed their normal morphology with the typical indeterminate nodule zonation and the stained bacteria present in the infection and inter-zones (Zone II and Zone II-III). Additional blue staining, present in some of the images, was caused by endogenous plant ß-galactosidase activity. Plants transformed using the empty vector at 21dai continued to demonstrate the previously-described *lyk3-1* phenotype (Catoira et al., 2001). In addition to the observed earlier deformation of root hairs, periodical thickenings of the roots caused by several rounds of cortical cells division in these areas were also observed (Fig.1B). After LYK3 was shown to stay active in the epidermis in the symbiotic conditions, we proceeded further to the development of Phos-tag™ assay.

A
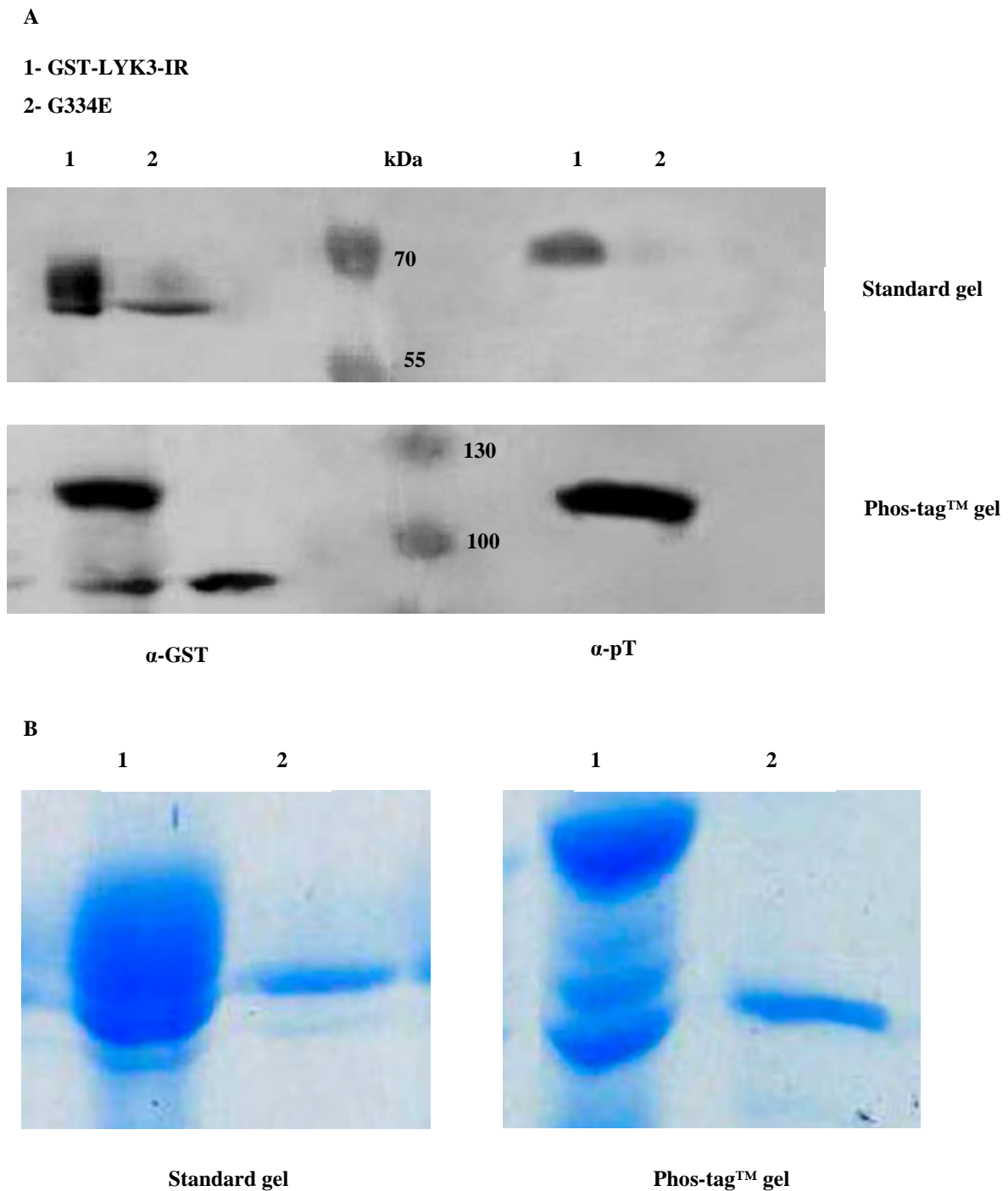
1- GST-LYK3-IR

2- G334E

Fig.2 Immunodetection of the GST-LYK3-IR and G334E proteins after their separation on standard and Phos-tag^{Tm} acrylamide gels.

GST-LYK3-IR and G334E proteins were migrated on the Standard and Phos-tag^{Tm} gels and next detected with anti-GST-HRP (α-GST) or anti- rabbit -phospho-Threonine (α-pT) antibodies (**A**) or via coomassie blue staining (**B**). In all cases GST-LYK3-IR protein was retarded in the presence of Phos-tag^{Tm} molecule.

92

Development of Phos-tag™ SDS-PAGE assay.

To develop the Phos-tag™ assay for detection of NFP and LYK3 phosphorylation we decided to use previously obtained proteins consisting of the GST tag fused to the N terminus of the intracellular regions of LYK3 wild type (GST-LYK3-IR) and point mutated (G334E) proteins. By analyzing both purified proteins with anti-phospho-Thr (-pT) and anti-phospho-Ser (-pS) antibodies it was demonstrated that GST-LYK3-IR is capable of auto and trans-phosphorylation whereas G334E has lost this ability (Klaus-Heisen et al., 2011). GST-LYK3-IR and G334E thus represent a pair of equivalent proteins only differing in their phosphorylation status and therefore were expected to show no differences during migration on the standard acrylamide gel, but to get separated during Phos-tag™ SDS PAGE. Regular SDS-PAGE and western blotting performed with GST-LYK3-IR and G334E showed a similarly migrating polypeptide observed with anti-GST antibodies for both proteins, except that GST-LYK3-IR migrated as a pronounced smear. Optimization of the conditions for Phos-tag™ SDS PAGE took several trials and resulted in finding conditions in which GST-LYK3-IR migrated as two separated bands, one highly retarded and one migrating at the same level as G334E (Fig.2A). Detection of the proteins with anti-phospho-Thr (-pT) antibodies resulted in the visualization of only the retarded band belonging to the GST-LYK3-IR sample. These observations suggested that the shift of the band observed in the case of GST-LYK3-IR was caused by the Phos-tag™ dependent separation of its phosphorylated and non-phosphorylated forms. These GST-LYK3 proteins were used as the Phos-tag™ quality controls during the study of NFP and LYK3 phosphorylation. In some experiments, to simplify and speed up the procedure of the control proteins detection the treatment with anti-GST antibodies, which was used previously, was replaced by Coomassie blue (CB) staining, which was shown to provide similar visualization of the GST-LYK3 proteins to the one obtained with antibodies. The presence of several retarded bands in the over-loaded sample of GST-LYK3-IR (Fig.2B), suggests that it consists of several different phosphorylated forms.

Study of LYK3 and NFP phosphorylation in the roots of M. truncatula plants after their treatment with Sinorhizobium meliloti or with pure LCO obtained from this bacterium.

After Phos-tag™ SDS PAGE was shown to work satisfactorily we proceeded further to the *in vivo* NFP and LYK3 phosphorylation study. For the experimental procedures we used two homozygous transgenic lines of *M. truncatula* stably expressing in epidermis FLAG tagged NFP (pLeEXT1:NFP line M51A7) and LYK3 (pLeEXT1:LYK3 line M52B12). Receptor activation experiments were performed on the transgenic plants grown for one month in aeroponic system and starved of nitrogen during three days before treatment with symbiotic molecules. At this stage some of the transgenic roots were harvested to serve as the untreated controls in future phosphorylation detection by Phos-tag™ SDS-PAGE. To study LYK3 phosphorylation, roots of the transgenic plants were soaked for twenty minutes in the liquid medium containing purified *S. meliloti* Nod factor- LCO-IV (Ac, S, C16:2 $\Delta 2$, $\Delta 9$) at 10^{-8} molar concentration. After the treatment, transgenic roots were harvested, frozen in liquid nitrogen and ground to a powder. Next, to analyze the changes in receptor

1- GST-LYK3-IR

2- G334E

3- LYK3+Nod

4- LYK3-Nod

Fig.3 Immunodetection of LYK3 proteins after electrophoresis analysis on standard and Phos-tag^{Tm} gels.

Crude extracts obtained from roots expressing pLeEXT1:LYK3-FLAG, treated (+Nod) or not treated (-Nod) with *S. meliloti* Nod factor, were analyzed by electrophoresis on Standard and Phos-tag^{Tm} gels. After transfer on nitrocellulose, LYK3 was detected with anti-FLAG-HRP antibodies. To validate the Phos-tag^{Tm} approach, GST-LYK3-IR (lane 1) and G334E (lane 2) proteins were separated on the same gels and visualized after coomassie blue staining. GST-LYK3-IR protein and minor bands corresponding to LYK3 +/-Nod factor (lane 3 and 4) were clearly retarded on Phos-tag^{Tm} gel.

phosphorylation, crude extracts from the transgenic roots treated with purified Nod factor (LYK3+Nod) together with the extracts obtained from untreated roots (LYK3-Nod) were migrated on the standard 9% acrylamide gel and the gel supplemented with Phos-tag™ (Fig.3). Phos-tag™ capability of phosphorylated proteins detection was validated by the separation of GST-LYK3-IR protein performed in the same gel. No differences in migration during standard SDS-PAGE were observed for LYK3+Nod and LYK3-Nod samples. In both cases migration profiles consisted of a main 90 kDa band corresponding to whole FLAG tagged LYK3 protein and several bands of 30 kDa-50 kDa probably belonging to the products of LYK3 degradation. However, LYK3 bands from both Nod factor treated and untreated roots demonstrated strong similarity also while migrating on the Phos-tag™ gel. Interestingly, for both Nod + and Nod- samples bands placed below the main 90 kDa band were shifted with respect to each other and present in higher amounts on the Phos-tag™ gel than on the standard one. This observation provides evidence that the degradation products may be phosphorylated.

In the case of NFP, roots of the transgenic plants were exposed for two hours with *S. meliloti* strain GMI6526 which was added to the nutrient solution of the aeroponic system reaching the final concentration of $2x10^7$ bacteria/ml. Before starting the experiment bacteria were preactivated in terms of LCO production by the incubation for five hours in luteolin containing media. Migration profiles obtained for NFP in the lack of Phos-tag™ were identical for the samples extracted from *Rhizobium* treated (NFP+Rhz) and non-treated (NFP-Rhz) roots (Fig.4). Polypeptides observed on the standard gel were represented by the main 100 kDa band corresponding to the FLAG tagged NFP and several bands placed below originating, probably, from the degraded NFP protein. Phos-tag™ analysis resulted in the detection of a strongly retarded band placed above the main 100 kDa band in the130-170 kDa area for the NFP-Rhz sample. This band was absent in the extract obtained from the NFP+Rhz roots. In addition all bands placed below 100 kDa band were retarded in NFP+Rhz sample in relation to the same bands from NFP-Rhz sample. Further comparison of migration profiles obtained during standard and Phos-tag™ SDS-PAGE revealed general differences for both treated and untreated proteins in their modes of migration in presence and absence of Phos-tag™. Firstly, in both NFP-Rhz and NFP+Rhz samples, the100 kDa band was followed by a smaller 90 kDa band which was not observed on the standard gel. Secondly, bands placed below 100 kDa area were organized differently in relation to each other in the presence of Phos-tag™. On the Phos-tag™ gel minor bands were migrating as one 70 kDa band separated from the pack of smaller bands (starting around 60 kDa) whereas on the standard gel two 70 kDa and 60 kDa bands were divided from the number of smaller bands (starting at 50 kDa) (Fig. 4).

The obtained results suggested that both LYK3 and NFP samples could contain phosphorylated proteins. Most promising data was produced for NFP particularly when a highly retarded polypeptide, probably corresponding to the phosphorylated form of the protein, was detected in NFP-Rhz sample. To verify the NFP phosphorylation, the experiment was repeated but using a new homozygous *M. truncatula* line expressing pLeEXT1:NFP (M51C9.11). This line was selected for the

1- G334E

2- GST-LYK3-IR

3- NFP+Rhz
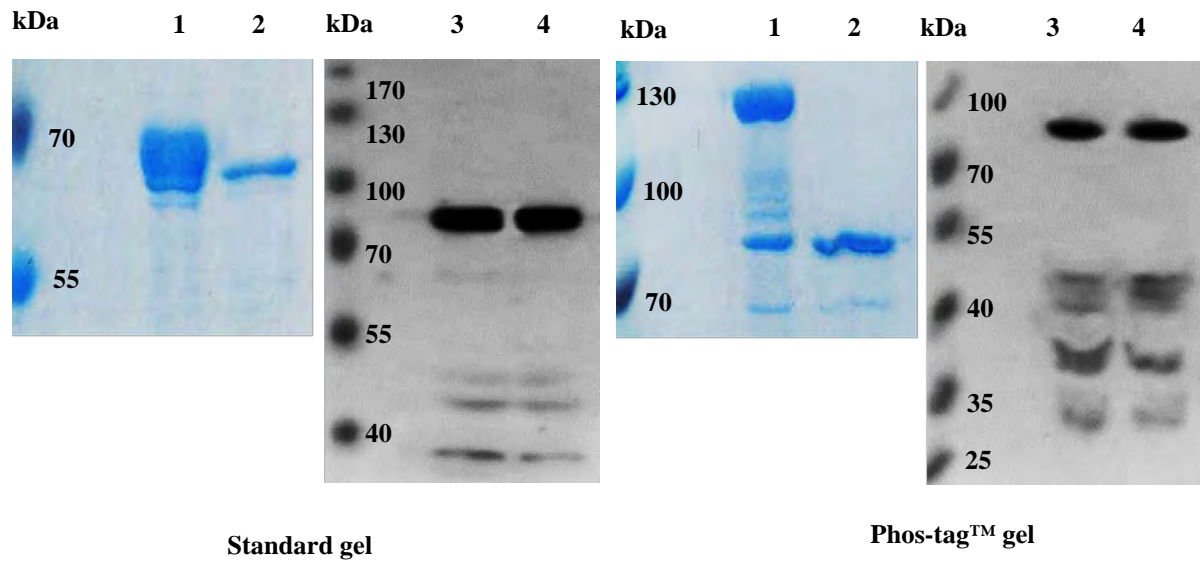
4- NFP-Rhz

Standard gel

Phos-tag™ gel

Fig.4 . Immunodetection of NFP proteins after electrophoresis analysis on standard and Phos-tag[Tm] gels.

Crude extracts obtained from roots expressing pLeEXT1:NFP-FLAG, treated (+Rhz) or not treated (-Rhz) with *S. meliloti*, were analyzed by electrophoresis on Standard and Phos-tag[Tm] gels. NFP proteins were detected after transfer on nitrocellulose with anti-FLAG-HRP antibodies. GST-LYK3-IR and G334E proteins were separated on the same gels and next detected with anti-GST-HRP antibodies. GST-LYK3-IR protein was strongly retarded in the presence of Phos-tag[Tm] validating its phosphate binding functionality. For NFP-Rhz, a strongly retarded polypeptide was detected on the Phos-tag[Tm] gel. All minor bands corresponding to NFP+Rhz polypeptides were shifted in Phos-tag[Tm] gel.

96

reason that the NFP signal was weakening in the previously used M51A7 line probably caused by a problem of gene silencing. The NFP phosphorylation experiment was performed in a similar way as was done previously. On the standard gel no differences in the migration profiles were observed for NFP+Rhz and NFP-Rhz samples (Fig.5). The detected polypeptides were represented by the main 100 kDa band followed by a much less abundant 90 kDa band and several smaller size bands (starting from 55 kDa) with the most pronounced band of 45 kDa. On the fully functional Phos-tag™ gel no differences in the separation were observed for the proteins extracted from the treated and un-treated with bacteria roots. The migration profiles obtained during the Phos-tag™ SDS-PAGE were consisting of one main 100 kDa band and several smaller size bands placed in the 55-25 kDa area with the most abundant 50 kDa band. Possessing similarity in terms of migration within one gel, both NFP samples were, however, behaving differently in the presence or absence of Phos-tag™. Present on the standard gel, the 90 kDa band accompanying the main 100 kDa NFP band was lacking on the Phos-tag™ gel, perhaps due to retardation and co-migration with the major 100 kDa band. High amount of equally distanced minor bands consisting of bands of 55 kDa and 50 kDa, a sharp 45 kDa band possessing the strongest signal and several bands placed below was observed in the presence of Phos-tag™. Minor bands detected on the standard gel were represented by one 55 kDa band separated from the stronger 45 kDa band, which migrates with a smear and several bands placed below.

In both NFP phosphorylation experiments the bands placed below the main 100 kDa band were shifted in the presence of Phos-tag™ probably due to their phosphorylation. The predicted size of the intracellular region of NFP with the 3xFLAG tag is 38 kDa. Therefore the size of some of the minor bands suggested that some of the corresponding truncated proteins could still include the TM region and hence be attached to the plasma membrane (PM), whereas the smaller bands might correspond to soluble proteins. To examine the association of the phosphorylated derivatives of NFP with the PM, the studied samples were fractionated by performing differential centrifugation.

Fractionation of NFP extracts and Phos-tag™ analysis of the proteins from different fractions.

During the fractionation both NFP+Rhz and NFP-Rhz samples were separated by differential centrifugation into the $3x10^3$g supernatant, the $20x10^3$g supernatant and the $20x10^3$g pellet fractions. It was expected that in the chosen conditions the $3x10^3$g supernatant would contain both soluble and membrane attached proteins whereas at $20x10^3$g the membrane associated proteins will be pelleted and divided from the soluble ones which will stay in the supernatant.

To show that the observed bands are specific to the tagged NFP protein the $3x10^3$g supernatant was prepared from the roots of wild type *M. truncatula* (A17). All fractions were analyzed by standard and Phos-tag™ SDS-PAGE. On both supplemented with Phos-tag™ and standard gels no differences were observed in the migration profiles of the NFP+Rhz and NFP-Rhz samples as well as no bands were detected in the $3x10^3$g supernatant corresponding to the A17 sample (Fig.6). Migration profiles observed on the standard gel for the NFP proteins consisted of two bands of 100 kDa and 90 kDa detected in the $3x10^3$g supernatant and the $20x10^3$g pellet. These bands were missing in the $20x10^3$g

Standard gel
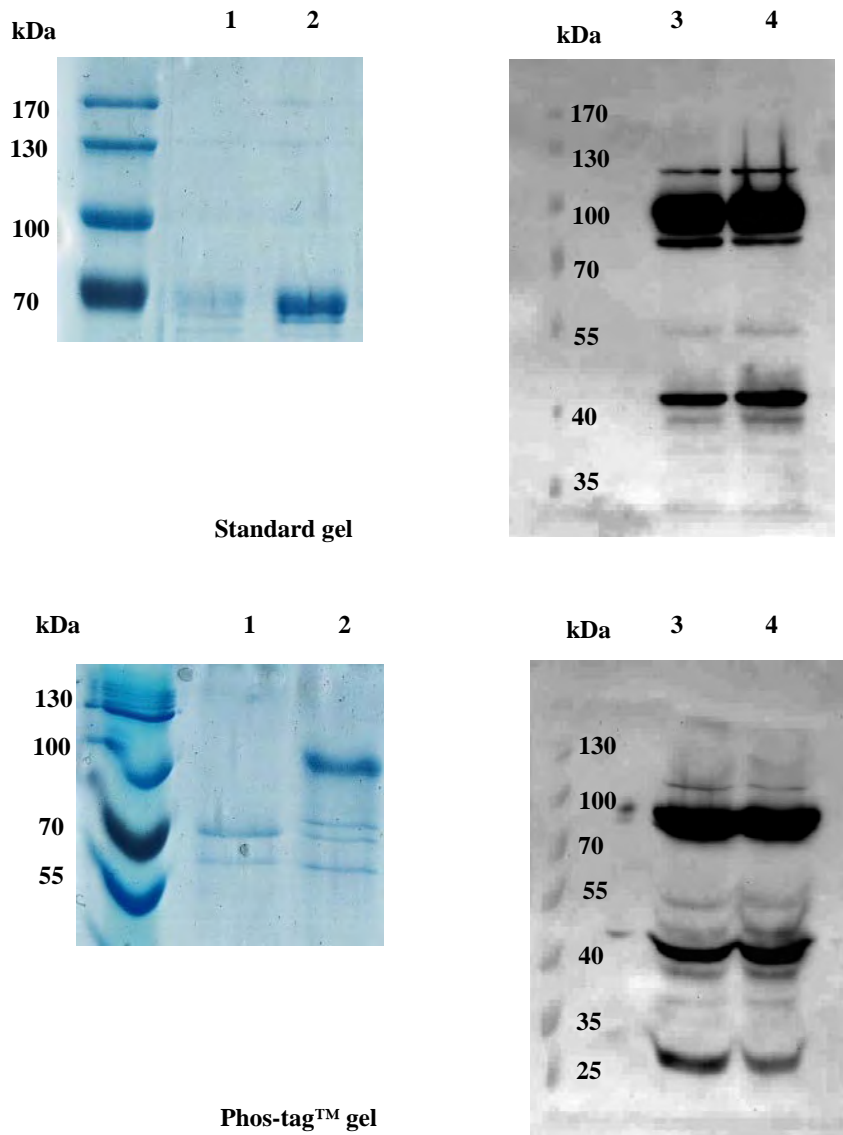
Phos-tag™ gel

Fig.5 . Second immunodetection of NFP proteins after electrophoresis analysis on standard and Phos-tag^{Tm} gel of crude extracts from roots expressing pLeEXT1:NFP-FLAG, treated (+Rhz) or not treated (-Rhz) with *S. meliloti*.

NFP proteins were analysed on Standard and Phos-tag^{Tm} gels and detected after transfer on nitrocellulose with anti-FLAG-HRP antibodies. GST-LYK3-IR and G334E proteins were separated on the same gels and next detected via coomassie blue staining.GST-LYK3-IR protein was strongly retarded on Phos-tag^{Tm}. No differences in the migration of NFP+Rhz and NFP-Rhz samples were observed on standard and Phos-tag^{Tm} gels.

supernatant. The most abundant protein was represented by a 45 kDa band which was observed in all fractions. On the Phos-tag™ gel, the two 100 kDa and 90 kDa bands were detected only in the $3x10^3$g supernatant. Both the $3x10^3$g and $20x10^3$g supernatants contained the 45 kDa band. This band was however slightly shifted down in the $20x10^3$g supernatant samples. In the $20x10^3$g pellet the band with the strongest signal was migrating at 50 kDa level and therefore was shifted in comparison to the 45 kDa band of equal intensity observed in the two other fractions.

The obtained data was unexpected in several aspects. Firstly, the observed 45 kDa band in the standard gel was present in both $20x10^3$g supernatant and pellet fractions, whereas other experiments had not shown bands remaining in the supernatant (see Fig. 7). This could suggest that the centrifugation force at $20x10^3$ g was insufficient to pellet completely the membrane associated 45 kDa protein and part of it was remaining in the $20x10^3$ g supernatant. Secondly, retardation of the band to 50 kDa from the $20x10^3$g pellet observed on the Phos-tag™ gel in comparison to its migration at 45 kDa level in all fractions on the standard gel showed that this 50 kDa band is clearly phosphorylated. However, it was surprising that no equally retarded band was detected in the $3x10^3$g supernatant on the Phos-tag™ gel. Looking for the possible explanation for the observed phenomenon we identified a slight difference in the composition of the two buffers routinely used during the differential centrifugation and for the resuspension of the obtained pellets. The extraction buffer in which all supernatants were obtained was supplemented with ethylenediaminetetraacetic acid (EDTA) whereas the $20x10^3$g pellet was resuspended in EDTA free buffer. It is known that EDTA acts as a Phos-tag™ inhibitor due to its ability to chelate the Mn^{2+} ions, leading to the interruption of the phosphate binding sites of the Phos-tag™ molecules. It is therefore possible that EDTA present in the $3x10^3$g and $20x10^3$ supernatants could protect phosphorylated proteins in these samples from their retardation during Phos-tag™ SDS-PAGE.

The fractionation was therefore repeated but with excluding EDTA from all types of buffers and increasing the centrifugation force up to 45 $x10^3$ g. Since on the Phos-tag™ and standard gels migration profiles of NFP+Rhz and NFP-Rhz samples were identical, the new fractionation experiment was performed only for the NFP-Rhz sample. For the $3x10^3$g supernatant on the standard gel one 100 kDa main band and several minor bands including the separated 55 kDa band and several smaller bands migrating as a smear were detected (Fig.7). The 115 kDa band detected in the 45 $x10^3$ g supernatant, suggests that it is a non-specific soluble protein. The migration profile obtained for the 45 $x10^3$ g pellet was similar to the one observed for the $3x10^3$g supernatant. On the Phos-tag™ gel in the $3x10^3$g supernatant and in the 45 $x10^3$ g pellet we observed the main 100 kDa band and at least five minor bands approximately equally distanced and migrating in the 55 kDa – 40 kDa area. The spacing of some of these bands in relation to the standard gel suggests that some of them are phosphorylated. As on the standard gel no specific bands were detected in the 45 $x10^3$ g supernatant.

1- GST-LYK3-IR

2- extract from A17

3- NFP+Rhz 3×10^3 g supernatant +EDTA

4- NFP-Rhz 3×10^3 g supernatant +EDTA

5- NFP+Rhz 45×10^3 g supernatant +EDTA

6- NFP-Rhz 45×10^3 g supernatant +EDTA

7- NFP+Rhz 45×10^3 g microsomal fraction

8- NFP-Rhz 45×10^3 g microsomal fraction
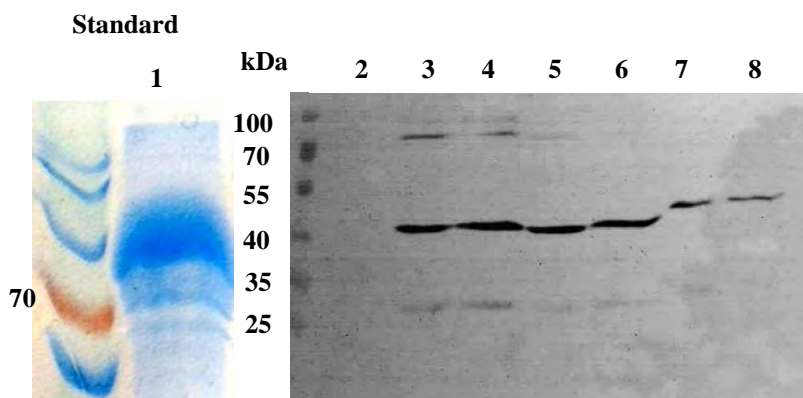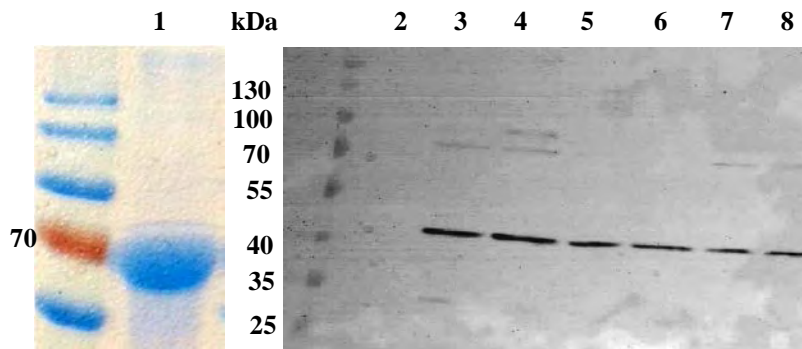
Standard

Phos-tag™

Fig.6 Immunodetection of NFP proteins after electrophoresis analysis on standard and Phos-tag^{Tm} gel of different fractions obtained for roots expressing pLeEXT1:NFP-FLAG, treated (+Rhz) or not treated (-Rhz) with *S. meliloti*.

The roots were extracted and three cell fractions were obtained by differential centrifugation. 3×10^3 g supernatant, 45×10^3 g supernatant both supplemented with EDTA and 45×10^3 g pellet were analysed on standard and Phos-tag^{Tm} gels. NFP was detected with anti-FLAG-HRP antibodies. On the same gels extract obtained from A17 wild type plants and GST-LYK3-IR protein were analysed, corresponding respectively to a negative control and a positive control for Phos-tag^{Tm} functionality. GST-LYK3-IR protein was retarded in the presence of Phos-tag^{Tm}. Immunoreactive polypeptides detected in the 45×10^3 g pellet corresponding to NFP+/- Rhz were retarded on the Phos-tag^{Tm} gel in comparison to the similar ones observed in 3×10^3 g supernatant and 45×10^3 g supernatant fractions.

Study of NFP and LYR3 phosphorylation in the roots of M. truncatula LYK3 (lyk3-1) or DMI2 (dmi2-1) mutants.

In all NFP phosphorylation experiments a slight retardation of minor bands on the Phos-tag™ was detected. This could be interpreted in favor of NFP phosphorylation. It is known that NFP has an inactive kinase (Arrighi, Barre, 2006) and thus would require another protein kinase for its phosphorylation. To study whether two receptors LYK3 and DMI2 possessing active kinases are involved in NFP trans-phosphorylation expression of NFP in the *LYK3* (*lyk3-1*) and *DMI2* (*dmi2-1*) mutated backgrounds was performed.

For NFP trans-phosphorylation study, *M. truncatula* lines B56 (*lyk3-1*) and Tr25G (*dmi2-1*) as well as wild type line A17 were transformed by *Agrobacterium rhizogenes* with the pLeEXT1:NFP-FLAG construction. The plants, containing transgenic roots were grown for two weeks on the selective medium and were then transferred to the aeroponic system and grown for another two weeks. For the reason that phosphorylation of symbiotic receptors might be sensitive to the abundance of nitrogen, even without further treatment with *Rhizobium*, it was decided to starve the plants for nitrogen for three days before harvesting. To analyze the phosphorylation of NFP, extracts obtained from the roots of wild type plants and the two mutated lines were migrated on the standard and Phos-tag™ acrylamide gels (Fig.8). Migration profiles obtained on the standard gel were similar for all examined samples consisting of the main 100 kDa band corresponding to the FLAG tagged NFP, a 55 kDa band and three smaller size bands migrating below. Comparing the behavior of NFP extracted from the wild type plants and *lyk3-1* or *dmi2-1* mutants on the Phos-tag™ gel we were not able to find any differences in terms of migration of either the main 100 kDa band or the smaller sized bands placed in the 55 kDa-25 kDa area. For all samples the minor bands seemed to be in higher amounts and to be more equally distanced in the presence of Phos-tag™ in comparison to the profiles observed on the standard gel.

In parallel with NFP, a similar experiment was performed for LYR3. To study LYR3 phosphorylation *lyk3-1* and wild type plants were transformed *A. rhizogenes* carrying pLeEXT1-LYR3-HAST. Samples obtained from the transgenic plants were simultaneously analyzed with the NFP samples described above by standard and Phos-tag™ SDS-PAGE (Fig.9). Migration profiles observed on the standard gel were similar for both wild type and *lyk3-1* samples consisting of a main 90 kDa band and few faint minor bands of 40 kDa and 35 kDa. On the Phos-tag™ gel for both samples no differences in migration of the main 90 kDa band was observed. The minor bands present in higher amount on Phos-tag™ gel in comparison to the standard were migrating similarly for *lyk3-1* and wild type samples in case of 45 kDa, 40 kDa and 25 kDa bands whereas the 35 kDa band was slightly retarded in the *lyk3-1* sample, suggesting that it is phosphorylated. In comparison to the standard gel, the 40 kDa band resolved into two bands on the Phos-tag™ gel, suggesting that at least the upper one is phosphorylated.

1- GST-LYK3-IR

2- G334E

3- NFP-Rhz 3x10^3 g supernatant

4- NFP-Rhz 45x10^{3}g supernatant

5- NFP-Rhz 45x10^{3}g microsomal fraction

Standard gel
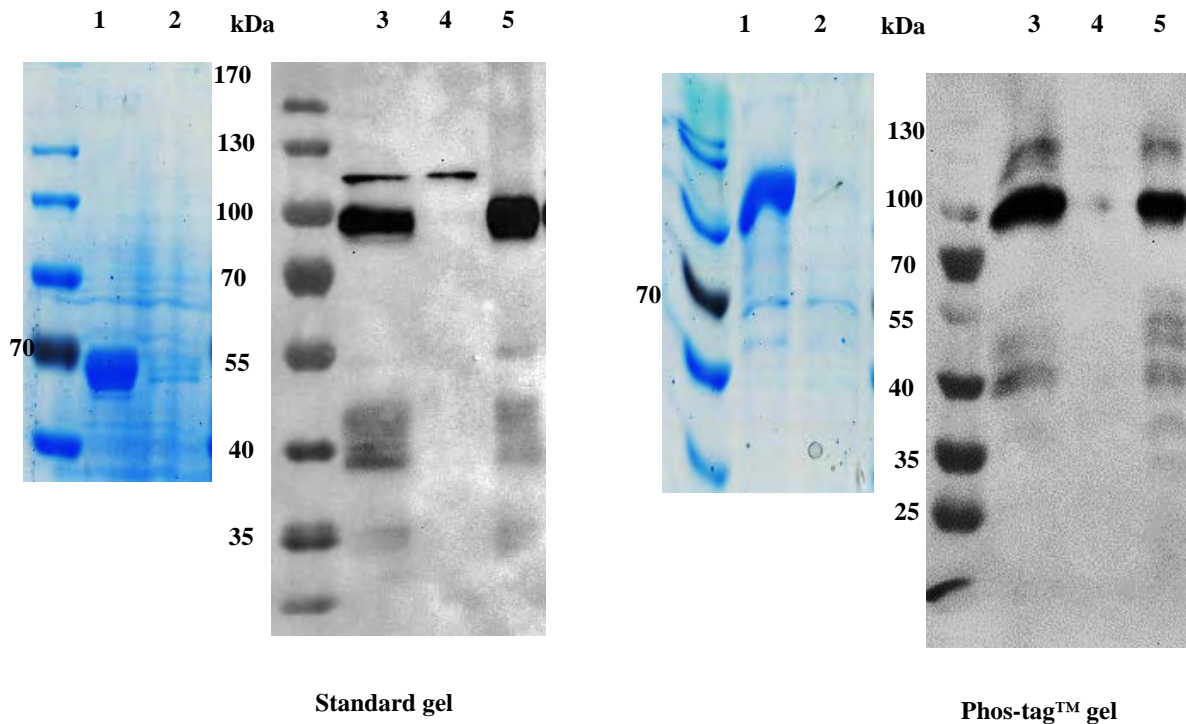
Phos-tag™ gel

Fig.7 Second immunodetection of NFP proteins after electrophoresis analysis on standard and Phos-tag^{Tm} gel of different fractions, free of EDTA, obtained for roots expressing pLeEXT1:NFP-FLAG not treated (-Rhz) with *S. meliloti*.

The roots were extracted and three cell fractions were obtained by differential centrifugation. 3x10^{3}g supernatant, 45x10^{3}g supernatant and 45x10^{3}g pellet all lacking EDTA were analysed on standard and Phos-tag^{Tm} gels. NFP was detected with anti-FLAG-HRP antibodies. On the same gels GST-LYK3-IR protein was analysed and used as a positive control for Phos-tag^{Tm} functionality. GST-LYK3-IR protein was retarded in the presence of Phos-tag^{Tm}. The immunoreactive polypeptides detected in the 3x10^{3}g supernatant and 45x10^{3}g pellet were migrating equally possessing better separation on Phos-tag^{Tm} gel.

Conclusions and discussion.

Expression of *LYK3* in the epidermis of *lyk3-1* plants has shown that LYK3 stays biologically active in this tissue and serves as an entry receptor promoting invasion of *Rhizobium*. In our experiment epidermal-expressed LYK3 complemented the *lyk3-1* mutant phenotype for such symbiotic responses as root hair curling, and the formation and progression of infection threads (Fig.1). However, the infection process was still strongly affected by the limitations in *LYK3* expression, with the ITs, becoming arrested before reaching the cortical tissue. This indicates the importance of LYK3 cortical expression for normal development of infection. Surprisingly, epidermal LYK3 was shown to trigger the formation of visible bumps in the *lyk3-1* plants, suggesting that it has the ability to signal downstream from the epidermis to the cortex and evoke such symbiotic response as cortical cell division (CCD). Such a finding puts LYK3 in line with NFP which was previously shown to rescue the CCD response while being expressed from the epidermal promoter in the *nfp* mutant background (Rival et al., 2012). However, in contrast to *LYK3*, epidermal expression of *NFP* was insufficient for initiating infection thread formation. Participation of LYK3 in infection at the level of the epidermis makes it similar to DMI3, for which epidermal expression was recently shown to rescue bacterial infection in epidermal tissue of *dmi3-1* plants (Rival et al., 2012). However unlike LYK3 and NFP, epidermal expression of DMI3 did not lead to bumps. Together our observations are suggesting that epidermal LYK3 contributes to both infection and nodule organogenesis combining therefore both NFP and DMI3 activities. After showing the symbiotic role of LYK3 in the epidermis, by analogy with the similar study performed for NFP and DMI3, it would be interesting to continue the research by investigating in which symbiotic responses LYK3 participates in the cortex and how epidermal NFP and LYK3 activate cortical cell division.

The development of PhosTag gels, allowed a study of LYK3 phosphorylation and possible changes in its phosphorylation following symbiotic treatments. No clear differences in the migration on the standard and Phos-tag™ gels were observed for the major 90 kDa band corresponding to whole LYK3 proteins in both Nod factor treated and non-treated samples (Fig.3). This observation suggests that LYK3 might not be phosphorylated although it is possible that the phosphorylated form may not be retarded enough to be resolved at this molecular weight. However, slight Phos-tag™ dependent retardation, identical in the presence and absence of symbiotic treatment, was detected for the LYK3 50 kDa-30 kDa minor bands. This work, although preliminary, suggests that LYK3 is phosphorylated *in vivo* independently of symbiotic stimulation. The fact that LYK3 seems to be phosphorylated is in agreement with its capability for auto-phosphorylation which was discovered using the GST-LYK3-IR protein expressed in *E. coli* (Klaus-Heisen et al., 2011) The very strong retardation of this GST-LYK3-IR protein on the Phos-tag™ gel (which is known to be phosphorylated in 15 different residues) compared to the very weak shift of the bands corresponding to the LYK3 protein from roots, suggests that in *M. truncatula* LYK3 may be phosphorylated to a much lower degree then in *E. coli*. To detect LYK3 phosphorylation sites, mass spectrometry analysis of LYK3+Nod and LYK3-Nod samples should be performed. The capability of auto-phosphorylation does not exclude the possibility

1- GST-LYK3-IR
2- pExt:NFP A17
3- pExt:NFP *lyk3-1*
4- pExt:NFP *dmi2-1*

Standard gel

Phos-tag™ gel

Fig.8 Immunodetection of NFP proteins after electrophoresis analysis on standard and Phos-tag^Tm gel of crude extracts from roots of wild type A17 plants or *lyk3-1* or *dmi2-1* mutant plants transiently expressing pLeEXT1:NFP-FLAG.

NFP proteins from wild type A17 plants and *lyk3-1* or *dmi2-1* mutants were analysed on the standard and Phos-tag^Tm gels and next detected by immunoblotting with anti-FLAG-HRP antibodies. GST-LYK3-IR protein was separated on the same gels and visualized by coomassie blue staining. GST-LYK3-IR protein was strongly retarded in the presence of Phos-tag^Tm. Migration profiles were similar for NFP obtained from A17, *lyk3-1* or *dmi2-1* plants, however better separation and higher amount of the minor bands was observed for all three samples on the Phos-tag^Tm gel.

that in *M. truncatula* LYK3 could be trans-phosphorylated by another protein with an active kinase. To study LYK3 trans-phosphorylation mutated LYK3 protein possessing an inactive kinase (for example G334E) and therefore blocked in auto-phosphorylation could be used. Phos-tag™ and mass spectrometry analyses performed for wild type and mutated LYK3 proteins after their expression in *M. truncatula* should clarify which out of the two possible mechanisms of phosphorylation takes place in the case of root-expressed LYK3. As the nitrogen status could play an important role in the activation of symbiotic receptors and because both LYK3+Nod and LYK3-Nod samples were obtained from nitrogen starved plants, phosphorylation of LYK3 in nitrogen sufficient conditions should also be investigated.

Phosphorylation of NFP in the presence and absence of *Rhizobium* was studied in several Phos-tag™ experiments. Results of the first experiment suggested that the NFP protein being initially phosphorylated in nitrogen-starved conditions gets degraded after treatment with symbiotic bacteria (Fig. 4). The NFP phosphorylated status is suggested by the highly retarded band detected on the Phos-tag™ gel in the extract obtained from non-treated with *Rhizobium* plants (Fig.4). The fact that the highly retarded band is absent in the sample treated with bacteria whereas all bands placed below the main 100 kDa band corresponding to whole NFP protein are retarded, could be explained by the degradation of phosphorylated NFP protein followed by the Phos-tag™ dependent retardation of the products of its degradation. However, repetition of this NFP activation experiment resulted in similar Phos-tag™ migration profiles for NFP+Rhz and NFP-Rhz samples, suggesting no effect of *Rhizobium* treatment on NFP phosphorylation (Fig.5). The differences between the two experiments could originate from some slight changes in the experimental conditions which could not be controlled in the aeroponic growth system and/or differences in the transgenic lines used. To clarify whether the bacteria affect NFP phosphorylation, additional experiments should be performed using another more reproducible system to produce the samples. Common to the two experiments was the Phos-tag™ dependent retardation of the minor bands placed below the 100 kDa band, probably corresponding to the phosphorylated products of NFP degradation. However, the main 100 kDa bands corresponding to the whole NFP protein seemed to be either not phosphorylated or so poorly phosphorylated that it could not be separated from its more abundant non-phosphorylated form, since no differences in their migration on the control and Phos-tag™ gels were detected. The retardation of the minor bands was detected for samples from roots both treated and non-treated with bacteria, suggesting that NFP is phosphorylated in both symbiotic and non-treated conditions. Both Phos-tag™ experiments were performed by using plants starved of nitrogen and since this may affect NFP phosphorylation similar experiments should be done with plants grown in the presence of nitrogen. Two fractionation experiments (Fig.6, Fig.7) performed to study the membrane association of NFP truncated forms (migrating below 100 kDa) indicated that all these polypeptides (with apparent molecular weights between 35 kDa and 55 kDa) are associated with the PM since they were detected in the microsomal fractions sedimenting at $20x10^3$ g and $45x10^3$ g. An interesting outcome from the first fractionation experiment is the validation of phosphorylation of the 45 kDa polypeptide which arises from the

1- pExt:LYR3 A17

2-pExt:LYR3 *lyk3-1*

| kDa | 1 | 2 | kDa | 1 | 2 |

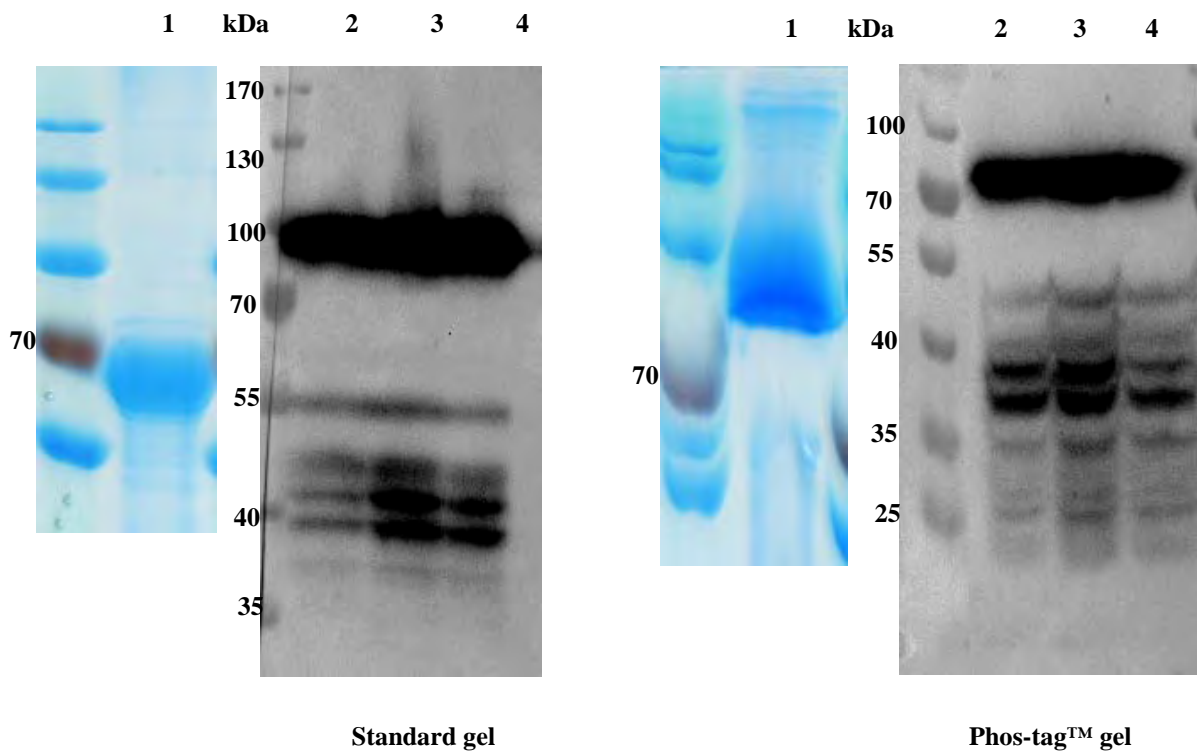Standard gel   Phos-tag™ gel
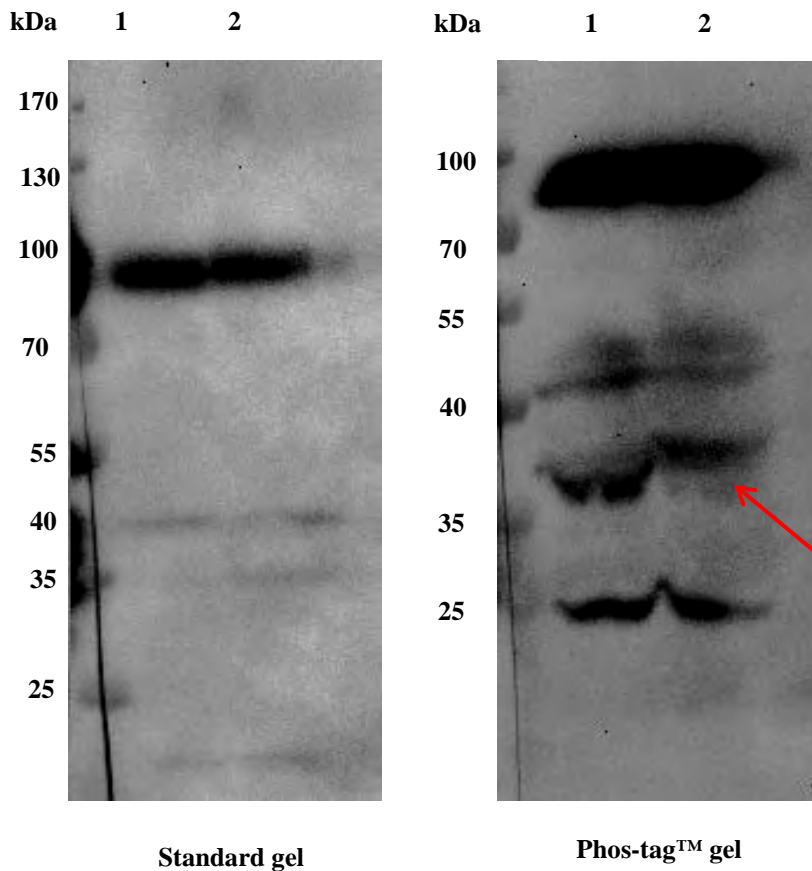
Fig.9 Immunodetection of LYR3 proteins after electrophoresis analysis on standard and Phos-tag^{Tm}gel of crude extracts obtained from roots of wild type A17 or *lyk3-1* mutant plants transiently expressing pLeEXT1:LYR3-HAST.

LYR3 proteins from wild type A17 and *lyk3-1* mutant plants were analysed on standard and Phos-tag^{Tm} gels and next detected with anti-HA-HRP antibodies by immunoblotting. Migration profiles were similar for LYR3 obtained from A17 or *lyk3-1* plants on the standard gel, however on the Phos-tag^{Tm} gel retardation of the minor immunoreactive polypeptide in the 35-40 kDa area was observed for LYR3 extracted from *lyk3-1* mutant plants.

difference in its migration on the Phos-tag™ gel in the presence and absence of EDTA (Fig.6).The fact that the phosphorylated forms of NFP are associated to the membrane suggests that they result from a truncation targeting the extracellular region. This could be a result of so called ectodomain shedding which from studies on some mammalian receptors is known to play an important role in protein activation (Higashiyama et al., 2011). Recently, it was shown that ectodomain shedding is also crucial for the biological functioning of the LRR-RLK SYMRK from *L. japonicus* (Antolín-Llovera, Ried, 2014). Whether such a mechanism of activation also takes place for NFP remains to be discovered. With that purpose, further study of truncated forms of NFP and particularly detection and mutation of the cleavage sites located in its ECD followed by complementation experiments should be performed.

For the reason that in several experiments NFP seemed to be phosphorylated, its phosphorylation was investigated in *lyk3* or *dmi2* mutant backgrounds. The obtained results suggest that neither LYK3 nor DMI2 are essential for NFP phosphorylation since no differences in the Phos-tag™ migration profiles were observed for the samples of NFP obtained from A17, *lyk3-1* or *dmi2-1* plants (Fig.8). The presence of NFP phosphorylation in the mutants is shown by the Phos-tag™ dependent retardation of the minor bands observed in all samples. According to the obtained results, NFP can be phosphorylated by kinase(s) expressed in the epidermis, which are different to LYK3 and DMI2. The search for the protein(s) that trans-phosphorylates NFP should be continued and to facilitate the selection of the protein-candidates, the SYMbiMICs database, which includes transcriptomics of laser-dissected epidermal cells, could be used.

A study of LYR3 phosphorylation by LYK3, was also performed since, like NFP, LYR3 possesses an inactive kinase and thus would require trans-phosphorylation. Also the kinase like domain of LYR3 has been shown to be phosphorylated by the kinase domain of LYK3 *in vitro* (J. Fliegmann, unpublished). The detection of slightly retarded minor bands in both *lyk3-1*and A17 samples on the Phos-tag™ gel in comparison to the standard one (Fig.9), could indicate that, independently of LYK3, LYR3 is phosphorylated at a low level in *vivo*. Additionally, one of the minor bands from the *lyk3-1* sample was shown to be retarded in comparison to the same band in the A17 sample, suggesting that LYR3 undergoes supplementary phosphorylation in the absence of LYK3. This in turn could mean that LYK3 plays a negative role in LYR3 phosphorylation. However, this extra phosphorylation, shown only for the truncated form of LYR3, requires further validation by the repetition of the experiment followed by purification of the protein and mass spectrometry analysis.

Conclusions and perspectives

Mutualistic plant microbe symbioses are known to play very important biological, agricultural and ecological roles. In the last twenty years it has been revealed that a key element required for symbiosis establishment is the molecular dialog between the host plant and its microsymbiont. Initially this was demonstrated for the rhizobial symbiosis, where the legume plant activates its rhizobial partner to produce LCO signal molecules, which were shown to be essential for nodulation, infection and specific recognition between Rhizobia and legumes. Following their discovery in 1990, within a few years Nod factors were shown to trigger a number of plant responses, such as root growth stimulation and increase in nodulation. In1994 LCOs were commercialized and used to improve yield of several important legume crops. Subsequently arbuscular mycorrhizal fungi were shown to produce signals, structurally similar to Nod factors, called the Myc-LCOs, which display stimulatory effects on mycorrhization. These signal molecules potentially extend LCOs application to all plants susceptible to AM fungi, which includes 90% of the land plants, and LCO products are now available for maize. Despite the biological and commercial importance of LCOs, to date little is known about the mechanisms underlying their perception and discrimination in plants. Recently a high affinity LCO binding protein LYR3 was identified in *M. truncatula.* Due to its ability to perceive LCOs, LYR3 could be expected to be a part of the plant symbiotic machinery.

The characterization of the LYR3 protein and its interaction with LCOs was the main focus of my thesis.

Through the characterization of LYR3 in different legumes (*P. sativum, G. max, P. vulgaris*, *L. japonicus* and *L. angustifolius*) I showed that LYR3 proteins from all these species, except *L. angustifolius,* possess high affinity binding to both Nod factors and Myc-LCOs but not to COs. Although demonstrating specificity for LCOs versus COs, LYR3 proteins were unable to discriminate different structures of LCOs determined by their chemical decorations. The lack of specificity for LCO decorations present on rhizobial and mycorrhizal LCOs, may suggest a generic role of LYR3 in both the bacterial and fungal symbioses. The LYR3 protein from *L. angustifolius* was shown to be impaired in LCO binding and since this species is known to be a non-host for mycorrhizal fungi it is tempting to link these two phenomena and suggest a role of LYR3 in mycorrhization. However, recent studies have shown that *L. angustifolius* lacks several other genes implicated in mycorrhization, suggesting that the loss of binding to LYR3 could not be the sole determinant for the Myc$^-$ phenotype (Delaux et al., 2014).

The inability of LYR3 from *L. angustifolius* to bind LCO was used to study the involvement of different LysM domains of LYR3 protein in LCO binding. For that, domain swapping was performed between the three LysM domains of *M. truncatula* (Mt) and *L. angustifolius* (Lan) LYR3 proteins. According to the obtained results, the third LysM domain (LysM3) plays a crucial role in LCO accommodation. This was concluded since all chimeric proteins containing MtLysM3 were shown to conserve their ability to bind LCO. Subsequent site directed mutagenesis pinpointed a particular amino-acid in the third LysM domain, Y228, which is conserved in all the legume LYR3

binding proteins and which is crucial for LCO binding. Since this residue was never reported to be a component of CO binding site it seems to be specifically involved in LCO recognition.

Structural studies are now revealing the molecular basis of CO recognition. For example, chitin and COs have been shown to be recognized by the second LysM domain of both rice CEBiP (Hayafune et al., 2014) and Arabidopsis CERK1 receptors (Liu et al., 2012). A fungal LysM receptor, Ecp6, carries two CO binding sites, one is located in the LysM2 and exhibits a low affinity for CO (in the μM range) and the other, a high affinity binding site, is formed at the interface between the LysM1 and the LysM3 domains (Sánchez-Vallet et al., 2013). In all these cases CO binding involves the same groove in the conserved βααβ structure of a LysM domain. Our results show a clear role of LysM3 of LYR3 in LCO perception. Whether the other two domains of LYR3, LysM1 and LysM2 also participate in LCO perception or play a structural role remains to be discovered. To study this, site directed mutagenesis could be performed by targeting residues of the LysM1 or LysM2 of *M. truncatula* LYR3 corresponding to those identified in the LysM1 of Ecp6 or LysM2 of AtCERK1. However, for a complete understanding of the mechanism of LCO perception structural analyses by X-ray crystallography or NMR of the extracellular domain of LYR3 in interaction with LCO is needed.

As LYR3 is a target for LCOs, experiments were aimed to investigate whether its ECD could be used to trigger responses in non-legume plants after their treatment with LCOs. These studies have shown that the LYR3 ECD could be combined with the kinase domain of other proteins to form a biologically functional chimeric receptor. Thus, LYR3/CERK1 chimeric receptors were found to trigger a cell death response following expression in *N. benthamiana.* In turn LYR3/EFR chimeras expressed together with a LYR3/BAK1 co-receptor were shown to evoke a cell death response and emission of ethylene in tobacco leaves. However, both types of chimeric proteins were auto-active and insensitive to LCO, suggesting that the creation of regulatable chimeric constructions requires some improvements. One of the possible reasons for auto-activation of the chimeras could be their ligand independent dimerization, probably triggered by their overexpression from the strong 35S promoter. Thus selection of a new, weaker promoter could be proposed as one of the possible future improvements. For LYR3/EFR, co-expression together with a LYR3/BAK1 chimera was required for response activation. The ligand independent activation observed in this case could be due to the interaction of the LYR3 ECDs in the heteromeric chimeras, as it has been shown recently that the complete LYR3 protein is capable of homodimerization (J. Fliegmann, unpublished). Deeper exploration of LYR3 by revealing the residues involved in its dimerization could be used for introducing some changes in the LYR3 ECD to improve its functionality in a composition of chimeric receptors. However, for possible agricultural application, it would be more convenient to base LCO response activation on single chimeric receptors. The recently identified *A. thaliana* lipochitooligosaccharide (LPS) binding RLK, SD1-29, which does not require the co-receptor BAK1, but activates defense responses (Ranf et al., 2015) could be used for the creation of new chimeric receptors with LYR3 ECD.

Recent studies in the group, using *lyr3* mutants, have not revealed a clear role for this protein in symbiosis. In contrast the LysM-RLKs NFP and LYK3 have clear genetically-defined roles in LCO responses and in the *Rhizobium* symbiosis and LYK3 also participates in the mycorrhizal symbiosis (Zhang et al., 2015). These two proteins, unlike LYR3, do not appear to bind Nod factors (J.J. Bono, unpublished). Thus an alternative technique (PhosTag) was developed, which allowed us to detect the phosphorylation of these proteins in the epidermal cells in *planta*. An experiment aimed to investigate the symbiotic role of LYK3 in the level of epidermis revealed a previously unknown ability of LYK3 to trigger a CCD response demonstrating its involvement in the signal transduction from the epidermis to the cortex. This role is in addition to its role in infection (Smit et al., 2007). Results obtained from our studies of LYK3 phosphorylation in the root epidermis suggest that it is phosphorylated in both symbiotic and normal conditions. In the case of NFP, this protein was shown to be phosphorylated independently of the symbiotic treatments. Interestingly, phosphorylation was detected only for the truncated forms of LYK3 and NFP. Some of the phosphorylated minor proteins belonging to NFP were associated with the membrane fraction and according to their molecular weights, appear to lack the extracellular domains. By analogy with SYMRK (Antolín-Llovera et al., 2014) it is tempting to hypothesize that the NFP ECD removal could be caused by so called ectodomain shedding which was shown to be essential for SYMRK biological functioning.

Mass spectrometric analysis of truncated forms of LYK3 and NFP is an obvious next step in the characterization of these two proteins since it should define the LYK3 and NFP phosphorylation sites and also the cleavage sites in the case of NFP. Subsequent site directed mutagenesis of the residues involved in phosphorylation or cleavage, followed by complementation studies of the appropriate mutants, would clarify whether these two processes are essential for LYK3 and NFP biological functioning.

The study of NFP phosphorylation in *dmi2-1* and *lyk3-1* mutant backgrounds suggests that neither DMI2 nor LYK3 are responsible for the phosphorylation of NFP, which contains a dead kinase. Therefore another receptor possessing trans-phosphorylation activity serves for this posttranslational modification of NFP. Future search for this interacting kinase protein could recruit such tactics as exploiting the SYMbiMICs epidermal transcriptomics database (https://iant.toulouse.inra.fr/symbimics) and identifying NFP interactors by co- immunopurification, from root tissue.

Together this work has contributed to our knowledge of three receptors, LYR3, NFP, and LYK3, involved in LCO perception. Further studies are required to understand the interaction between these receptors and how different Nod and Myc LCOs are discriminated to activate symbiotic responses.

References

Akiyama K, Matsuzaki K, Hayashi H. Plant sesquiterpenes induce hyphal branching in arbuscular mycorrhizal fungi. Nature. 2005;435:824-27.

Albert M, Jehle AK, Mueller K, Eisele C, Lipschis M, Felix G. The Arabidopsis thaliana pattern recognition receptors for bacterial EF-TU and flagellin can be combined to form functional chimeric receptors. Journal of Biological Chemistry. 2010:-.

Allen DG, Blinks JR, Prendergast FG. AEQUORIN LUMINESCENCE - RELATION OF LIGHT-EMISSION TO CALCIUM CONCENTRATION - CALCIUM-INDEPENDENT COMPONENT. Science. 1977;195:996-98.

Antolín-Llovera M, Ried Martina K, Parniske M. Cleavage of the SYMBIOSIS RECEPTOR-LIKE KINASE Ectodomain Promotes Complex Formation with Nod Factor Receptor 5. Current Biology. 2014;24:422-27.

Ardourel M, Demont N, Debellé F, Maillet F, de Billy F, Prome JC, et al. Rhizobium meliloti lipooligosaccharide nodulation factors: different structural requirements for bacterial entry into target root hair cells and induction of plant symbiotic developmental responses. Plant Cell. 1994;6:1357-74.

Arrighi J-F, Barre A, Ben Amor B, Bersoult A, Soriano LC, Mirabella R, et al. The Medicago truncatula lysin motif-receptor-like kinase gene family includes NFP and new nodule-expressed genes. Plant Physiol. 2006;142:265-79.

Bago B, Pfeffer PE, Shachar-Hill Y. Carbon metabolism and transport in arbuscular mycorrhizas. Plant Physiology. 2000;124:949-57.

Barker D, Bianchi S, Blondon F, Dattée Y, Duc G, Essad S, Flament P, Gallusci P, Génier G, Guy P, Muel X, Tourneur J, Dénarié J, Huguet T (1990) Medicago truncatula, a model plant for studying the molecular genetics of the Rhizobium-legume symbiosis. Plant Mol Biol Rep 8: 40-49

Ben Amor B, Shaw SL, Oldroyd GE, Maillet F, Penmetsa RV, Cook D, et al. The NFP locus of Medicago truncatula controls an early step of Nod factor signal transduction upstream of a rapid calcium flux and root hair deformation. Plant J. 2003;34:495-506.

Bensmihen S, de Billy F, Gough C. Contribution of NFP LysM domains to the recognition of Nod Factors during the Medicago truncatula/Sinorhizobium meliloti symbiosis. PLoS ONE. 2011;6:e26114.

Besserer A, Puech-Pages V, Kiefer P, Gomez-Roldan V, Jauneau A, Roy S, et al. Strigolactones stimulate arbuscular mycorrhizal fungi by activating mitochondria. Plos Biology. 2006;4:1239-47.

Broghammer A, Krusell L, Blaise M, Sauer J, Sullivan JT, Maolanon N, et al. Legume receptors perceive the rhizobial lipochitin oligosaccharide signal molecules by direct binding. Proc Natl Acad Sci USA. 2012;109:13859-64.

Brutus A, Sicilia F, Macone A, Cervone F, De Lorenzo G. A domain swap approach reveals a role of the plant wall-associated kinase 1 (WAK1) as a receptor of oligogalacturonides. Proceedings of the National Academy of Sciences of the United States of America. 2010;107:9452-57.

Cao Y, Liang Y, Tanaka K, Nguyen CT, Jedrzejczak RP, Joachimiak A, et al. The kinase LYK5 is a major chitin receptor in Arabidopsis and forms a chitin-induced complex with related kinase CERK1. eLife. 2014.

Capoen W, Sun J, Wysham D, Otegui MS, Venkateshwaran M, Hirsch S, et al. Nuclear membranes control symbiotic calcium signaling of legumes. Proceedings of the National Academy of Sciences. 2011;108:14348-53.

Catoira R, Galera C, de Billy F, Penmetsa RV, Journet EP, Maillet F, et al. Four genes of Medicago truncatula controlling components of a Nod factor transduction pathway. Plant Cell. 2000;12:1647-66.

Catoira R, Timmers AC, Maillet F, Galera C, Penmetsa RV, Cook D, et al. The HCL gene of Medicago truncatula controls Rhizobium-induced root hair curling. Development. 2001;128:1507-18.

Chen T, Zhu H, Ke D, Cai K, Wang C, Gou H, et al. A MAP Kinase Kinase Interacts with SymRK and Regulates Nodule Organogenesis in Lotus japonicus. The Plant Cell Online. 2012.

Chinchilla D, Bauer Z, Regenass M, Boller T, Felix G. The Arabidopsis Receptor Kinase FLS2 Binds flg22 and Determines the Specificity of Flagellin Perception. Plant Cell. 2006;18:465-76.

Clough SJ, Bent AF. Floral dip: a simplified method for Agrobacterium-mediated transformation of Arabidopsis thaliana. Plant Journal. 1998;16:735-43.

Cook DR. Medicago truncatula - a model in the making! Commentary. Current Opinion in Plant Biology. 1999;2:301-04.

Cullimore J, Dénarié J. How legumes select their sweet talking symbionts. Science. 2003;302:575-8.

D'Haeze W, Holsters M. Nod factor structures, responses, and perception during initiation of nodule development. Glycobiology. 2002;12:79R-105.

da Silva DKA, Freitas ND, Cuenca G, Maia LC, Oehl F. Scutellospora pernambucana, a new fungal species in the Glomeromycetes with a diagnostic germination orb. Mycotaxon. 2008;106:361-70.

De Lorenzo G, Brutus A, Savatin DV, Sicilia F, Cervone F. Engineering plant resistance by constructing chimeric receptors that recognize damage-associated molecular patterns (DAMPs). FEBS Letters. 2011;585:1521-28.

Delaux P-M, Varala K, Edger PP, Coruzzi GM, Pires JC, Ané J-M. Comparative phylogenomics uncovers the impact of symbiotic associations on host genome evolution. PLoS Genet. 2014;10:e1004487.

Denison RF, Kiers ET. Life Histories of Symbiotic Rhizobia and Mycorrhizal Fungi. Current Biology. 2011;21:R775-R85.

Dénarié J, Debellé F, Promé JC. Rhizobium lipo-chitooligosaccharide nodulation factors: signaling molecules mediating recognition and morphogenesis. Annu Rev Biochem. 1996;65:503-35.

Faulkner C, Petutschnig E, Benitez-Alfonso Y, Beck M, Robatzek S, Lipka V, et al. LYM2-dependent chitin perception limits molecular flux via plasmodesmata. Proceedings of the National Academy of Sciences of the United States of America. 2013;110:9166-70.

Felix G, Duran JD, Volko S, Boller T. Plants have a sensitive perception system for the most conserved domain of bacterial flagellin. Plant Journal. 1999;18:265-76.

Fliegmann J, Canova S, Lachaud C, Uhlenbroich S, Gasciolli V, Pichereaux C, et al. Lipo-chitooligosaccharidic symbiotic signals are recognized by LysM Receptor-Like Kinase LYR3 in the legume Medicago truncatula. ACS Chem Biol. 2013;8:1900-06.

Gage DJ. Infection and invasion of roots by symbiotic, nitrogen-fixing rhizobia during nodulation of temperate legumes. Microbiology and Molecular Biology Reviews. 2004;68:280-+.

Galibert F, Finan TM, Long SR, Puhler A, Abola P, Ampe F, et al. The Composite Genome of the Legume Symbiont Sinorhizobium meliloti. Science. 2001;293:668-72.

Genre A, Chabaud M, Balzergue C, Puech-Pages V, Novero M, Rey T, et al. Short-chain chitin oligomers from arbuscular mycorrhizal fungi trigger nuclear Ca2+ spiking in Medicago truncatula roots and their production is enhanced by strigolactone. New Phytologist. 2013;198:179-89.

Genre A, Chabaud M, Faccio A, Barker DG, Bonfante P. Prepenetration Apparatus Assembly Precedes and Predicts the Colonization Patterns of Arbuscular Mycorrhizal Fungi within the Root Cortex of Both Medicago truncatula and Daucus carota. The Plant Cell. 2008:tpc.108.059014.

Geurts R, Lillo A, Bisseling T. Exploiting an ancient signalling machinery to enjoy a nitrogen fixing symbiosis. Current Opinion in Plant Biology. 2012;15:438-43.

Gherbi H, Markmann K, Svistoonoff S, Estevan J, Autran D, Giczey G, et al. SymRK defines a common genetic basis for plant root endosymbioses with arbuscular mycorrhiza fungi, rhizobia, and Frankia bacteria. Proceedings of the National Academy of Sciences. 2008:0710618105.

Giraud E, Moulin L, Vallenet D, Barbe V, Cytryn E, Avarre J-C, et al. Legumes Symbioses: Absence of Nod Genes in Photosynthetic Bradyrhizobia. Science. 2007;316:1307-12.

Goodin MM, Zaitlin D, Naidu RA, Lommel SA. Nicotiana benthamiana: Its history and future as a model for plant-pathogen interactions. Molecular Plant-Microbe Interactions. 2008;21:1015-26.

Gough C, Jacquet C. Nod factor perception protein carries weight in biotic interactions. Trends Plant Sci. 2013;18:566-74.

Gutjahr C, Novero M, Guether M, Montanari O, Udvardi M, Bonfante P. Presymbiotic factors released by the arbuscular mycorrhizal fungus Gigaspora margarita induce starch accumulation in Lotus japonicus roots. New Phytologist. 2009;183:53-61.

Handberg K, Stougaard J. LOTUS-JAPONICUS, AN AUTOGAMOUS, DIPLOID LEGUME SPECIES FOR CLASSICAL AND MOLECULAR-GENETICS. Plant Journal. 1992;2:487-96.

Harrison MJ. Signaling in the arbuscular mycorrhizal symbiosis. Annual Review of Microbiology. Palo Alto: Annual Reviews; 2005. p. 19-42.

Hassan S, Mathesius U. The role of flavonoids in root-rhizosphere signalling: opportunities and challenges for improving plant-microbe interactions. Journal of Experimental Botany. 2012;63:3429-44.

Hayafune M, Berisio R, Marchetti R, Silipo A, Kayama M, Desaki Y, et al. Chitin-induced activation of immune signaling by the rice receptor CEBiP relies on a unique sandwich-type dimerization. Proc Natl Acad Sci USA. 2014.

Higashiyama S, Nanba D, Nakayama H, Inoue H, Fukuda S. Ectodomain shedding and remnant peptide signalling of EGFRs and their ligands. Journal of Biochemistry. 2011;150:15-22.

Hocher V, Alloisio N, Auguy F, Fournier P, Doumas P, Pujic P, et al. Transcriptomics of actinorhizal symbioses reveals homologs of the whole common symbiotic signaling cascade. Plant Physiology. 2011a.

Hocher V, Alloisio N, Bogusz D, Normand P. Early signaling in actinorhizal symbioses. Plant signaling & behavior. 2011b;6:1377-9.

Indrasumunar A, Searle I, Lin M-H, Kereszt A, Men A, Carroll BJ, et al. Nodulation factor receptor kinase 1α controls nodule organ number in soybean (Glycine max L. Merr). The Plant Journal. 2011;65:39-50.

Kaku H, Nishizawa Y, Ishii-Minami N, Akimoto-Tomiyama C, Dohmae N, Takio K, et al. Plant cells recognize chitin fragments for defense signaling through a plasma membrane receptor. Proc Natl Acad Sci USA. 2006;103:11086-91.

Kevei Z, Lougnon G, Mergaert P, Horvath GV, Kereszt A, Jayaraman D, et al. 3-Hydroxy-3-Methylglutaryl Coenzyme A Reductase1 Interacts with NORK and Is Crucial for Nodulation in Medicago truncatula. The Plant Cell. 2007;19:3974-89.

Kishimoto K, Kouzai Y, Kaku H, Shibuya N, Minami E, Nishizawa Y. Perception of the chitin oligosaccharides contributes to disease resistance to blast fungus Magnaporthe oryzae in rice. The Plant Journal. 2010;64:343-54.

Klaus-Heisen D, Nurisso A, Pietraszewska-Bogiel A, Mbengue M, Camut S, Timmers T, et al. Structure-function similarities between a plant receptor-like kinase and the human interleukin-1 receptor-associated kinase-4. J Biol Chem. 2011;286:11202-10.

Kosuta S, Chabaud M, Lougnon G, Gough C, Dénarié J, Barker DG, et al. A diffusible factor from arbuscular mycorrhizal fungi induces symbiosis-specific MtENOD11 expression in roots of Medicago truncatula. Plant Physiol. 2003;131:952-62.

Kouchi H, Imaizumi-Anraku H, Hayashi M, Hakoyama T, Nakagawa T, Umehara Y, et al. How Many Peas in a Pod? Legume Genes Responsible for Mutualistic Symbioses Underground. Plant cell physiol. 2010;51:1381-97.

Kretzschmar T, Kohlen W, Sasse J, Borghi L, Schlegel M, Bachelier JB, et al. A petunia ABC protein controls strigolactone-dependent symbiotic signalling and branching. Nature. 2012;483:341-U135.

Kucho K-i, Hay A-E, Normand P. The Determinants of the Actinorhizal Symbiosis. Microbes and Environments. 2010;25:241-52.

Kuhn H, Küster H, Requena N. Membrane steroid-binding protein 1 induced by a diffusible fungal signal is critical for mycorrhization in Medicago truncatula. New Phytologist. 2010;185:716-33.

Lakatos L, Szittya G, Silhavy D, Burgyan J. Molecular mechanism of RNA silencing suppression mediated by p19 protein of tombusviruses. Embo Journal. 2004;23:876-84.

Liang Y, Tóth K, Cao Y, Tanaka K, Espinoza C, Stacey G. Lipochitooligosaccharide recognition: an ancient story. New Phytologist. 2014;204:289-96.

Limpens E, Franken C, Smit P, Willemse J, Bisseling T, Geurts R. LysM domain receptor kinases regulating rhizobial Nod factor-induced infection. Science. 2003;302:630-03.

Liu T, Liu Z, Song C, Hu Y, Han Z, She J, et al. Chitin-induced dimerization activates a plant immune receptor. Science. 2012;336:1160-64.

Madsen EB, Antolín-Llovera M, Grossmann C, Ye J, Vieweg S, Broghammer A, et al. Autophosphorylation is essential for the in vivo function of the Lotus japonicus Nod factor receptor 1 and receptor-mediated signalling in cooperation with Nod factor receptor 5. Plant J. 2011;65:404-17.

Madsen EB, Madsen LH, Radutoiu S, Olbryt M, Rakwalska M, Szczyglowski K, et al. A receptor kinase gene of the LysM type is involved in legume perception of rhizobial signals. Nature. 2003;425:637-40.

Madsen LH, Tirichine L, Jurkiewicz A, Sullivan JT, Heckmann AB, Bek AS, et al. The molecular network governing nodule organogenesis and infection in the model legume Lotus japonicus. Nat Commun. 2010;1:10.

Maillet F, Poinsot V, André O, Puech-Pages V, Haouy A, Gueunier M, et al. Fungal lipochitooligosaccharide symbiotic signals in arbuscular mycorrhiza. Nature. 2011;469:58-63.

Markmann K, Parniske M. Evolution of root endosymbiosis with bacteria: how novel are nodules? Trends in Plant Science. 2009;14:77-86.

Masson-Boivin C, Giraud E, Perret X, Batut J. Establishing nitrogen-fixing symbiosis with legumes: how many rhizobium recipes? Trends in Microbiology. 2009;17:458-66.

Mbengue M, Camut S, de Carvalho-Niebel F, Deslandes L, Froidure S, Klaus-Heisen D, et al. The Medicago truncatula E3 Ubiquitin Ligase PUB1 interacts with the LYK3 symbiotic receptor and negatively regulates infection and nodulation. Plant Cell.22:3474-88.

Mesnage S, Dellarole M, Baxter NJ, Rouget J-B, Dimitrov JD, Wang N, et al. Molecular basis for bacterial peptidoglycan recognition by LysM domains. Nat Commun. 2014;5.

Miya A, Albert P, Shinya T, Desaki Y, Ichimura K, Shirasu K, et al. CERK1, a LysM receptor kinase, is essential for chitin elicitor signaling in Arabidopsis. Proc Natl Acad Sci USA. 2007;104:19613-18.

Moling S, Pietraszewska-Bogiel A, Postma M, Fedorova E, Hink MA, Limpens E, et al. Nod factor receptors form heteromeric complexes and are essential for intracellular infection in Medicago nodules. The Plant Cell. 2014;26:4188-99.

Mulder L, Lefebvre B, Cullimore J, Imberty A. LysM domains of Medicago truncatula NFP protein involved in Nod factor perception. Glycosylation state, molecular modeling and docking of chitooligosaccharides and Nod factors. Glycobiology. 2006;16:801-09.

Olah B, Briere C, Bécard G, Dénarié J, Gough C. Nod factors and a diffusible factor from arbuscular mycorrhizal fungi stimulate lateral root formation in Medicago truncatula via the DMI1/DMI2 signalling pathway. The Plant J. 2005;44:195-207.

Oldroyd GED. Speak, friend, and enter: signalling systems that promote beneficial symbiotic associations in plants. Nat Rev Micro. 2013;11:252-63.

Oldroyd GED, Murray JD, Poole PS, Downie JA. The rules of engagement in the legume-Rhizobial symbiosis. Annu Rev Genetics. 2011;45:119-44.

Op den Camp R, Streng A, De Mita S, Cao Q, Polone E, Liu W, et al. LysM-Type Mycorrhizal Receptor Recruited for Rhizobium Symbiosis in Nonlegume Parasponia. Science. 2011;331:909-12.

Op den Camp RHM, Polone E, Fedorova E, Roelofsen W, Squartini A, Op den Camp HJM, et al. Nonlegume Parasponia andersonii Deploys a Broad Rhizobium Host Range Strategy Resulting in Largely Variable Symbiotic Effectiveness. Molecular Plant-Microbe Interactions. 2012;25:954-63.

Parniske M. Plant-fungal associations - Cue for the branching connection. Nature. 2005;435:750-51.

Parniske M. Arbuscular mycorrhiza: the mother of plant root endosymbioses. Nat Rev Micro. 2008;6:763-75.

Pawlowski K, Demchenko KN. The diversity of actinorhizal symbiosis. Protoplasma. 2012;249:967-79.

Perret X, Staehelin C, Broughton WJ. Molecular basis of symbiotic promiscuity. Microbiology and Molecular Biology Reviews. 2000;64:180-+.

Petutschnig EK, Jones AME, Serazetdinova L, Lipka U, Lipka V. The Lysin motif receptor-like kinase (LysM-RLK) CERK1 is a major chitin-binding protein in Arabidopsis thaliana and subject to chitin-induced phosphorylation. J Biol Chem. 2010;285:28902-11.

Pietraszewska-Bogiel A, Lefebvre B, Koini MA, Klaus-Heisen D, Takken FLW, Cullimore JV, et al. Interaction of Medicago truncatula Lysin motif receptor-like kinases, NFP and LYK3, produced in Nicotiana benthamiana leaf induces defence-like responses. PLoS One. 2013;8:e65055.

Popovici J, Comte G, Bagnarol E, Alloisio N, Fournier P, Bellvert F, et al. Differential Effects of Rare Specific Flavonoids on Compatible and Incompatible Strains in the Myrica gale-Frankia Actinorhizal Symbiosis. Applied and Environmental Microbiology. 2010;76:2451-60.

Radutoiu S, Madsen LH, Madsen EB, Felle HH, Umehara Y, Gronlund M, et al. Plant recognition of symbiotic bacteria requires two LysM receptor-like kinases. Nature. 2003;425:585-92.

Radutoiu S, Madsen LH, Madsen EB, Jurkiewicz A, Fukai E, Quistgaard EM, et al. LysM domains mediate lipochitin-oligosaccharide recognition and Nfr genes extend the symbiotic host range. EMBO J. 2007;26:3923-35.

Ranf S, Gisch N, Schaffer M, Illig T, Westphal L, Knirel YA, et al. A lectin S-domain receptor kinase mediates lipopolysaccharide sensing in Arabidopsis thaliana. Nature immunology. 2015;16:426-33.

Rival P, de Billy F, Bono J-J, Gough C, Rosenberg C, Bensmihen S. Epidermal and cortical roles of NFP and DMI3 in coordinating early steps of nodulation in Medicago truncatula. Development. 2012;139:3383-91.

Roche P, Lerouge P, Ponthus C, Promé D. Structural determination of bacterial nodulation factors involved in the Rhizobium meliloti-alfalfa symbiosis. J Biol Chem. 1991;266:10933-40.

Roux M, Schwessinger B, Albrecht C, Chinchilla D, Jones A, Holton N, et al. The Arabidopsis Leucine-Rich Repeat Receptor-Like Kinases BAK1/SERK3 and BKK1/SERK4 Are Required for Innate Immunity to Hemibiotrophic and Biotrophic Pathogens. Plant Cell. 2011;23:2440-55.

Saito K, Yoshikawa M, Yano K, Miwa H, Uchida H, Asamizu E, et al. Nucleoporin 85 Is Required for Calcium Spiking, Fungal and Bacterial Symbioses, and Seed Production in Lotus japonicus. Plant Cell. 2007:tpc.106.046938.

Sanchez-Vallet A, Mesters JR, Thomma BPHJ. The battle for chitin recognition in plant-microbe interactions. FEMS microbiology reviews. 2015;39:171-83.

Sanders IR, Croll D. Arbuscular Mycorrhiza: The Challenge to Understand the Genetics of the Fungal Partner. In: Campbell A, Lichten M, Schupbach G, editors. Annual Review of Genetics, Vol 44. Palo Alto: Annual Reviews; 2010. p. 271-92.

Sato S, Tabata S. Lotus japonicus as a platform for legume research. Current Opinion in Plant Biology. 2006;9:128-32.

Segovia L, Pinero D, Palacios R, Martinezromero E. GENETIC-STRUCTURE OF A SOIL POPULATION OF NONSYMBIOTIC RHIZOBIUM-LEGUMINOSARUM. Applied and Environmental Microbiology. 1991;57:426-33.

Shimizu T, Nakano T, Takamizawa D, Desaki Y, Ishii-Minami N, Nishizawa Y, et al. Two LysM receptor molecules, CEBiP and OsCERK1, cooperatively regulate chitin elicitor signaling in rice. The Plant Journal. 2010;64:204-14.

Shinya T, Motoyama N, Ikeda A, Wada M, Kamiya K, Hayafune M, et al. Functional characterization of CEBiP and CERK1 homologs in Arabidopsis and rice reveals the presence of different chitin receptor systems in plants. Plant Cell Physiol. 2012;53:1696-706.

Shiu SH, Bleecker AB. Plant receptor-like kinase gene family: diversity, function, and signaling. Science's STKE : signal transduction knowledge environment. 2001;2001:re22-re22.

Singh S, Katzer K, Lambert J, Cerri M, Parniske M. CYCLOPS, A DNA-Binding Transcriptional Activator, Orchestrates Symbiotic Root Nodule Development. Cell host & microbe. 2014;15:139-52.

Smit P, Limpens E, Geurts R, Fedorova E, Dolgikh E, Gough C, et al. Medicago LYK3, an entry receptor in rhizobial nodulation factor signaling. Plant Physiol. 2007;145:183-91.

Smith SE, Smith FA, Jakobsen I. Mycorrhizal fungi can dominate phosphate supply to plants irrespective of growth responses. Plant Physiology. 2003;133:16-20.

Sun J, Miller JB, Granqvist E, Wiley-Kalil A, Gobbato E, Maillet F, Cottaz S, Samain E, Venkateshwaran M, Fort S, Morris RJ, Ané J-M, Dénarié J, Oldroyd GED (2015) Activation of Symbiosis Signaling by Arbuscular Mycorrhizal Fungi in Legumes and Rice. The Plant Cell doi: http://dx.doi.org/10.1105/tpc.114.131326

Svistoonoff S, Hocher V, Gherbi H. Actinorhizal root nodule symbioses: what is signalling telling on the origins of nodulation? Current Opinion in Plant Biology. 2014;20:11-18.

Sánchez-Vallet A, Saleem-Batcha R, Kombrink A, Hansen G, Valkenburg D-J, Thomma B, P. H. J, et al. Fungal effector Ecp6 outcompetes host immune receptor for chitin binding through intrachain LysM dimerization. eLife. 2013;2:e00790.

Timmers AC, Auriac MC, Truchet G. Refined analysis of early symbiotic steps of the Rhizobium-Medicago interaction in relationship with microtubular cytoskeleton rearrangements. Development. 1999;126:3617-28.

Tomida J, Kitao H, Kinoshita E, Takata M. Detection of phosphorylation on large proteins by Western blotting using Phos-tag containing gel. Nat Protoc. 2008.

Venkateshwaran M, Volkening JD, Sussman MR, Ané J-M. Symbiosis and the social network of higher plants. Current Opinion in Plant Biology. 2012.

Wall LG. The actinorhizal symbiosis. Journal of Plant Growth Regulation. 2000;19:167-82.

Wan J, Tanaka K, Zhang X-C, Son GH, Brechenmacher L, Nguyen THN, et al. LYK4, a Lysin motif receptor-like kinase, is important for chitin signaling and plant innate immunity in Arabidopsis. Plant Physiol. 2012;160:396-406.

Wan J, Zhang X-C, Neece D, Ramonell KM, Clough S, Kim S-y, et al. A LysM receptor-like kinase plays a critical role in chitin signaling and fungal resistance in Arabidopsis. Plant Cell. 2008;20:471-81.

Wang W, Xie Z-P, Staehelin C. Functional analysis of chimeric LysM domain receptors mediating Nod factor-induced defense signaling in Arabidopsis thaliana and chitin-induced nodulation signaling in Lotus japonicus. The Plant Journal. 2014:n/a-n/a.

Weidmann S, Sanchez L, Descombin J, Chatagnier O, Gianinazzi S, Gianinazzi-Pearson V. Fungal elicitation of signal transduction-related plant genes precedes mycorrhiza establishment and requires the dmi3 gene in Medicago truncatula. Molecular Plant-Microbe Interactions. 2004;17:1385-93.

Willmann R, Lajunen HM, Erbs G, Newman M-A, Kolb D, Tsuda K, et al. Arabidopsis lysin-motif proteins LYM1 LYM3 CERK1 mediate bacterial peptidoglycan sensing and immunity to bacterial infection. Proc Natl Acad Sci USA. 2011;108:19824-29.

Young ND, Debelle F, Oldroyd GED, Geurts R, Cannon SB, Udvardi MK, et al. The Medicago genome provides insight into the evolution of rhizobial symbioses. Nature. 2011;480:520-24.

Zhang X, Dong W, Sun J, Feng F, Deng Y, He Z, et al. The receptor kinase CERK1 has dual functions in symbiosis and immunity signalling. Plant Journal. 2015;81:258-67.

Zhukov V, Radutoiu S, Madsen LH, Rychagova T, Ovchinnikova E, Borisov A, et al. The pea Sym37 receptor kinase gene controls infection-thread initiation and nodule development. Mol Plant Microbe Interact. 2008;21:1600-8.

Zipfel C, Kunze G, Chinchilla D, Caniard A, Jones JDG, Boller T, et al. Perception of the bacterial PAMP EF-Tu by the receptor EFR restricts Agrobacterium-Mediated Transformation. Cell. 2006;125:749-60.